UCSF
UC San Francisco Electronic Theses and Dissertations

Title
Role of MARCH1 in Dendritic Cells During Airway Allergic Immunity

Permalink
https://escholarship.org/uc/item/7zb7r394

Author
Castellanos, Carlos Andres

Publication Date
2021

Supplemental Material
https://escholarship.org/uc/item/7zb7r394#supplemental

Peer reviewed|Thesis/dissertation

eScholarship.org Powered by the California Digital Library
University of California

Role of MARCH1 in Dendritic Cells During Airway Allergic Immunity

by
Carlos Andres Castellanos Rincon

DISSERTATION
Submitted in partial satisfaction of the requirements for degree of
DOCTOR OF PHILOSOPHY

in

Biomedical Sciences

in the

GRADUATE DIVISION
of the
UNIVERSITY OF CALIFORNIA, SAN FRANCISCO

Approved:

DocuSigned by:
Dean Sheppard
101CEA27F0AF442...

Dean Sheppard
Chair

DocuSigned by:
Jeoung-Sook Shin

Jeoung-Sook Shin

DocuSigned by:
Averil Ma

Averil Ma

DocuSigned by:
Jason Cyster
5FFFC327038A40D...

Jason Cyster

Committee Members

Copyright 2021

by

Carlos Andrés Castellanos

"Knowledge and wonder are the dyad of our worthy lives as intellectual beings."

Stephen Jay Gould, "The Horn of Triton", Bully for Brontosaurus

Dedicated to
Sixta Julia Prieto

may her memory be a blessing and continue to bring joy to those whose lives she touched

Dedicada a
Sixta Julia Prieto

que su recuerdo sea una bendición y continúe alegrando a aquellos cuyas vidas tocó

Acknowledgements

I am indebted to Dr. Jeoung-Sook Shin who took me under her tutelage for my PhD thesis research. Over the last six years, I have grown tremendously as a scientist and researcher. My growth would not have been possible without the guidance and advice that Jeoung-Sook provided me regularly. I truly admire her mentorship style which centered around patient listening, reliability, fairness, and honesty. I will miss learning from her and the many inspiring conversations that we had, which conferred on me the perseverance needed to perform rigorous and curiosity-driven scientific research. Most importantly, I will miss the joy of sharing the bricks of data for the first time with her, after many weeks, months, or years of planning complex experiments. Over the last few years, I feel these bricks have built the following house, my dissertation. I am grateful to Jeoung-Sook and the mortar of knowledge and critical thought that she imparted on me which has given me the confidence to continue building brick houses on a solid foundation of scientific understanding and reasoning.

I am indebted to my dissertation committee consisting of Dr. Dean Sheppard, Dr. Jason Cyster, and Dr. Averil Ma. They were instrumental in fostering a supportive environment for me to receive critical feedback on my research when I needed it eagerly. Dean was a remarkable dissertation chair and I admire the time, support, and interest that he took from the very beginning on my scientific research. Dean provided me with critical expertise on pulmonary biology and physiology. I find his passion to perform rigorous biomedical research admirable. Jason was also a fantastic mentor and easily one of the most reliable and steadfast scientists that I know. I will miss the difficult and insightful questions that he would pose during the yearly dissertation meetings. I am also grateful for Jason providing me with critical resources for my

research project. Last, Averil was very supportive, reliable, and always happy to provide me with scientific and career advice. Averil helped me greatly in crafting well-written and elegant research proposals. I am glad he was part of my dissertation committee. I will miss my dissertation committee dearly. I look forward to the day when I will see them again and rejoice in our common scientific interests.

I am indebted to K. Mark Ansel, the director of the UCSF BMS PhD Program and another outstanding mentor that took me under his wing during many times when I struggled during my PhD journey. He provided a safe environment for me to talk with him about any issues not limited to the happenings of the lab. Mark took a genuine interest in my growth as a scientist and did not let me fall through the cracks. I am grateful because he also welcomed me to his lab. I truly admire Mark for his friendship and mentorship over the years, and I will miss him dearly. He is a great role model, an exemplary scientist and kind-hearted person.

I am also indebted to many other people at UCSF. For the interest of space and time I will only mention their names in this paragraph, yet they all provided critical support, help, advice, kindness, and generosity. Of the UCSF faculty, I am indebted to Dr. Julie Zikherman, Dr. Anthony Shum, Dr. Mehrdad Matloubian, Dr. Marlys Fassett, Dr. Matthew Krummel, Dr. Jeroen Roose, Dr. Hilde Schjerven, Dr. Ari Molofsky, Dr. Mallar Bhattacharya, Dr. Aparna Sundaram, Dr. Harold Chapman, Dr. Michael Rosenblum, Dr. Mark Anderson, Dr. Esteban Burchard, Dr. Arthur Weiss, Dr. Diane Barber, and Dr. Rushika Perera. Of the UCSF Graduate Division or administrative staff, I am indebted to Demian Sainz, Dr. D'Anne Duncan, Fleur Reynolds, Annie Chan, Julia Clark, Ned Molyneux, Dr. Elizabeth Silva, and Dr. Elizabeth Watkins. I am indebted

to my lab mates on the HSW 2nd floor, including Dr. Jaehak Oh, Hong-Kun Li, and Steven Lomeli Gonzalez, of the Shin Lab, Dr. Paola Torre, Dr. Aritra Bhattacharyya, Tracy Chen and Kaveh Boostanpour of the Bhatacharya Lab, Dr. Olivier Bernard, Sheyla Yamato, Raquel Alvarez of the Gordon Lab, Grace Ngo of the Sundaram Lab, and Dr. Claude LeSaux, Dr. Jaymin Kathiriya, Dr. Tsung-Che Ho, Dr. Ying Wei, and Alexis Brumwell of the Chapman lab. I am also indebted to the staff of Student Health and Support Services at UCSF, and particularly, my general practitioner, Lisa DiGiorgio-Haag. I am indebted to my graduate school cohort especially Dr. Daniel Bunis, Dr. Jessica Cortez, Dr. Ariane Panzer, Dr. Casey Beppler and Dr. Rebecca Jaszczak. I cherish the many interactions I had over the years with my graduate school cohort and thank them for being an amazing support system for me.

I am indebted to Dr. Laura Walker of Adimab, LLC who has been and will always continue to be my personal champion. I would not have chosen to undertake a PhD if it were not for Laura and the example she set forth for me when I was under her mentorship. Laura has supported me very dearly and I treasure our friendship. To this day, I am still in awe of her and the exemplary career and fascinating scientific life she has pursued. Laura continues to be a critical role model for me.

I am indebted to the many friends that I made in high school, at MIT (particularly from my fraternity, Skullhouse, at 530 Beacon St. in Boston), in the Upper Valley, and in San Francisco that have been such an amazing support network and whose friendships have carried me through tough and dark days. In no particular order, I am indebted to Oscar Vela, Jessica Greil, Shannon Von See, Christopher Graves, Ryan Keating, Jay Baxter, Kevin Fisher, Tim Wall, Raymond Nguyen, Benjamin Mayne, Alex Salazar, Sean Robertson, Seth Berg, Michael Pohl, Baker

Logan, Bryn Waldwick, Vince Agard, Benjamin Harvatine, Amiria Harper-Rose, Carrie Perna, Leah Huiting, Katie McAlpine, Katie Waldwick (Vogel), Katie Chasins, Katalina Sher Wall, Kimia Mavon, Erica Jutras, Lauren Wisbeski, Brian Stirling, Kevin Rivera, Pawel Dominik, Eric Martina, Wilian Cortopassi, Parinaz Fozouni, Naoaki Sugimura – and many more, please do forgive me if I omitted you in this list.

I am indebted to my best friend and partner, Robert Van Noord (Bob), who I met in San Francisco in my first year of my PhD studies. Bob has been by my side throughout my lowest points throughout this journey and lifted me up. I would not be half the person I am today without his love and support. I am also indebted to his wonderful family who welcomed me as one of their own and who have been so generous and kind with me throughout this journey.

I am indebted to my own family who have been so supportive, loving, and accepting of all my life decisions, including my PhD journey. I love them with all my heart, my father Carlos Humberto Castellanos, my mother Luz Nelly Rincon, my brother Juan Camilo Castellanos, and my sister Adriana Camila Castellanos. I am also indebted to my amazing extended family who have also supported me and been so kind and generous with me. I dedicate this dissertation to my grandmother, Sixta Julia Prieto, who passed away before I started my PhD. I hope she is beaming from another realm at this achievement. I love her with all my heart.

Last, and not least, I am indebted to Kiki, a beautiful chihuahua which I welcomed into my life in the last year of my PhD and who has offered me one of life's true treasures – the love and affection that only a dog has for his owner.

Contributions to the Dissertation

All work presented in this dissertation was performed under the supervision of Dr. Jeoung-Sook Shin. Chapter 2 was published in *Science Immunology* as "Lymph node-resident dendritic cells drive T_H2 cell development involving MARCH1" (Castellanos et al. 2021)[1]. The co-authors for this publication were Xin Ren, Steven Lomeli Gonzalez, Hong Kun Li, Andrew W. Schroeder, Hong-Erh Liang, Brian J. Laidlaw, Donglei Hu, Angel C.Y. Mak, Celeste Eng, José R. Rodríguez-Santana, Michael LeNoir, Qi Yan, Juan C. Celedón, Esteban G. Burchard, Scott S. Zamvil, Satoshi Ishido, Richard M. Locksley, Jason G. Cyster, Xiaozhu Huang, and Jeoung-Sook Shin. The author contributions are listed in the Acknowledgements section of Chapter 2.

[1] Castellanos, C. A., X. Ren, S. L. Gonzalez, H. K. Li, A. W. Schroeder, H. E. Liang, B. J. Laidlaw, D. Hu, A. C. Y. Mak, C. Eng, J. R. Rodriguez-Santana, M. LeNoir, Q. Yan, J. C. Celedon, E. G. Burchard, S. S. Zamvil, S. Ishido, R. M. Locksley, J. G. Cyster, X. Huang, and J. S. Shin. 2021. Lymph node-resident dendritic cells drive TH2 cell development involving MARCH1. Sci Immunol 6: eabh0707.

Role of MARCH1 in Dendritic Cells During Airway Allergic Immunity

Carlos Andrés Castellanos

Abstract

Dendritic cells (DCs) are critical for the differentiation and activation of type 2 T helper (T_H2) cells, which provide protection from parasitic worm infections, yet also aggravate inflammation as seen in asthma and other allergic diseases. Yet little is known concerning the mechanisms employed by DCs to induce T_H2 cells in the draining lymph node (LN) or to sustain activation of the T cells in the tissue during ongoing inflammation. In the lymph node, we show that DC induction of T_H2 cells depends on the MARCH1 ubiquitin ligase. This pro-T_H2 effect of MARCH1 relied on LN-resident DCs, which triggered T cell receptor (TCR) signaling and induced GATA-3 expression from naïve $CD4^+$ T cells independent of tissue-driven migratory DCs. Mice with mutations in the ubiquitin acceptor sites of the antigen-presenting molecule MHCII and costimulatory ligand CD86, the substrates of MARCH1, failed to develop T_H2 cells. In the allergen-exposed tissue, we also found that MARCH1 in DCs played an essential role in sustaining effector $CD4^+$ T cells. MARCH1-mediated turnover of MHCII and CD86 restrained exhaustion of effector $CD4^+$ T cells, permissive with the robust proliferation of the T cells and the establishment of allergic inflammation. MARCH1 ablation in mice with established asthma reduced tissue infiltration of disease-associated eosinophils and T_H2 cells. Thus, T_H2 cell development and function in the lymph node and tissue depend on MARCH1-mediated turnover of antigen-presenting and costimulatory molecules by DCs to control TCR signaling and T cell exhaustion. MARCH1 may serve as a novel therapeutic target in asthma and other allergic diseases.

Papel de MARCH1 en las células dendríticas durante la inmunidad alérgica de las vías respiratorias

Carlos Andrés Castellanos

Resumen

Las células dendríticas (DCs) son cruciales para la diferenciación y activación de las células T cooperadoras tipo 2 (Th2), que prestan protección contra las infecciones por lombrices parasitarias, pero también agudizan la inflamación que se observa en el asma y otras enfermedades alérgicas. Sin embargo, poco se sabe acerca de los mecanismos empleados por las DCs para inducir células Th2 en el ganglio linfático de drenaje (LN) o para mantener la activación de las células T en el tejido durante la inflamación continua. En el ganglio linfático, demostramos que la inducción de células Th2 por las DCs depende de la ubiquitina ligasa MARCH1. Este effecto pro-Th2 de MARCH1 se baso en las DCs residentes en los LNs, que desencadenaron señalización de la receptora de las células T (TCR) y estimularon la expressión de GATA-3 de células $CD4^+$ T naive independiente de las DCs migratorias promovidas por el tejido. Los ratones con mutaciones en los sitios aceptores de ubiquitina de la molécula presentadora de antígeno MHCII y el ligando coestimulador CD86, los sustratos de MARCH1, no lograron desarrollar células Th2. En el tejido expuesto al alérgeno, también encontramos que MARCH1 en las DCs desempeñaba un papel esencial en el mantenimiento de las células $CD4^+$ T efectoras. La renovación mediada por MARCH1 de MHCII y CD86 restringió el agotamiento de las células $CD4^+$ T efectoras, permisivo con la proliferación robusta de las células T y el establecimiento de inflamación alérgica. La ablación de MARCH1 en ratones con asma establecida redujo la infiltración de eosinófilos y células Th2 en el tejido asociados con la enfermedad. Por lo tanto, el desarrollo y la función de las células Th2 en el ganglio linfático y el

tejido dependen del recambio mediado por MARCH1 de moléculas presentadoras de antígeno y coestimuladoras por las DCs para controlar la señalización de la TCR y el agotamiento de las células T. MARCH1 puede servir como una diana terapéutica novedosa en el asma y otras enfermedades alérgicas.

Table of Contents

Chapter 1: Dendritic Cell Involvement in Allergic Asthma and a Potential Role for MARCH1 in Allergic Immunity……1

Introduction……1

Dendritic cells and T_H2 cells: Major Culprits in Allergic Immunity……1

MARCH1: An Intriguing Ubiquitin Ligase……3

Hypothesis: Role for MARCH1 in DCs in Instruction of T_H2 Cell Immunity……4

References……6

Chapter 2: Lymph Node-Resident Dendritic Cells Drive T_H2 Cell Development Involving MARCH1……11

One sentence summary……11

Abstract……11

Introduction……12

Results ……14

MARCH1 is required for the development of T_H2 cell immunity but not T_H1, T_H17, or cytotoxic $CD8^+$ T cell immunity……14

The role of MARCH1 in promoting T_H2 cell immunity depends on its expression by DCs……15

MARCH1 promotes T_H2 cell development through LN-resident DCs……16

MARCH1 expression in LN-resident DCs promotes up-regulation of GATA-3 and down-regulation of T-bet in developing T_H2 cells……19

Ubiquitin-dependent turnover of MHCII and CD86 promotes up-regulation of GATA-3 and down-regulation of T-bet in developing T_H2 cells……20

Ubiquitination of MHCII and CD86 promotes T_H2 cell immune development in a cooperative manner……...22

Combined GWAS and eQTL analysis implicate low expression of MARCH1 associates with a low risk of asthma in humans……22

Discussion……23

Materials and Methods……....24

References and Notes…….…..44

Acknowledgements…….…….56

List of Supplementary Files……58

Chapter 3: MARCH1-Dependent Restraint of $CD4^+$ T Cell Exhaustion Establishes Airway Allergic Inflammation…….……...82

One sentence summary……....82

Abstract……82

Introduction & Results……....84

Materials and Methods……....91

References……96

List of Figures

Chapter 2: Lymph Node-Resident Dendritic Cells Drive T_H2 Cell Development Involving MARCH1……11

Figures…….....60

Fig. 2.1. MARCH1 is required for the development of T_H2 cell immunity and experimental asthma.……60

Fig. 2.2. The role of MARCH1 in promoting T_H2 cell immunity depends on its expression by DCs.……..……..……..……...61

Fig. 2.3. MARCH1 promotes T_H2 cell development through LN-resident DCs.……..……..……..……..62

Fig. 2.4. MARCH1 expression in LN-resident DCs promotes up-regulation of GATA-3 and down-regulation of T-bet in developing T_H2 cells.…….……63

Fig. 2.5. Ubiquitin-dependent turnover of MHCII and CD86 promotes up-regulation of GATA-3 and down-regulation of T-bet in developing T_H2 cells.……..……..……..……65

Fig. 2.6. Ubiquitination of MHCII and CD86 promotes T_H2 cell immune development in a cooperative fashion.…….……66

Supplementary Figures……....67

Fig. S2.1. Flow cytometry gating strategy.……..67

Fig. S2.2. MARCH1 is required for the development of T_H2 cell immunity to *Aspergillus fumigatus* extract and parasitic worms.……..68

Fig. S2.3. MARCH1 is dispensable for the development of T_H1, T_H17, or cytotoxic $CD8^+$ T cell immunity to influenza virus or autoimmune self-antigen. ……..69

Fig. S2.4. MARCH1 deletion efficiency in $MARCH1^{fl/fl}Zbtb46^{Cre}$ mice.……70

Fig. S2.5. MARCH1 expressed by macrophages, plasmacytoid DCs, or B cells does not play a significant role in T_H2 cell priming.……71

Fig. S2.6. MARCH1 is dispensable for pulmonary DC homeostasis, capture of HDM allergen, migration to the draining lymph node, or transcriptional reprograming during migration.……..72

Fig. S2.7. FACS gating strategy for purifying pulmonary or medLN DC populations.……74

Fig. S2.8. Gating of OT-II T cells and extent of expression of activation markers, GATA-3 and T-bet.…….75

Fig. S2.9. Gating of LN-resident DCs.…….76

Fig. S2.10. MARCH1 facilitates MHCII turnover.……...77

Fig. S2.11. eQTL violin plots of associations between genotypes of rs6815724, rs6815345, rs2036903 with MARCH1 expression in lung tissue....78

Chapter 3: MARCH1-Dependent Restraint of $CD4^+$ T Cell Exhaustion Establishes Airway Allergic Inflammation……82

Figures…….101

Fig. 3.1. MARCH1 negatively regulates the expression of inhibitory receptors by effector $CD4^+$ T cells and suppresses exhaustion of these T cells during allergic airway inflammation.…….……...……101

Fig. 3.2. MARCH1 promotes expansion of effector CD4$^+$ T cells during allergic airway inflammation.……102

Fig. 3.3. Ubiquitination of MHCII and CD86 negatively regulates the expression of inhibitory receptors by effector CD4$^+$ T cells and suppresses exhaustion of these cells during allergic airway inflammation.……..103

Fig. 3.4. MARCH1 ablation after establishment of allergic airway inflammation reduces Th2 cell effector function and eosinophilia to chronic HDM exposure.……104

Supplementary Figures……..105

Fig. S3.1. Flow cytometry plots of effector CD4$^+$ T cells in the lungs of WT and MARCH1$^{-/-}$ mice.……105

Fig. S3.2. MARCH1 in myeloid APCs promotes effector CD4$^+$ T cell accumulation and controls inhibitory receptor expression during HDM-induced allergic airway inflammation.……..106

Fig. S3.3. Tamoxifen treatment increases the surface expression of MHCII and CD86 by lung APCs and increases the expression of inhibitory receptors by effector CD4$^+$ T cells in MARCH1$^{fl/fl}$ UBC$^{ERT2\text{-}Cre}$ mice.……107

List of Tables

Chapter 2: Lymph Node-Resident Dendritic Cells Drive T_H2 Cell Development Involving MARCH1……**11**

Supplementary Tables……**79**

Table S2.1. Demographics of GALA II and SAGE participants included in this study.……..**79**

Table S2.2. Top ten genetic associations with asthma in trans-ethnic meta-analysis.……...**80**

Table S2.3. Replication analysis of the top ten associations in the trans-ethnic meta-analysis.…….……..……**81**

Chapter 1: Dendritic Cell Involvement in Allergic Asthma and a Potential Role for MARCH1 in Allergic Immunity

Introduction

Allergic asthma is a disease characterized by narrowing of the airways due to ongoing airway inflammation resulting in chronic pulmonary obstruction and reduced lung function. Innocuous inhaled allergens are main environmental triggers for the development and establishment of allergic asthma. The increased incidence of asthma in the United States of America, other industrialized countries, and the developing world mandate a thorough understanding of the cells responsible for initiating and progressing the disease. The dendritic cell (DC) has recently been identified as a crucial mediator in asthma through its antigen-presenting and migratory function from the lung, the site of inhaled allergen exposure, to the regional mediastinal lymph node (medLN). In the medLN, DCs activate allergen-specific $CD4^+$ T helper cells through the cognate molecular interaction of the peptide-major histocompatibility class II (MHCII) complex on the DC and the T cell receptor (TCR) on the $CD4^+$ T cell. After activation, allergen-specific T cells migrate from the medLN to the lung and elicit a response that permits allergic inflammation in asthma. The processes by which DCs activate, polarize, and sustain T helper cells in allergic immunity are incompletely understood.

Dendritic cells and T_H2 cells: Major Culprits in Allergic Immunity

The dendritic cell (DC) is a hematopoietic-derived differentiated cell belonging to the family of professional antigen-presenting cells (APCs) in the mononuclear phagocyte system. Among the APCs, DCs are instrumental in initiating adaptive immunity [Merad et al. ARI 2014].

Encounter and capture of foreign antigen and microbial stimulation promotes a process called "maturation", whereby tissue-resident DCs enhance surface expression of MHCII and CD86 and migrate to draining lymph nodes to activate naïve $CD4^+$ T cells (*1, 2*). Activated $CD4^+$ T cells polarize into distinct differentiation pathways depending on the specific pathogen invader; T_H1 cells combat intracellular microbes, T_H2 cells promote metazoan parasite expulsion, and T_H17 cells protect from extracellular bacteria and fungi (*3*). Due to these modalities, a prevailing model for helper T cell specialization calls for distinct DC populations bearing differential responsibility in their abilities to instruct differential T cell responses, among them the myeloid-derived conventional DC (DC1 and DC2) or the lymphoid-derived plasmacytoid DC (pDC) (*4, 5*). One subset of the DC2 expresses the transcription factor IRF4 and is required for the T_H2 cell response (*6, 7*). In asthma and allergic diseases, exaggerated T_H2 cell responses are coordinated by IL-4, IL-5, and IL-13 cytokines that permit eosinophilic airway allergic inflammation and IgE and IgG1 antibody production (*8*). These immune reactions further coordinate the airway smooth muscle contraction and the mucus secretion that obstructs the airways, the major manifestations of asthma.

Of the T_H2 characteristic cytokines, IL-4 is produced in significant quantities by primed T_H2 cells and IL-4 further coordinates T_H2 differentiation into effector cells that produce additional IL-13 and IL-5 cytokines (*9*). IL-4 also facilitates class switching and differentiation of activated B cells into $IgG1^+$ and IgE^+ plasma cells (*10*). These plasma cells produce IgG1 and IgE antibodies, the latter which are specifically pathological in asthma (*11*). Recently, T follicular helper (T_{FH}) cells have been proposed to impart relevant function on the IgE response in airway allergic inflammation (*12, 13*). Importantly, subsets of T_{FH} actively produce IL-4 during an immune response including T_{FH} cells in the germinal center (GC), a major site for antibody affinity maturation, memory B cell and plasma cell differentiation (*14, 15*).

Antigen-bearing DCs that migrate from the tissues upregulate the chemokine receptor CCR7 which mediates chemotaxis of these cells to the T cell zone of the lymph node (*16*). These DCs present antigens and activate naïve antigen specific $CD4^+$ T cells. Migratory DCs may also transfer antigen to lymph node-resident DCs and both are instrumental in coordinating the adequate T cell response (*17, 18*). In the context of induction of T_H2 immunity, DCs expressing the surface molecules MGL2 and CXCR5 and the transcription factors IRF4 and KLF4 have been implicated in the priming of Th2 cells during helminth parasitic infection and allergen exposure (*19-21*). In the spleen, DCs also instruct T_{FH} cell fate by producing and solubilizing CD25 which promotes T_{FH} cell priming after sheep red blood cells immunization(*22*). None of these models implicating DCs in T_H2 or T_{FH} cell priming, however, involve the DC producing a driving cytokine. The mechanisms by which DCs instruct T_H2 or T_{FH} cells in the lymph node during the primary response are unknown.

MARCH1: An Intriguing Ubiquitin Ligase

The membrane-associated RING-CH-1 (MARCH1) E3 ubiquitin ligase is expressed primarily by hematopoietic-derived antigen presenting cells (APCs) including DCs but not expressed by T cells (*23*). MARCH1 belongs to a family of E3 ubiquitin ligases called the MARCH proteins. Unlike other ubiquitin ligases which are mostly expressed in the cytosol, most MARCH proteins are anchored to plasma membranes and contain transmembrane domains (*24*). Due to this restriction in cellular localization, most MARCH proteins appear to target membrane-bound molecules. The MARCH proteins, including MARCH1, were discovered after searching for mammalian homologs of the Kaposi's Sarcoma-associated herpesvirus K3 and K5 ligases which ubiquitinate MHC class I (MHCI) and other immune-associated molecules, such as PECAM-1,

ICAM-1, IFN-γR1 and others, for lysosomal degradation (*25, 26*). By downregulating these immune-associated molecules, K3 and K5 ligases are employed by the virus to evade the immune system. Intriguingly, though many other MARCH proteins appear to be expressed ubiquitously by many cell types, MARCH1 expression appears to be mostly restricted to APCs, suggesting that MARCH1 might play a fundamental role in APC function. In accordance with this notion, MARCH1 in DCs and other APCs ubiquitinate the MHC class II (MHCII) antigen-presenting molecule and the CD86 costimulatory ligand to target them for degradation (*23, 27-30*). Along with the closely related MARCH8 protein, which is not expressed by DCs, MARCH1 shares the most homology with the K3 and K5 ligases compared to other MARCH proteins, so there may be a possibility that MARCH1 may ubiquitinate other immune-associated molecules. MARCH1 may play a relevant role in adaptive immunity by controlling expression of MHCII, CD86, or other immune-associated molecules which might support DC or other APC function of promoting development and activation of T cells.

Hypothesis: Role for MARCH1 in DCs in Instruction of T_H2 Cell Immunity

Given the importance of the peptide-MHCII complex and the TCR interaction in T cell activation, regulation of surface expression of MHCII molecules on antigen-presenting DCs likely plays crucial functions in immune responses (*31*). The membrane-associated RING-CH-1 (MARCH1) E3 ligase ubiquitinates MHCII and CD86 on the DC surface and variations in MARCH1 expression may influence the ability of DCs to initiate a specific $CD4^+$ T cell response(*32*). Aside from the peptide-MHCII and TCR interaction, costimulatory ligation of CD86 with the CD28 molecule expressed on the T cell also lowers thresholds for T cell activation and may affect T cell polarization (*33, 34*). In the context of T cell polarization, TCR

signal strength mediated by the TCR and peptide-MHCII interaction and influenced by costimulatory ligation has been proposed for instruction of the T_H1 and T_H2 cell fate, with T_H2-committed cells favoring weaker signals as opposed to T_H1-committed cells (*35, 36*). Due to the role of MARCH1 in controlling MHCII and CD86 levels on the DC surface, MARCH1 may be an instrumental molecule in regulating the T cell signal strength necessary to maintain optimal T cell polarity. In the following sections, I demonstrate how MARCH1 in DCs, by enabling ubiquitination of MHCII molecules and CD86 costimulatory ligands, guides functional T_H2 differentiation in the initiation of allergic immunity. Moreover, I further establish a secondary physiological role for MARCH1 in APCs for continuous activation of effector $CD4^+$ T cells in the airways. These findings provide rationale for the development of therapeutic agents that target MARCH1 in asthma and other allergic diseases.

References

1. M. Dalod, R. Chelbi, B. Malissen, T. Lawrence, Dendritic cell maturation: functional specialization through signaling specificity and transcriptional programming. *EMBO J* **33**, 1104-1116 (2014).
2. L. Ardouin, H. Luche, R. Chelbi, S. Carpentier, A. Shawket, F. Montanana Sanchis, C. Santa Maria, P. Grenot, Y. Alexandre, C. Gregoire, A. Fries, T. P. Vu Manh, S. Tamoutounour, K. Crozat, E. Tomasello, A. Jorquera, E. Fossum, B. Bogen, H. Azukizawa, M. Bajenoff, S. Henri, M. Dalod, B. Malissen, Broad and Largely Concordant Molecular Changes Characterize Tolerogenic and Immunogenic Dendritic Cell Maturation in Thymus and Periphery. *Immunity* **45**, 305-318 (2016).
3. J. Zhu, H. Yamane, W. E. Paul, Differentiation of effector CD4 T cell populations (*). *Annu Rev Immunol* **28**, 445-489 (2010).
4. V. Durai, K. M. Murphy, Functions of Murine Dendritic Cells. *Immunity* **45**, 719-736 (2016).
5. R. J. Dress, C. A. Dutertre, A. Giladi, A. Schlitzer, I. Low, N. B. Shadan, A. Tay, J. Lum, M. Kairi, Y. Y. Hwang, E. Becht, Y. Cheng, M. Chevrier, A. Larbi, E. W. Newell, I. Amit, J. Chen, F. Ginhoux, Plasmacytoid dendritic cells develop from Ly6D(+) lymphoid progenitors distinct from the myeloid lineage. *Nat Immunol* **20**, 852-864 (2019).
6. Y. Gao, S. A. Nish, R. Jiang, L. Hou, P. Licona-Limon, J. S. Weinstein, H. Zhao, R. Medzhitov, Control of T helper 2 responses by transcription factor IRF4-dependent dendritic cells. *Immunity* **39**, 722-732 (2013).
7. J. W. Williams, M. Y. Tjota, B. S. Clay, B. Vander Lugt, H. S. Bandukwala, C. L. Hrusch, D. C. Decker, K. M. Blaine, B. R. Fixsen, H. Singh, R. Sciammas, A. I. Sperling,

Transcription factor IRF4 drives dendritic cells to promote Th2 differentiation. *Nat Commun* **4**, 2990 (2013).

8. B. N. Lambrecht, H. Hammad, J. V. Fahy, The Cytokines of Asthma. *Immunity* **50**, 975-991 (2019).
9. W. E. Paul, History of interleukin-4. *Cytokine* **75**, 3-7 (2015).
10. F. D. Finkelman, J. Holmes, I. M. Katona, J. F. Urban, Jr., M. P. Beckmann, L. S. Park, K. A. Schooley, R. L. Coffman, T. R. Mosmann, W. E. Paul, Lymphokine control of in vivo immunoglobulin isotype selection. *Annu Rev Immunol* **8**, 303-333 (1990).
11. M. J. Robinson, M. Prout, H. Mearns, R. Kyle, M. Camberis, E. E. Forbes-Blom, W. E. Paul, C. D. Allen, G. Le Gros, IL-4 Haploinsufficiency Specifically Impairs IgE Responses against Allergens in Mice. *J Immunol* **198**, 1815-1822 (2017).
12. T. Kobayashi, K. Iijima, A. L. Dent, H. Kita, Follicular helper T cells mediate IgE antibody response to airborne allergens. *J Allergy Clin Immunol* **139**, 300-313 e307 (2017).
13. A. Noble, J. Zhao, Follicular helper T cells are responsible for IgE responses to Der p 1 following house dust mite sensitization in mice. *Clin Exp Allergy* **46**, 1075-1082 (2016).
14. I. Yusuf, R. Kageyama, L. Monticelli, R. J. Johnston, D. Ditoro, K. Hansen, B. Barnett, S. Crotty, Germinal center T follicular helper cell IL-4 production is dependent on signaling lymphocytic activation molecule receptor (CD150). *J Immunol* **185**, 190-202 (2010).
15. R. L. Reinhardt, H. E. Liang, R. M. Locksley, Cytokine-secreting follicular T cells shape the antibody repertoire. *Nat Immunol* **10**, 385-393 (2009).

16. A. Braun, T. Worbs, G. L. Moschovakis, S. Halle, K. Hoffmann, J. Bolter, A. Munk, R. Forster, Afferent lymph-derived T cells and DCs use different chemokine receptor CCR7-dependent routes for entry into the lymph node and intranodal migration. *Nat Immunol* **12**, 879-887 (2011).

17. H. K. Lee, M. Zamora, M. M. Linehan, N. Iijima, D. Gonzalez, A. Haberman, A. Iwasaki, Differential roles of migratory and resident DCs in T cell priming after mucosal or skin HSV-1 infection. *J Exp Med* **206**, 359-370 (2009).

18. S. Srivastava, J. D. Ernst, Cell-to-cell transfer of M. tuberculosis antigens optimizes CD4 T cell priming. *Cell Host Microbe* **15**, 741-752 (2014).

19. Y. Kumamoto, M. Linehan, J. S. Weinstein, B. J. Laidlaw, J. E. Craft, A. Iwasaki, CD301b(+) dermal dendritic cells drive T helper 2 cell-mediated immunity. *Immunity* **39**, 733-743 (2013).

20. B. Leon, A. Ballesteros-Tato, J. L. Browning, R. Dunn, T. D. Randall, F. E. Lund, Regulation of T(H)2 development by CXCR5+ dendritic cells and lymphotoxin-expressing B cells. *Nat Immunol* **13**, 681-690 (2012).

21. R. Tussiwand, B. Everts, G. E. Grajales-Reyes, N. M. Kretzer, A. Iwata, J. Bagaitkar, X. Wu, R. Wong, D. A. Anderson, T. L. Murphy, E. J. Pearce, K. M. Murphy, Klf4 expression in conventional dendritic cells is required for T helper 2 cell responses. *Immunity* **42**, 916-928 (2015).

22. J. Li, E. Lu, T. Yi, J. G. Cyster, EBI2 augments Tfh cell fate by promoting interaction with IL-2-quenching dendritic cells. *Nature* **533**, 110-114 (2016).

23. Y. Matsuki, M. Ohmura-Hoshino, E. Goto, M. Aoki, M. Mito-Yoshida, M. Uematsu, T. Hasegawa, H. Koseki, O. Ohara, M. Nakayama, K. Toyooka, K. Matsuoka, H. Hotta, A.

Yamamoto, S. Ishido, Novel regulation of MHC class II function in B cells. *EMBO J* **26**, 846-854 (2007).

24. T. Samji, S. Hong, R. E. Means, The Membrane Associated RING-CH Proteins: A Family of E3 Ligases with Diverse Roles through the Cell. *Int Sch Res Notices* **2014**, 637295 (2014).

25. E. Bartee, M. Mansouri, B. T. Hovey Nerenberg, K. Gouveia, K. Fruh, Downregulation of major histocompatibility complex class I by human ubiquitin ligases related to viral immune evasion proteins. *J Virol* **78**, 1109-1120 (2004).

26. M. Ohmura-Hoshino, E. Goto, Y. Matsuki, M. Aoki, M. Mito, M. Uematsu, H. Hotta, S. Ishido, A novel family of membrane-bound E3 ubiquitin ligases. *J Biochem* **140**, 147-154 (2006).

27. J. S. Shin, M. Ebersold, M. Pypaert, L. Delamarre, A. Hartley, I. Mellman, Surface expression of MHC class II in dendritic cells is controlled by regulated ubiquitination. *Nature* **444**, 115-118 (2006).

28. M. Ohmura-Hoshino, Y. Matsuki, M. Aoki, E. Goto, M. Mito, M. Uematsu, T. Kakiuchi, H. Hotta, S. Ishido, Inhibition of MHC class II expression and immune responses by c-MIR. *J Immunol* **177**, 341-354 (2006).

29. G. Baravalle, H. Park, M. McSweeney, M. Ohmura-Hoshino, Y. Matsuki, S. Ishido, J. S. Shin, Ubiquitination of CD86 is a key mechanism in regulating antigen presentation by dendritic cells. *J Immunol* **187**, 2966-2973 (2011).

30. K. Corcoran, M. Jabbour, C. Bhagwandin, M. J. Deymier, D. L. Theisen, L. Lybarger, Ubiquitin-mediated regulation of CD86 protein expression by the ubiquitin ligase membrane-associated RING-CH-1 (MARCH1). *J Biol Chem* **286**, 37168-37180 (2011).

31. T. ten Broeke, R. Wubbolts, W. Stoorvogel, MHC class II antigen presentation by dendritic cells regulated through endosomal sorting. *Cold Spring Harb Perspect Biol* **5**, a016873 (2013).

32. R. Ishikawa, M. Kajikawa, S. Ishido, Loss of MHC II ubiquitination inhibits the activation and differentiation of CD4 T cells. *Int Immunol* **26**, 283-289 (2014).

33. V. K. Kuchroo, M. P. Das, J. A. Brown, A. M. Ranger, S. S. Zamvil, R. A. Sobel, H. L. Weiner, N. Nabavi, L. H. Glimcher, B7-1 and B7-2 costimulatory molecules activate differentially the Th1/Th2 developmental pathways: application to autoimmune disease therapy. *Cell* **80**, 707-718 (1995).

34. M. A. Linterman, A. E. Denton, D. P. Divekar, I. Zvetkova, L. Kane, C. Ferreira, M. Veldhoen, S. Clare, G. Dougan, M. Espeli, K. G. Smith, CD28 expression is required after T cell priming for helper T cell responses and protective immunity to infection. *Elife* **3**, (2014).

35. S. Constant, C. Pfeiffer, A. Woodard, T. Pasqualini, K. Bottomly, Extent of T cell receptor ligation can determine the functional differentiation of naive CD4+ T cells. *J Exp Med* **182**, 1591-1596 (1995).

36. N. van Panhuys, F. Klauschen, R. N. Germain, T-cell-receptor-dependent signal intensity dominantly controls CD4(+) T cell polarization In Vivo. *Immunity* **41**, 63-74 (2014).

Chapter 2: Lymph Node-Resident Dendritic Cells Drive T_H2 Cell Development Involving MARCH1

One Sentence Summary

Type 2 immune development depends on MARCH1-mediated turnover of MHCII and CD86 by lymph node-resident dendritic cells.

Abstract

Type 2 T helper (T_H2) cells are protective against parasitic worm infections but also aggravate allergic inflammation. Although the role of dendritic cells (DCs) in T_H2 cell differentiation is well established, the underlying mechanisms are largely unknown. Here, we show that DC induction of T_H2 cells depends on membrane-associated-RING-CH-1 (MARCH1) ubiquitin ligase. The pro-T_H2 effect of MARCH1 relied on lymph node (LN)-resident DCs, which triggered T cell receptor (TCR) signaling and induced GATA-3 expression from naïve $CD4^+$ T cells independent of tissue-driven migratory DCs. Mice with mutations in the ubiquitin acceptor sites of MHCII and CD86, the two substrates of MARCH1, failed to develop T_H2 cells. These findings suggest that T_H2 cell development depends on ubiquitin-mediated clearance of antigen-presenting and costimulatory molecules by LN resident DCs and consequent control of TCR signaling.

Introduction

Dendritic cells (DCs) play an instrumental role in inducing antigen-specific T cell immunity (*1*). Encounter and capture of foreign antigens in the tissues activate DCs and induce migration to the draining lymph node (LN) (*2*). Migrated DCs present antigens to naïve T cells through the major histocompatibility complex (MHC) antigen-presenting molecules and provide the T cells with costimulatory signals that lowers threshold of activation (*3*). Activated T cells differentiate into specific types of effector cells depending on the nature of the antigens (*4*). Type 1 T helper (T_H1) effector cells develop in response to intracellular pathogens playing a critical role in activating macrophages to facilitate pathogen clearance and inducing robust cytotoxic $CD8^+$ T cell responses (*5, 6*). DC production of interleukin-12 (IL-12) is important for differentiation of T_H1 and cytotoxic $CD8^+$ T cells (*7, 8*). T_H17 cells develop in response to extracellular bacteria or fungi, and IL-1β, IL-6, IL-23, or transforming growth factor-β1 produced by DCs plays a key role in driving development of these cells (*9*). T_H2 cells develop in response to extracellular parasites and environmental substances including common allergens (*10*). Unlike the defined role for DC-derived cytokines in driving T_H1 or T_H17 cell differentiation, specific cytokines produced by DCs that drive T_H2 cell differentiation are not known (*11*). DC expression of the transcription factors interferon regulatory factor 4 (IRF4) or Krüppel-like factor 4 (KLF4) have been implicated in T_H2 cell development, but these factors also profoundly alter DC development (*12-14*). DC surface molecules such as OX40 ligand and CD40 have been also implicated for T_H2 cell development (*15, 16*), but many of these molecules serve as general costimulatory molecules rather than specifically promoting T_H2 cell development (*17, 18*). Weak T cell receptor (TCR) signal strength has been proposed to foster T_H2 cell differentiation (*4*). Priming of naïve antigen-specific T cells with a low dose of antigens

promoted IL-4 secretion and GATA-3 expression from the T cells in vitro *(19, 20)*. Adoptive transfer of DCs loaded with a low dose of antigens preferentially gave rise to T_H2 over T_H1 cells in vivo (*21*). However, whether TCR signal strength is modulated during T_H2 cell development under physiological conditions, and if so, how such modulation is achieved have not been defined.

DCs control the surface expression of the antigen-presenting molecule MHCII and the costimulatory molecule CD86 through ubiquitination by membrane-associated-RING-CH-1 (MARCH1) E3 ligase (*22, 23*). MARCH1 enables transfer of ubiquitin moieties from a ubiquitin-conjugating enzyme to a cytoplasmic lysine amino acid on its substrates (*24*). MARCH1 targets MHCII only after the MHCII is loaded with antigenic peptide and transported to the plasma membrane, thus mediating surface turnover of peptide-MHCII complexes (*25*). Despite being a well-characterized molecular pathway and mechanism, the functional role of MHCII ubiquitination is not clearly understood (*26*). We have reported that deficiency of MARCH1 or MHCII ubiquitination reduces the competitiveness of germinal center B cells during immune responses, implicating MHCII turnover in B cell function of producing high affinity antibodies (*27*). Mice deficient in MARCH1 or the ubiquitin-accepting lysine of MHCII in DCs exhibited a decrease in the number and repertoire of thymic regulatory T cells, implicating MARCH1 in DC function of selecting natural regulatory T cells (*28, 29*). However, the role of MARCH1 in driving antigen-specific T cell immunity has not been explored extensively.

Here, we investigated the role of MARCH1 in the development of T cell immunity using mouse models of microbial and parasitic infections or immune-stimulatory diseases. This study reveals that MARCH1 plays an essential role in the development of T_H2 cells by enabling LN-

resident DCs to transmit TCR signaling optimal for T_H2 cell differentiation involving turnover of MHCII and CD86.

Results

MARCH1 is required for the development of T_H2 cell immunity but not T_H1, T_H17, or cytotoxic $CD8^+$ T cell immunity

We explored the role of MARCH1 in the development of type 2 T cell immunity by employing a mouse model of allergic asthma driven by house dust mite (HDM) allergen (Fig. 2.1A). Strikingly, MARCH1-deficient mice failed to induce IL-4- or IL-13-producing T_H2 cells in the lungs (Fig. 2.1B and fig. S2.1A). These mice also failed to elicit eosinophilia in the lungs (Fig. 2.1C and fig. S2.1B). Total and HDM-specific immunoglobulin E (IgE) antibody responses were also impaired (Fig. 2.1D). However, airway infiltration of neutrophils, DCs, or monocyte-derived macrophages occurred to a similar extent to WT mice (Fig. 2.1, E to G), indicating that immune activation was not entirely impaired in these mice. These mice were resistant to developing airway hyper-responsiveness (AHR) or severe airway goblet cell metaplasia (Fig. 2.1, H and I), denoting that MARCH1 contributes to the pathology associated with allergic asthma. To determine whether the observed defect is restricted to HDM or reflects a general type 2 immune development defect, we treated mice with two additional type 2 immune stimuli, the fungal cellular extract from *Aspergillus fumigatus* or the parasitic worm *Nippostrongylus brasiliensis*. MARCH1-deficient mice elicited poor T_H2 cells, eosinophilia, or IgE antibodies against both stimuli (fig. S2.2, A to F). MARCH1 thus plays an essential role in the development of type 2 immunity independent of specific antigens.

We next examined the role of MARCH1 in the development of type 1 immunity using a mouse model of viral infection induced by the influenza virus (X31). MARCH1-deficient mice elicited interferon-γ (IFN-γ)-producing T_H1 cells at similar levels to WT mice (fig. S2.3A). MARCH1-deficient mice also elicited robust clonal expansion of viral nucleoprotein (NP)-specific $CD8^+$ T cells and production of IFN-γ and granzyme B by these cells (fig. S2.3B). Influenza-reactive IgG antibodies were produced similarly to WT mice (fig. S2.3C), and the kinetics of viral clearance were also similar (fig. S2.3D). Thus, MARCH1 is not required for the development of type 1 immunity and host protection against the influenza virus. We further assessed the role of MARCH1 in the development of experimental autoimmune encephalomyelitis (EAE), a mouse model of multiple sclerosis driven by T_H1 and T_H17 cells. MARCH1-deficient mice expanded myelin-specific $CD4^+$ T cells as robustly as WT mice (fig. S2.3E), and these T cells committed to IFN-γ, IL-17A, or granulocyte-macrophage conlony-stimulating factor (GM-CSF) production (fig. S2.3F). MARCH1-deficient mice developed this neuroinflammatory disease as severely as WT mice as determined by daily assessments of the clinical score of EAE (fig. S2.3G). Taken together, MARCH1 is required for the development of T_H2 cell immunity but not T_H1, T_H17, or cytotoxic $CD8^+$ T cell immunity.

The role of MARCH1 in promoting T_H2 cell immunity depends on its expression by DCs

To understand the cellular mechanism by which MARCH1 selectively supports T_H2 cell immune development, we aimed to identify the specific cell type(s) that uses MARCH1 for this event. Among the antigen-presenting cells that express MARCH1, DCs are best implicated in their role in type 2 immunity by their abilities of priming T_H2 cells (*30*). To examine the role of DC-expressed MARCH1, we generated mice lacking MARCH1 in cells expressing CD11c

(MARCH1$^{fl/fl}$ CD11c^{Cre}). We found MARCH1$^{fl/fl}$ CD11c^{Cre} mice recapitulated the absence of T_H2 cells, eosinophils, IgE and HDM-specific IgE antibodies observed in MARCH1-deficient mice (Fig. 2.2, A to C), supporting a role for DC-expressed MARCH1 in type 2 immune development. Because CD11c is not only expressed in DCs but also in some macrophages (*31, 32*), we generated mice in which MARCH1 is deleted in cells expressing the more selective marker for DCs, Zbtb46 (*33*). Unexpectedly, MARCH1$^{fl/fl}$ Zbtb46^{Cre} mice displayed incomplete MARCH1 deletion with about 30% of DCs persistently expressing MARCH1 (fig. S2.4A). This incomplete deletion was also shown by the surface expression of MHCII, a substrate of MARCH1, which increased only in a fraction of DCs (fig S2.4, B and C). Despite this partial deletion, we examined whether MARCH1$^{fl/fl}$ Zbtb46^{Cre} mice would still exhibit appreciable defects in developing type 2 immune responses to HDM. We performed correlation analyses between MHCII surface levels in pulmonary DCs, an indicator of MARCH1 deletion efficiency, and the extent of HDM-induced inflammatory and IgE responses. We found that the number of T_H2 cells, eosinophils, and IgE titers were each inversely correlated with the surface expression of MHCII on pulmonary DCs (Fig. 2.2, D to F), corroborating a crucial role for DC-expressed MARCH1 in the development of type 2 immunity.

MARCH1 promotes T_H2 cell development through LN-resident DCs

We sought to identify the specific role that MARCH1 plays in DC activation of type 2 immunity. We examined whether MARCH1 would be necessary for DC instruction of T_H2 cell polarization in the LN. We found that MARCH1$^{fl/fl}$ CD11c^{Cre} mice possessed significantly fewer IL-4$^+$CD4$^+$ T cells in the mediastinal LN (medLN) compared to control mice at day 7 after HDM administration (Fig. 2.3, A and B), suggesting DC MARCH1 involvement in T_H2 cell

polarization. We corroborated this finding by employing mixed bone marrow (BM) chimeric mice reconstituted with MARCH1$^{-/-}$:Zbtb46^{DTR} BM, in which after diphtheria toxin (DT) treatment, all remaining DCs lack MARCH1 (Fig. 2.3, C and D). These mice failed to prime as many IL-4^{+}CD4^{+} T cells in the medLN as control mice (Fig. 2.3E). MARCH1 in macrophages was not required as MARCH1$^{fl/fl}$ MafB^{Cre} mice, in which MARCH1 was specifically ablated in macrophages mounted normal IL-4^{+}CD4^{+} T cell development (fig. S2.5A). MARCH1 in plasmacytoid DCs (pDCs) was also dispensable because mixed BM chimeric mice reconstituted with MARCH1$^{-/-}$:CLEC4C^{DTR} BM and treated with DT, which would confine MARCH1-deficieny to pDCs, were fully competent at inducing IL-4^{+}CD4^{+} T cells (fig. S2.5B). MARCH1 in B cells was also dispensable because mixed BM chimeric mice reconstituted with MARCH1$^{-/-}$:μMT BM, in which all developing B cells lack MARCH1, were also fully competent at inducing IL-4^{+}CD4^{+} T cells (fig. S2.5C).

Pulmonary DCs that capture allergens and migrate to medLN have been implicated in driving T_H2 cell polarization (*34*). We investigated whether MARCH1 is involved in homeostasis of pulmonary DCs, allergen capturing activity of the DCs, or their migration to medLN. The number of DCs in the lungs or the efficiency of these DCs to capture HDM was not impaired by MARCH1 deficiency (fig. S2.6, A to C). The frequency of HDM-bearing DCs in the medLN of MARCH1-deficient mice was not significantly different from that of WT mice (fig. S2.6, D and E). We then investigated whether MARCH1 is involved in transcriptional reprograming of migratory DCs, which has been suggested to condition the DCs to drive T_H2 cell development (*12*). Single-cell transcriptome analysis of HDM-bearing medLN DCs revealed that these DCs consist of two subsets marked by differential expression of genes highly expressed by DC1 but not DC2, such as *IRF8*, and vice versa, genes highly expressed in DC2 but

not DC1, such as *IRF4* (*35*) (fig S2.6, F and G). Subsequent analysis indicated the gene *AY036118* was the only differentially expressed gene between WT and MARCH1-deficient DCs by more than twofold (fig S2.6H). Together, pulmonary DC homeostasis, capture of allergens, migration to medLN, or transcriptional reprograming during migration does not require MARCH1.

DCs rapidly down-regulate the expression of MARCH1 after maturation (*36*). Because DC migration to lymph node is accompanied by maturation (*2*), we examined whether MARCH1 is perhaps down-regulated during pulmonary DCs' migration to the medLN. Pulmonary DCs and medLN migratory DCs were isolated from mice at the steady state (fig. S2.7, A and B). HDM-bearing medLN migratory DCs were isolated from mice 24 hours after instillation with HDM (fig. S2.7C). medLN-resident DCs were also isolated for comparison (fig. S2.7D). The isolated DCs were analyzed for the expression of MARCH1 by quantitative reverse transcription polymerase chain reaction (PCR). We detected appreciable amount of MARCH1 in pulmonary DCs and LN-resident DCs but a very minor amount in migratory DCs both in the steady state and after HDM administration (Fig. 2.3F), suggesting that pulmonary DCs down-regulate MARCH1 during travel from the airway to the medLN. This finding raised a possibility that the effect of MARCH1 in promoting T_H2 cell development may be exerted independent of migratory DCs. To test this, we generated chimeric mice reconstituted with MARCH1$^{fl/fl}$ CD11c^{Cre}:CCR7$^{-/-}$ BM, in which all migratory DCs are MARCH1-deficient. These mice were fully competent at eliciting IL-4^{+}CD4^{+} T cells to HDM (Fig. 2.3G), indicating that the T_H2-promoting effect of MARCH1 does not depend on migratory DCs; then, it must depend on nonmigratory LN-resident DCs.

MARCH1 expression in LN-resident DCs promotes up-regulation of GATA-3 and down-regulation of T-bet in developing T_H2 cells

To explore the role of LN-resident DCs in T_H2 cell priming, we blocked migration of DCs by treating mice with pertussis toxin (PTx) (*37, 38*) and subsequently monitored activation and polarization of allergen-specific $CD4^+$ T cells. PTx inhibited accumulation of HDM-bearing DCs in the medLN up to 48 hours (Fig. 2.4, A and B), validating its efficacy as a DC migration blocker. To monitor the activation of antigen-specific T cells, mice were transferred with $CD4^+$ T cells isolated from ovalbumin (OVA)-specific TCR transgenic OT-II mice and subsequently challenged with HDM mixed with OVA. The activation of OT-II T cells in the medLN was examined by determining the expression of Nur77, CD44, and CD69, the early or later T cell activation markers. PTx treatment did not impair the extent of expression of these markers nor altered the kinetics of expression. (Fig. 2.4C, left three panels), indicating that migratory DCs are not necessary to induce activation of antigen-specific naïve $CD4^+$ T cells. Moreover, GATA-3 and T-bet, the transcription factors responsible for guiding T_H2 or T_H1 cell polarization, respectively, were also induced in mice treated with PTx at comparable levels to the mice not treated with PTx (Fig. 2.4C, right two panels). This finding suggests that migratory DCs are not necessary to initiate T_H cell polarization.

Having found that early activation and polarization of T_H cells do not depend on migratory DCs, we tested whether these events depend on MARCH1. MARCH1 deficiency resulted in a decrease in the expression of GATA-3 and an increase in the expression of T-bet. This alteration was accompanied by sustained expression of CD69, whereas no difference was observed in the expression of Nur77 or CD44 (Fig. 2.4D and fig. S2.8, A and B). A follow-up analysis on day 7 confirmed poor differentiation of these T cells to T_H2 cell fate (Fig. 2.4E).

These findings suggest that LN-resident DCs are sufficient to activate and initiate polarization of T_H2 cells during allergic airway sensitization and that MARCH1 in the LN-resident DCs plays a key role by promoting GATA-3 and repressing T-bet in developing T_H2 cells.

Ubiquitin-dependent turnover of MHCII and CD86 promotes up-regulation of GATA-3 and down-regulation of T-bet in developing T_H2 cells

The sustained expression of CD69 in OT-II T cells in MARCH1-deficient mice suggested that these T cells might have received persistent TCR signaling compared with those in WT mice. Because MARCH1 mediates ubiquitin-dependent turnover of MHCII and CD86 from DC surface, deficiency of MARCH1 would result in excessive accumulation of MHCII and CD86 on the DCs, which, in turn, would result in persistent TCR signaling in antigen-specific $CD4^+$ T cells. LN-resident DCs of MARCH1-deficient mice displayed MHCII and CD86 molecules 7- to 10-fold higher than those of WT mice (Fig. 2.5A and fig. S2.9). To determine whether this accumulation reflects delayed MHCII turnover, we used DCs cultured from bone marrow of mice using Fms-related tyrosine kinase 3 ligand (FLT3L) (BMDCs), the in vitro counterpart of lymphoid organ-resident DCs (*39*), and compared the rate of MHCII degradation in DCs derived from WT and MARCH1-deficient BM. For this assay, we made retrovirus encoding MHCII β chain fused with a photoconvertible tag (I-A^b-mKikGR) (*27*) and transduced the BMDCs with this virus. Violet light exposure irreversibly photoconverted I-A^b-mKikGR on both WT and MARCH1-deficient DCs. At 16 hours after photoconversion, WT DCs had degraded most of the photoconverted I-A^b-mKikGR molecules, whereas MARCH1-deficient DCs retained substantial amounts of the photoconverted fusion protein (fig S2.10, A and B). This finding confirms MARCH1 deficiency significantly delays MHCII turnover in DCs.

Having confirmed delayed MHCII turnover in MARCH1-deficient DCs, we tested whether this delay is indeed the cause of sustained CD69, decreased GATA-3, and increased T-bet expression in OT-II T cells in the mice. To test this, we employed MHCII$^{K>R}$ knock-in mice, which have the ubiquitin-accepting lysine (K) of MHCII replaced by arginine (R). These mice exhibited markedly elevated surface MHCII on LN-resident DCs similar to that observed in MARCH1-deficient mice, whereas the level of CD86 was not altered (Fig. 2.5B and fig. S2.9). OT-II cells transferred to MHCII$^{K>R}$ mice sustained CD69 and expressed less GATA-3 than those transferred to WT mice, although T-bet level did not differ (Fig. 2.5C). Next, we tested whether delayed turnover of CD86 may also alter the expression or regulation of CD69, GATA-3, or T-bet in T cells. CD86$^{K>R}$ mice, which have all ubiquitin accepting lysines (K) of CD86 replaced by arginines (R), exhibited an increase in the level of CD86 in the LN-resident DCs similar to that observed in MARCH1-deficient mice, whereas that of MHCII was not altered (Fig. 2.5D and fig. S2.9). OT-II cells transferred to CD86$^{K>R}$ mice did not exhibit any significant difference in the expression of CD69, GATA-3 or T-bet from those transferred to WT mice (Fig. 2.5E). Last, we generated MHCII$^{K>R}$CD86$^{K>R}$ mice in which MHCII and CD86 both fail to be ubiquitinated and thus both highly accumulate on the surface of LN-resident DCs (Fig. 2.5F and fig. S2.9). OT-II cells transferred to MHCII$^{K>R}$CD86$^{K>R}$ mice fully recapitulated the retention of CD69, reduced GATA-3, and enhanced T-bet (Fig. 2.5G) observed in MARCH1-deficient mice (Fig. 2.4D). This finding suggests that ubiquitin-mediated turnover of MHCII and CD86 contributes to regulating activation and polarization of developing T_H2 cells in a cooperative manner.

Ubiquitination of MHCII and CD86 promotes T_H2 cell immune development in a cooperative manner

We further tested the individual or cooperative effect of MHCII or CD86 ubiquitination in T_H2 cell immune development and inflammation following HDM exposure. $MHCII^{K>R}$ mice elicited IL-4^+CD4^+ T cells in the medLN normally (Fig. 2.6A) but exhibited a partial deficit in IL-4- or IL-13-producing T_H2 cells in the lung (Fig. 2.6B). $CD86^{K>R}$ mice were competent at both of these responses (Fig. 2.6, C and D). $MHCII^{K>R}CD86^{K>R}$ mice exhibited significant deficits both in T_H2 cell priming in the medLN and in T_H2 cell inflammation in the lungs (Fig. 2.6, E and F). These findings demonstrate a cooperative role of MHCII and CD86 ubiquitination in driving T_H2 cell immune development against respiratory allergens.

Combined GWAS and eQTL analysis implicate low expression of MARCH1 associates with a low risk of asthma in humans

We tested for the association between genetic variants in *MARCH1* and physician-diagnosed asthma status using asthma case and healthy control composed of 1353 Mexican American, 2118 Puerto Rican, and 1379 African American youths aged 8 to 21 (table S2.1). Association analyses were performed in each population separately and then combined in a trans-ethnic meta-analysis. The top 10 genetic associations with asthma are shown in table S2.2. Sensitivity analyses showed that downsampling to sample size without missingness in smoking status (~80% of the original sample size), rather than smoking status itself, had an impact on the meta-analysis results (data file S2.1), consistent with the relatively young study participants and hence low percentage of smokers (<10% overall). Three of the top 10 genetic variants (rs7666847, rs4691973 and rs2036903) were replicated at nominal significance level ($P < 0.05$)

using published asthma genome-wide association studies (GWASs) from the Hartford-Puerto Rico Study (table S2.3) (*40*) or Pan-UK Biobank (*41*). Flip-flop associations (nominally significant associations with different direction of effect) (*42*) were also observed from Pan-UK Biobank asthma GWAS (data file S2.2), indicating potential heterogenous effect size due to different study design and/or older populations (between 40 and 69 of age) who were likely to experience different asthma subtypes. Three of the top 10 genetic variants, rs6815724, rs6815345, and rs2036903, were expression quantitative trait loci (eQTL) in more than 29 tissues in the Genotype-Tissue Expression Project. Their alternative alleles were both associated with lower asthma risk and lower *MARCH1* gene expression (fig. S2.11 and data file S2.3). Together, these findings support that asthma risk in humans is associated with genetic variants of *MARCH1*.

Discussion

In the present study, we investigated the role of the MARCH1 ubiquitin ligase in the development of antigen-specific T cell immunity in vivo. We found MARCH1 is not necessary for the development of T_H1, T_H17, or cytotoxic $CD8^+$ T cell immunity but is required for T_H2 cell immune development. This T_H2-promoting effect depended on the expression of this molecule in LN-resident DCs. LN-resident DCs but not migratory DCs expressed MARCH1, and this molecule mediated active turnover of MHCII and CD86, enabling the DCs to provide allergen-specific T cells with modulated TCR signaling, which, in turn, resulted in a decrease in the expression of T-bet and an increase in the expression of GATA-3, leading to T_H2 cell differentiation. These findings not only reveal a specific and essential role of MARCH1 in the

development of T_H2 cell immunity but also uncover the role of LN-resident DC in T_H2 cell development together with an underlying mechanism.

MARCH1-deficient BMDCs have been shown to be incompetent at inducing production of IFN-γ and IL-17 from naïve $CD4^+$ T cells (*43*) and poor at activating antigen-specific $CD8^+$ T cells in vitro (*44*). More recently, splenic DCs derived from $MHCII^{K>R}$ mice have been shown to poorly stimulate naïve $CD4^+$ T cells in vitro and fail to expand adoptively transferred TCR transgenic T cells in vivo (*45*). Using mice immunized with OVA with alum and later challenged with OVA intranasally, Kishta *et al.* (*46*) identified that certain features of allergic asthma such as antigen-specific IgE antibody, IL-13-competent $CD4^+$ T cells, and AHR developed poorly in MARCH1-deficient mice compared to WT mice, consistent with our findings. However, the biological relevance of these findings has not been firmly established. We used various mouse models of infection and immune-stimulatory diseases and showed that MARCH1-deficient mice were competent at eliciting IFN-γ-producing T_H1 cells, IL-17-producing T_H17 cells, or cytotoxic $CD8^+$ T cells against virus or autoimmune self-antigens. However, these mice were resistant to developing T_H2 cell immune responses to environmental allergens or parasitic worms. Moreover, MARCH1-deficient mice cleared influenza virus as effectively as WT mice and developed EAE as severely as WT mice but were resistant to developing allergic airway inflammation and experimental asthma. Consistent with the asthma-resistant property of MARCH1-deficient mice, our data suggest that the alleles of two genetic variants in human *MARCH1* gene (rs6815724 and rs6815345), which were associated with lower *MARCH1* gene expression, were also associated with lower asthma risk in the trans-ethnic meta-analysis. These findings reveal a selective role of MARCH1 in inducing type 2 T cell immunity. Although the mechanisms underlying this selective role remain to be defined, MARCH1 being down-regulated following DC maturation

could be an attributing factor. DCs stop expressing MARCH1 upon Toll-like receptor (TLR) or other DC maturation inducing signals (*36, 47*). Because T_H1, T_H17, and cytotoxic $CD8^+$ T cell responses often develop after TLR-mediated activation and maturation of DCs (*48, 49*), MARCH1 would disappear from DCs during these immune responses rendering its role irrelevant for those responses. In contrast, type 2 immune stimuli often lack DC maturation stimuli and even have an activity of suppressing it. For example, papain, a well-known T_H2 immune stimulus, poorly induces DC maturation (*50*). The soluble egg antigen driven by *Schistosoma mansoni* parasite Omega-1 suppresses TLR signaling and inhibits DC maturation (*51, 52*). Because allergens are a complex mixture of many different antigens yet often contain endotoxin and other TLR stimulating agents, there might be some mechanisms used directly by allergens or activated in the host to suppress TLR signaling in DCs.

The T cell priming function of DCs has been largely attributed to migratory DCs that capture antigens in the peripheral tissue, migrate to draining LN, and present the antigens to antigen-specific $CD4^+$ T cells (*2*) . However, other studies have shown LN-resident DCs can directly capture antigens from lymphatics, present the antigens to antigen-specific $CD4^+$ T cells, and induce adaptive T cell immunity (*37, 53*). Most of these studies were done after skin immunization, and no prior studies exist regarding the role of LN-resident DCs in immune response to respiratory antigens. We showed that allergens administered intratracheally can reach the medLN and be presented to allergen-specific $CD4^+$ T cells as early as 4 hours after the administration. The T cells expressed T_H cell polarizing transcription factors such as GATA-3 and T-bet even when immigration of lung DCs to the LN was inhibited. Moreover, the expression of MARCH1 in DCs was crucial for T_H2 cell development, but its expression in migratory DCs was not, suggesting LN-resident DCs play a significant role in early instruction

of T_H2 cell development involving a MARCH1-dependent mechanism. Prevailing models for T_H2 cell development rely on migration of allergen-bearing tissue DCs to the draining LN, and recent models have also suggested the role of various cell types in tissue in promoting DC migration in association with type 2 immune development (*50, 54*). Although, undoubtedly, many T_H2 immune stimuli enhance DC migration, the specific role of these migratory DCs in T_H2 cell development has not been clearly defined (*55*). Identifying the specific role played by LN-resident versus migratory DCs represents a future avenue of investigation for a superior understanding of the mechanism of T_H2 cell development.

We found the role of MARCH1 in supporting T_H2 cell immune development depended on its activity of ubiquitinating MHCII and CD86 in DCs. MARCH1-deficient LN-resident DCs exhibited marked accumulation of MHCII and CD86 on the surface, and T cells activated by these DCs showed sustained expression of the TCR signaling reporter CD69, increased expression of T-bet, and repression of GATA-3. Because MARCH1-deficient DCs process and present antigens by the same kinetics as MARCH1-sufficient DCs (*28*), T cells that see either DCs would elicit the same strength of early TCR signaling, which seems to be reflected by the identical level of increase in the expression of Nur77 by these T cells. However, as time passes, the amounts of antigens staying on the surface of MARCH1-deficient and MARCH1-sufficient DCs would differ; more amounts of antigens would be present on MARCH1-deficient DCs than on MARCH1-sufficient DCs because of a defect in endocytosis and degradation of antigen-MHCII complexes in MARCH1-deficient DCs (*36*). This prolonged antigen presentation is likely to result in previously activated T cells receiving TCR signaling repeatedly. This persistent signaling appears to be reflected by the sustained expression of CD69 and also by the increased expression of T-bet and the decreased expression of GATA-3. Although the previous studies

have suggested that stronger TCR signaling preferentially induces the expression of T-bet to GATA-3 in activated T cells (*56, 57*), our finding suggests sustained TCR signaling may also exert the similar effect.

To confirm that the accumulation of MHCII and/or CD86 in DCs drove alteration in TCR signaling and T_H cell polarization, we employed mice in which ubiquitin-accepting sites of MHCII, CD86, or both were specifically mutated. T cells activated in mice where MHCII ubiquitination was ablated sustained the expression of CD69 and reduced expression of GATA-3, although the expression of T-bet was not altered. In contrast, T cells activated in mice where CD86 ubiquitination was ablated did not show any alteration in the expression of CD69, GATA-3, or T-bet, suggesting that the lack of CD86 ubiquitination alone is not sufficient to alter T_H cell differentiation. However, in mice where MHCII and CD86 ubiquitination were both ablated, activated T cells expressed CD69 in a sustained manner, down-regulated the expression of GATA-3, and up-regulated that of T-bet. This finding suggests that MHCII ubiquitination plays a dominant role in modulating TCR signaling and controlling the expression of T_H2 polarizing transcription factor, whereas CD86 ubiquitination plays a secondary role by contributing to repression of T_H1 polarization.

This study did not distinguish the contribution of MARCH1 expressed by DC1 or DC2 subsets to T_H2 cell development. Preliminary results using mixed BM chimeric mice reconstituted with MARCH1$^{-/-}$:XCR1^{DTR} BM support a contribution of MARCH1 expressed by DC1s . Whether MARCH1 expressed by DC2s also contributes to T_H2 cell development was not examined because the tools to address this question are not readily available. Given the facts that MARCH1 is expressed by both DC1 and DC2 lineages and that we observed that the defect in T_H2 cell development in MARCH1$^{-/-}$:XCR1^{DTR} chimeras was not as severe as what was seen in

MARCH1$^{-/-}$:Zbtb46^{DTR} chimeras, MARCH1 expressed by DC2 subset most likely also contributes to T_H2 cell development, although this needs confirmation.

In conclusion, we reveal an unappreciated role of LN-resident DCs in T_H2 cell immune development and demonstrate that MARCH1-dependent ubiquitination of MHCII and CD86 grants these DCs an ability to promote T_H2 cell differentiation through modulated TCR signaling. On the basis of these findings, we propose that LN-resident DCs and MARCH1 could serve as novel therapeutic targets for the prevention or treatment of type 2 immune-stimulatory diseases.

Materials and Methods

Study design

The study aimed to identify the role of MARCH1 in DC function in a T cell immune response. We used mouse models of allergic airway inflammation, pulmonary viral infection, systemic worm parasitic infection, and neuroinflammation and identified a selective role for MARCH1 in T_H2 cell immunity. We focused on the underlying molecular and cellular mechanisms in development of T_H2 cells in the LN to the HDM allergen using genetically engineered mouse models and other experimental manipulations of mice in vivo. Sample sizes for each experiment are indicated in the figure legends.

Mice

WT C57BL/6J and B6.SJL-PtprcaPepcb/BoyJ (CD45.1^{+}) mice were purchased from The Jackson Laboratory. MARCH1$^{-/-}$, 2D2, MARCH1$^{fl/fl}$, CD11c^{Cre}, Zbtb46^{Cre}, OT-II, Zbtb46^{DTR}, MafB^{Cre}, CLEC4C^{DTR}, μMt, Zbtb46^{GFP}, CCR7$^{-/-}$, MHCII$^{K>R}$, and CD86$^{K>R}$ mice were previously described (*28, 29, 33, 43, 58-67*). MARCH1$^{fl/fl}$ Zbtb46^{Cre} and MARCH1$^{fl/fl}$ MafB^{Cre} mice were

generated by breeding MARCH1$^{fl/fl}$ mice with Zbtb46^{Cre} or MafB^{Cre} mice, respectively. Our lab routinely genotypes the mice for adventitious germ-line deletion by checking the presence of intact loxp/loxp alleles in ear explants by PCR. We also examine the surface level of MHCII on blood B cells by flow cytometry because B cells are not supposed to be targeted by CD11c^{Cre} or MafB^{Cre}, but they express MARCH1 and thus increase MHCII surface level when MARCH1 is targeted. The mice that show surface MHCII expression on B cells increased compared to WT mice were excluded from experiments. CD45.1^{+} mice were mated to OT-II mice to generate CD45.1^{+} OT-II mice. MHCII$^{K>R}$ CD86$^{K>R}$ mice were generated by breeding MHCII$^{K>R}$ mice and CD86$^{K>R}$ mice. Mice were housed in a specific pathogen-free facility in the Laboratory Animal Research Center at the University of California, San Francisco (UCSF). Mice of both sexes were used at 5 to 12 weeks of age, except for EAE, AHR, and periodic-acid-Schiff (PAS) staining experiments, in which only female mice were used. Sample sizes were guided by previous studies. Mouse genotypes were not blinded from the investigator, except for EAE, AHR and PAS-stain scoring. All experiments conformed to ethical principles and guidelines approved by the Institutional Animal Care and Use Committee at UCSF.

HDM-induced allergic asthma protocol

On days 0 and 7 to 11, naïve mice were anesthetized with isoflurane and given 10 μg of HDM extract (*Dermatophagoides pteronyssinus*, Stallergenes Greer, catalog no. NC0419530) by oropharyngeal aspiration. On day 14, mice were euthanized, and lungs and sera were collected for flow cytometry and enzyme-linked immunosorbent assays (ELISAs).

Aspergillus extract-induced allergic inflammation protocol

On days 0 and 7 to 10, naïve mice were anesthetized with isoflurane and given of 10 μg *Aspergillus* cellular extract (*A. fumigatus*, Stallergenes Greer, catalog no. NC1677927) by

oropharyngeal aspiration. On day 13, mice were euthanized, and lungs and sera were collected for flow cytometry and ELISA.

N. brasiliensis infection

On day 0, naïve mice were infected subcutaneously with 500 *N. brasiliensis* (N.b.) stage 3 larvae (L3). On day 13, mice were euthanized, and lungs and sera were collected for flow cytometry and ELISA.

Influenza virus infection

On day 0, naïve mice were sedated with ketamine/xylazine and infected intranasally with 10^5 TCID50 (median tissue culture infectious dose) of the mouse attenuated H3N2 X31 influenza virus. On day 4, some mice were euthanized, and lungs were collected for qPCR. On day 10, the remaining mice were euthanized, and lungs and sera were collected for flow cytometry, ELISA, and qPCR.

Experimental autoimmune encephalomyelitis

On day 0, naïve mice were injected subcutaneously with 100 μg of myelin oligodendrocyte glycoprotein (MOG) peptide (35-55) (AnaSpec, catalog no. AS-60130-5) emulsified in complete Freund's adjuvant (CFA) consisting of 100 μg of heat-killed Mycobacterium tuberculosis (HKMT) (InvivoGen, catalog no. tlrl-hkmt-1)-supplemented incomplete Freund's adjuvant (Sigma-Aldrich, catalog no. F5506). On days 0 and 2, mice were also injected intraperitoneally with 200ng of PTx (EMD Millipore, catalog no. 516560). Mice were monitored for clinical signs of disease beginning on day 5 until day 20 using the following scores: grade 0, no disease; grade 1, loss of tail tone; grade 2, abnormal gait; mild hind limb paralysis; grade 3, hind limb paralysis; grade 4, front limb paralysis; grade 5, moribund.

Preparation of lung and LN cells for flow cytometry

Lungs were digested with collagenase D (Roche, catalog no. 11088882001) and deoxyribonuclease I (Roche, catalog no. 10104159001) for 30 min at 37°C and dissociated in C tubes with a gentleMACS dissociator (Miltenyi Biotec). The digest was stopped with cold fluorescence-activated cell sorting (FACS) buffer [0.5% bovine serum albumin (BSA) in phosphate-buffered saline (PBS)] and centrifuged at 500*g* for 5 min at 4°C. Cell pellets were resuspended in red blood cell lysis buffer for 5 min at room temperature (RT) and washed with FACS buffer. Cell suspensions were filtered with 70-μm nylon mesh strainers. Cells were centrifuged and resuspended in 1ml of FACS buffer and counted with a Z2 particle counter (Beckman Coulter). LNs were dispersed into cell suspensions with double frosted microscope slides in RPMI and filtered in 5-ml cell strainer tubes. Cells were centrifuged at 500*g* for 5 min at 4°C and cells were resuspended in FACS buffer. Lung and LN cells were prepared for surface or intracellular cytokine staining.

Surface staining of lung cells

Fc receptors of lung cells were blocked with anti-mouse CD16/32 (TruStain fcX, clone 93, catalog no. 101320, RRID: AB_1574975) antibody for 10 min on ice. For allergic inflammation or worm infection experiments, lung cells were stained with anti-mouse Pacific Blue I-A/I-E MHCII (M5/114.15.2, catalog no. 107620, RRID: AB_493527), anti-mouse BV605 CD4 (GK1.5, catalog no. 100451, RRID: AB_2564591 or RM4-5, catalog no. 116027, RRID: AB_2800581), anti-mouse BV650 Ly6G (1A8, catalog no. 127641, RRID: AB_2565881), anti-mouse fluorescein isothiocyanate (FITC) CD103 (2E7, catalog no. 121420, RRID: AB_10714791), anti-mouse phycoerythrin (PE) CD86 (GL-1, BD Pharmingen, catalog no. 553692), anti-mouse PerCP/Cy5.5 CD11b (M1/70, catalog no. 101228, RRID: AB_893232),

anti-mouse PE/Cy7 B220 (RA3-6B2 catalog no. 103222, RRID: AB_313005), anti-mouse allophycocyanin (APC) CD64 (X54-5/7.1, catalog no. 139306, RRID: AB_11219391), anti-mouse Alexa Fluor 700 CD11c (N418, catalog no. 117320, RRID: AB_528736), and anti-mouse APC/Cy7 Siglec-F (E50-2440, BD Pharmingen, catalog no. 565527) and with propidium iodide (BioLegend, catalog no. 421301 or Invitrogen, catalog no. P3566) as a live/dead stain for 30 min on ice. For influenza virus infection experiments, lung cells were stained with an APC tetramer with the immunodominant NP-ASNENMETM epitope (MBL Life Sciencem, catalog no. TS-M508-2) for 30 min on ice and subsequently stained with anti-mouse Pacific Blue I-A/I-E MHCII, anti-mouse BV605 CD4, anti-mouse BV650 Ly6G, anti-mouse FITC CD8a (53-6.7, catalog no. 100706, RRID: AB_312745), anti-mouse PE CD86, anti-mouse PerCP/Cy5.5 CD11b, anti-mouse PE/Cy7 CD44 (IM7, catalog no. 103030, RRID: AB_830787), anti-mouse Alexa Fluor 700 CD11c, and anti-mouse APC/Cy7 Siglec-F and with propidium iodide as a live/dead stain for 30 min on ice. Lung cells were washed and resuspended in FACS buffer for flow cytometry analysis on an LSRII machine. Antibodies were purchased from BioLegend unless stated otherwise.

Intracellular cytokine staining

Lung or LN cells were stimulated ex vivo with stimulation cocktail of phorbol 12-myristate 13-acetate (10 ng/ml; Sigma-Aldrich, catalog no. P1585) and ionomycin (1 μg/ml; Sigma-Aldrich, catalog no. I3909) in the presence of protein transport blocker brefeldin A (10 μg/ml; Sigma-Aldrich, catalog no. B5936) for 3 hours in a 37°C CO_2 incubator. After ex vivo stimulation, lung or LN cells were blocked with anti-mouse CD16/32 antibody for 10 min on ice, then stained with anti-mouse BV605 CD4 and anti-mouse Alexa Fluor 700 CD8α (53-6.7, catalog no. 100730, RRID: AB_493703) and with eFluor780 Fixable Viability Dye (eBioscience,

catalog no. 65-0865-14) as a live/dead stain for 30 min on ice. Lung or LN cells were fixed with IC fixation buffer (Invitrogen, catalog no. FB001) and permeabilized with permeabilization buffer (Invitrogen, catalog no. 00-8333-56). For allergic inflammation or worm infection experiments, lung cells were stained intracellularly with anti-mouse eFluor450 or FITC IFN-γ (XMG1.2, eBioscience, catalog no. 48-7311-82, RRID: AB_1834367 or catalog no. 11-7311-82, RRID: AB_465412), anti-mouse FITC IL-5 (TRFK5, Leinco Technologies), anti-mouse PE IL-13 (eBio13A, eBioscience, catalog no. 12-7133-82, RRID: AB_763559), anti-mouse PE/Cy7 IL-17A (TC11-18H10.1, catalog no. 506922, RRID: AB_2125010), and anti-mouse APC IL-4 (11B11, catalog no. 504106, RRID: AB_315320) for 30 min on ice. medLN cells were stained intracellularly with anti-mouse eFluor450 IFN-γ, anti-mouse PE/Cy7 IL-13 (eBio13A, eBioscience, catalog no. 25-7133-82, RRID: AB_2573530), anti-mouse PerCP/Cy5.5 IL-17A (TC11-18H10.1, catalog no.506920, RRID: AB_961384), and anti-mouse APC IL-4 for 30 min on ice. For influenza virus infection experiments, lung cells were also surface stained with an APC tetramer with the immunodominant NP-ASNENMETM epitope for 30 min on ice and stained intracellularly with anti-mouse eFluor450 IFN-γ, and anti-human/mouse PE granzyme B (GB12, ThermoFisher Scientific, catalog no. MHGB04, RRID: AB_10372671). Lung or LN cells were washed and resuspended in FACS buffer for flow cytometry analysis on an LSRII machine. Antibodies were purchased from BioLegend unless stated otherwise.

Enzyme-linked immunosorbent assay

Nunc or Immulon 96-well plates were coated overnight at 4°C with anti-mouse IgE (R35-72, BD Pharmingen, catalog no. 553413) antibody. Plates were washed with PBST (0.05% Tween in PBS) and blocked with 1% BSA for 1h. Serum samples were incubated at 1:25 dilution along with a mouse IgE standard (C48-2, BD Pharmingen, catalog no. 557080) to determine total

IgE or at 1:4 dilution to determine HDM-specific IgE at RT. Plates were washed with PBST and incubated with biotin-conjugated anti-mouse IgE (R35-118, BD Pharmingen, catalog no. 553419) for total IgE or biotin-conjugated HDM (prepared in house with the EZ-Link Sulfo-NHS-Biotinylation Kit, ThermoFisher Scientific, catalog no. 21425), for HDM-specific IgE. Plates were washed with PBST and incubated with horseradish peroxidase (HRP) streptavidin (BioLegend, catalog no. 405210) for 30 min at RT. Plates were washed with PBST and developed with trimethylboron substrate (eBioscience, catalog no. 00-4201-56). The reaction was stopped with 2N H_2SO_4 and plates were read at 450nm with a plate reader. For influenza-virus specific ELISA, plates were coated overnight with heat-inactivated X31 virus, serum samples were incubated at 1:1000, and HRP-conjugated anti-mouse IgG light chain (Jackson ImmunoResearch, catalog no. 115-035-174, RRID: AB_2338512) was used for detection.

AHR and PAS staining

Mice were sedated with ketamine/xylazine, attached to a rodent ventilator and pulmonary mechanics analyzer (FlexiVent; SCIREQ Inc.), and ventilated at a tidal volume of 9 ml/kg, a frequency of 150 breaths/min, and 2 cm H_2O positive end-expiratory pressure. Mice were paralyzed with pancuronium (0.1 mg/kg, ip). A 27-gauge needle was placed in the tail vein, and measurements of airway mechanics were made continuously using the forced oscillation technique. Mice were given increasing doses of acetylcholine (0.1, 0.3, 1, 3, and 9.6 μg/g of body weight) administered through the tail vein to generate a concentration response. HDM-induced AHR was measured. Lungs were then isolated, and paraffin-embedded lung sections were stained with PAS reagent and scored on the basis of the percentage of PAS positive cells among airway epithelial cells using the following score: grade 0: none; grade 1 <25% of airway

epithelial cells; grade 2, 25 to 50%, grade 3, 51 to 75%; and grade 4, >75%. Mice and samples were de-identified for blinding to the researcher performing these experiments.

qPCR for assessing viral burden

Lung lobes from influenza-infected mice were snap-frozen with liquid nitrogen, pulverized into powder, and dissolved in TRIzol LS reagent (Invitrogen, catalog no. 10296010). The RNA was purified and reverse-transcribed on the basis of equal amounts of RNA per sample into complementary DNA (cDNA) with oligo(dT) primers using the SuperScriptIV First Strand Synthesis System (Invitrogen, catalog no. 18091050). The cDNA was used as template for qPCR reactions in triplicates using SYBR Green reagents (Bio-Rad Laboratories, catalog no. 1725120) with primers to the influenza gene *PA* encoding the polymerase acidic (PA) protein (*PA* sense: cggtccaaattcctgctgat; *PA* antisense: cattgggttccttccataca) and normalized to qPCR reactions with primers to endogenous *Hprt*. qPCR was performed on a Bio-Rad CFX Connect System and relative viral titers were normalized to the sample from the least virally burdened mouse.

qPCR for assessing Cre-mediated MARCH1 deletion

Splenic DCs from MARCH1$^{fl/fl}$, MARCH1$^{fl/fl}$ Zbtb46^{Cre}, and MARCH1$^{fl/fl}$ CD11c^{Cre} mice were enriched using CD11c MicroBeads (Miltenyi Biotec, catalog no. 130-125-835) and sorted with a FACSAria from single-cell suspensions stained with anti-mouse Alexa Fluor488 I-A^{b} MHCII (AF6-120.1, BD Pharmingen, catalog no. 553551), anti-mouse Alexa Fluor647 CD11c (N418, BioLegend, catalog no. 117312, RRID: AB_389328), and anti-mouse PE/Cy7 B220. Genomic DNA from the sorted splenic DCs was purified using the PureLink genomic DNA Mini Kit (Invitrogen, catalog no. K182001). The genomic DNA was used as template for qPCR reactions in triplicates using SYBR Green reagents with primers spanning the 3' loxp site (MARCH1 sense: agctgtaagaactgacctcaa; MARCH1 antisense: ggaggatgcttgtcctgtaaa) and

normalized to qPCR reactions to control non-coding DNA site. qPCR was performed on a Bio-Rad CFX Connect System and MARCH1 expression was normalized to the MARCH1$^{fl/fl}$ samples.

qPCR for assessing MARCH1 expression

Pulmonary, LN migratory, or LN resident DCs from naïve or Alexa Fluor647-labeled HDM treated WT or Zbtb46^{GFP} mice (24 hours after oropharyngeal aspiration) were enriched from cell suspensions by depleting B220-, TCR-, and Ly6G-expressing cells through labeling with biotin-conjugated antibodies (RA3-6B2, BioLegend, catalog no. 103204, RRID: AB_312989; H57-597; catalog no. 13-5961-82, RRID: AB_466819; 1A8, catalog no. 127604, RRID: AB_1186108) and magnetic negative selection using EasySep RapidSpheres (STEMCELL Technologies, catalog no. 19860) and sorted with a FACSAria from the single-cell suspension stained with anti-mouse Pacific Blue I-A/I-E MHCII, anti-mouse PE/Cy7 CD11c (N418, BioLegend, catalog no. 117318, RRID: AB_493568), and anti-mouse PE Siglec-F (E50-2440, BD Pharmingen, catalog no. 562068, RRID: AB_394341) directly into TRIzol LS reagent. The RNA was purified and reverse-transcribed on the basis of equal amounts of RNA per sample into cDNA with oligo(dT) primers using the SuperScriptIV First Strand Synthesis System. The cDNA was used as template for qPCR reactions in triplicates using SYBR Green reagents with primers to *March1* isoform 2 (*March1* sense: gaccagcagccacatttgctgtaa; *March1* antisense: gctgcttgcctggagaaacaagtta) and normalized to qPCR reactions with primers to *Hprt*. qPCR was performed on a Bio-Rad CFX Connect System and relative expression of *March1* was calculated using the $2^{-\Delta\Delta Cq}$ method.

HDM capture assay

HDM extract was labeled with the Alexa Fluor 488 Protein Labeling Kit (Invitrogen, catalog no. A10235) or with Alexa Fluor 647 NHS Ester (Invitrogen, catalog no. A37573) and 10 μg of Alexa Fluor 488-labeled or Alexa Fluor 647-labeled HDM was administered to mice by oropharyngeal aspiration. Mice were euthanized 24h or 48h after and their lungs or medLNs were prepared for flow cytometric analysis. Control mice were untreated or given unlabeled HDM as negative controls.

2D2 T cell polarization

T cells were isolated using the EasySep Mouse Naïve $CD4^+$ T cell Isolation Kit (STEMCELL Technologies, catalog no. 19765) from single-cell suspensions of spleens derived from $CD45.1^+$ 2D2 donor mice. To determine IFN-γ^+, IL-$17A^+$ or GM-CSF^+ OT-II cells, mice were transferred with $CD45.1^+$ OT-II cells via retro-orbital injection. One day later, recipient mice were injected subcutaneously with 100 μg of MOG peptide (35-55) emulsified in 100 μg of HKMT-supplemented CFA. On day 0 and 2, mice were also injected intraperitoneally with 200ng of Pertussis Toxin (PTx). At day 6 after challenge, recipient mice were euthanized, and draining inguinal LNs were collected and stimulated *ex vivo* for intracellular cytokine staining (as mentioned previously). Briefly, the LN cells were surface stained with anti-mouse BV605 CD4, anti-mouse PE Vα3.2 (RR3-16, BioLegend, catalog no. 135406, RRID: AB_1937255), and anti-mouse Alexa Fluor 700 CD45.1 (A20, BioLegend, catalog no. 110724, RRID: AB_493733) and stained intracellularly with anti-mouse eFluor450 IFN-γ, anti-mouse PE/Cy7 IL-17A, and anti-mouse APC GM-CSF (MP1-22E9, BioLegend, catalog no. 505414, RRID: AB_2721461), and 2D2 polarization was determined by flow cytometry.

OT-II T cell polarization

T cells were isolated using the EasySep Mouse $CD4^+$ Naïve $CD4^+$ T cell Isolation Kit from single-cell suspensions of spleens derived from $CD45.1^+$ OT-II donor mice. To determine $IL\text{-}4^+$ OT-II cells, mice were transferred with $CD45.1^+$ OT-II cells via retro-orbital injection. One day later, recipient mice were challenged with 50 μg of OVA (Worthington, catalog no. LS003056) mixed with 10 μg of HDM by oropharyngeal aspiration. On day 7 after challenge, recipient mice were euthanized, and medLNs were collected and stimulated *ex vivo* for intracellular cytokine staining (as mentioned previously). Briefly, the medLN cells were surface stained with anti-mouse BV605 CD4, anti-mouse PerCP/Cy5.5 Vβ5 (MR9-4, BioLegend, catalog no. 139510, RRID: AB_2566807), and anti-mouse Alexa Fluor 700 CD45.1 and stained intracellularly with anti-mouse APC IL-4, and OT-II polarization was determined by flow cytometry. To determine TCR activation and polarizing transcription factors, at 4, 24, or 48 hours after challenge, recipient mice were euthanized, and medLNs were collected and surface stained with anti-mouse eFluor450 CD44 (IM7, eBioscience, catalog no. 48-0441-82, RRID: AB_1272246), anti-mouse BV605 CD4, anti-mouse FITC CD69 (H1.2F3, BioLegend, catalog no. 104506, RRID: AB_313109), anti-mouse PerCP/Cy5.5 Vβ5, and anti-mouseAlexa Fluor 700 CD45.1 and then prepared with the Foxp3 Transcription Factor Staining Buffer Kit (eBioscience, catalog no. 00-5523-00) for intracellular staining with anti-mouse PE GATA-3 (TWAJ, eBioscience, catalog no. 12-9966-42, RRID: AB_1963600), anti-mouse PE/Cy7 Nur77 (12.14, eBioscience, catalog no. 25-5965-82, RRID: AB_2811785), and anti-mouse eFluor660 T-bet (4B10, eBioscience, catalog no. 50-5825-82, RRID: AB_10596655), and OT-II activation and polarization were determined by flow cytometry.

BM chimeras and DT treatment

Mice were lethally irradiated (2×5.5 grays) and ~2×10^6 to 6×10^6 BM donor cells were injected through retro-orbital injection. Chimeras were reconstituted for at least 6 weeks before experimenting and were assessed for effective chimerism. Mice without effective chimerism were excluded from experiments. If chimeric mice received BM from Zbtb46^{DTR} or CLEC4C^{DTR} mice, then the mice were treated with DT (20 ng/g; Sigma-Aldrich, catalog no. D0564) on days -2, 0, 2, and 4 and medLNs were collected on day 7.

Pertussis Toxin (PTx)-induced DC migration blockade

Mice were administered with 1 μg of PTx mixed with 50 μg of OVA and 10 μg of Alexa Fluor 647-labeled or unlabeled HDM through oropharyngeal aspiration.

MHCII turnover assay

BMDCs were generated from BM of WT CD45.1$^+$ or MARCH1$^{-/-}$ CD45.2$^+$ mice and cultured in 1:1 ratio with FLT3L (100 ng/ml; Peprotech, catalog no. 250-31L) in 24-well plates. At day 2 or 3 of culture, the cells were spin-infected with a retrovirus with MSCV-I-Thy1.1 plasmid encoding an I-A_b-mKikGR fusion protein. At day 9 or 10 of culture, BMDCs were exposed to 415-nm violet light source set to a maximum intensity from a high numerical aperture polymer optical fiber (1.5mm core diameter) light guide and fiber collimator (Silver LED 415; Prizmatix). The cells were stained with anti-mouse Pacific Blue I-A/I-E MHCII, anti-mouse PerCP/Cy5.5 Thy1.1 (OX-7, BioLegend, catalog no. 202516, RRID: AB_961437), and anti-mouse Alexa Fluor647 CD45.2 (104, BioLegend, catalog no. 109818, RRID: AB_492870) and the cells were analyzed by flow cytometry using an LSRII machine. In the retrovirally transduced BMDCs, mKikGR^{green} fluorescence was detected using a blue laser whereas mKikGR^{red} fluorescence was detected using yellow-green laser, and MHCII turnover was

calculated as percentage of mKikGR^{red} fluorescence left at 16 hours after photoconversion compared with mKikGR^{red} fluorescence at 0 hours after photoconversion.

Study cohorts for genetic association with asthma

We examined 1,353 Mexican American, 2,118 Puerto Rican and 1,379 African American youth between 8 and 21 years of age with physician-diagnosed asthma from the Study of Genes-Environments and Admixture in Latino Americans (GALA II) and the Study of African Americans, Asthma, Genes and Environments (SAGE). A full description about the study design and recruitment has been previously described elsewhere(*68-70*). Briefly, participants were eligible for GALA II (SAGE) if they were 8 to 21 years of age and self-identified as African American (Latino) and had four African American (Latino) grandparents. Study exclusion criteria included the following: (i) any smoking within one year of the recruitment date, (ii) 10 or more pack-years of smoking, (iii) pregnancy in the third trimester, and (iv) history of lung diseases other than asthma (for cases) or chronic illness (for cases and controls). Local institutional review boards approved the studies (10-00889 for GALA II and IRB# 10-02877 for SAGE). All subjects and their legal guardians provided written informed consent.

Genetic association with asthma

Whole genome sequencing was performed in batches using whole blood samples from GALA II and SAGE participants under the Trans-Omics for Precision Medicine (TOPMed) program and the Centers for Common Disease Genomics of the Genome Sequencing Program as previously described (*71-73*). Since sequencing batch 1 included subjects with asthma cases only (table S2.1), we could not use the batch variable as a covariate directly in the case/control analysis. Instead, we used the strategies as described below to identify genetic variants associated with sequencing batch and removed them from downstream analysis. In each population, we

conducted logistic regression in PLINK to identify genetic variants associated with batch 1 and/or 3 in asthma cases, adjusting for age, sex and the first 5 genetic principal components. In Puerto Ricans, two additional logistic regression analyses were performed: 1) on sequencing batch 1 and 2 in subjects with asthma, adjusting for the same covariates; 2) on sequencing batch 2 and 3 in subjects with and without asthma using asthma status in addition to the same covariates. To minimize false positive discovery in downstream analysis, genetic variants with $P < 0.05$ in any of the above association analyses were removed from downstream analysis.

After removing genetic variants potentially associated with sequencing batches, 2492 common genetic variants (minor allele frequency ≥ 0.01) in MARCH1 and its 50kb flanking region (hg38 chr4:163,474,298-164,434,050) were used in genetic association analysis on asthma status. Association analysis was performed on each population separately using logistic regression in PLINK and then combined in a trans-ethnic meta-analysis using METAL (*74*). Age, sex and the first 5 genetic principal components were used as covariates in the discovery analysis. Sensitivity analysis with and without the smoking status was performed on the top ten associations from the discovery analysis by restricting to subset of samples with non-missing smoking status (table S2.1). The R (version 3.6.0) package coda (version 0.19-4) was used to estimate the effective number of tests for multiple testing correction in each population and meta-analysis separately. The statistical significance level was calculated by 0.05 divided by the effective number of tests. The effective number of tests for association analyses using African Americans (AA), Puerto Ricans (PR), Mexican Americans (MX) and meta-analysis (meta) were 166, 91, 255 and 122, respectively. Statistical significance levels were calculated by 0.05 divided by the number of effective tests, resulting in *P*-value thresholds of: 3.01×10^{-4} for AA, 5.49×10^{-4} for PR, 1.96×10^{-4} for MX and 4.10×10^{-4} for meta-analysis. Suggestive significance

levels were calculated by one divided by the number of effective tests, resulting in *P*-value thresholds of: 6.02×10^{-3} for AA, 1.10×10^{-2} for PR, 3.92×10^{-3} for MX and 8.20×10^{-3} for meta-analysis. Expression quantitative trait loci (eQTL) from Genotype-Tissue Expression (GTEx) Project version 8 were used for annotations (*75*). Replication of the top ten trans-ethnic meta-analysis asthma association were performed by querying previously published asthma association studies from Hartford-Puerto Rico Study(*40*) and Pan-UK Biobank (Phenocode 495, J45, 6152 22127 and 20002) (*41*).

Single cell RNA sequencing

HDM^+ WT DCs or HDM^+ $MARCH1^{-/-}$ DCs were enriched from the medLNs of CD45.1/.1 $Zbtb46^{GFP}$:CD45.2/.2 $Zbtb46^{GFP}$ $MARCH1^{-/-}$ mixed BM chimeric mice (24 hours after oropharyngeal aspiration) and the DCs were sorted using a FACSAria, as mentioned previously. Immediately after sorting, cells were run on the 10X Chromium (10X Genomics) and then through library preparation by the Institute for Human Genetics at UCSF following the recommended protocol for the Chromium Single Cell 3′ Reagent Kit (v3 Chemistry). Libraries were run on the NovaSeq 6000 for Illumina sequencing. Postprocessing and quality control were performed by the Genomics Core Facility at the Institute for Human Genetics at UCSF using the 10X Cell Ranger package (Cell Ranger version 3.0.2, 10X Genomics). Primary assessment with this software for WT DC sample reported 2441 cell-barcodes with 7,651 median unique molecular identifiers (transcripts) per cell and 2004 median genes per cell sequenced to 61.4% sequencing saturation with 48,559 mean reads per cell. Primary assessment with this software for $MARCH1^{-/-}$ DC sample reported 681 cell-barcodes with 6309 median unique transcripts per cell and 1774 median genes per cell sequenced to 73.1% sequencing saturation with 202,410 mean reads per cell.

RNA sequence data analysis

Using *Seurat* R package v3 (Satija Lab), we filtered cells to only keep those that had less than 7% mitochondrial genes and cells with numbers of features greater than 1800 and numbers of counts greater than 7500. For clustering, we determined the principal components (principal components analysis), then constructed a shared nearest neighbor graph (SNN), identified clusters with a resolution of 0.4, and lastly visualized the cells using uniform manifold approximate and projection (UMAP), per the typical Seurat workflow. To identify cluster-specific markers after the creation of UMAP plots, we used normalized RNA counts of all clusters, scaled the data, and performed differential gene expression (DE) testing by applying the Wilcoxon rank sum test using Seurat's FindMarkers function. To compare cell clusters of WT with MARCH1$^{-/-}$, we once again used normalized/scaled RNA counts and performed DE testing with FindMarkers.

Quantification and statistical analysis

Flow cytometry data were analyzed by FlowJo v5 or v10 software (TreeStar). Graphs were drawn using Prism v7 software (GraphPad). Data are presented as means ± SEM. One-way analysis of variance (ANOVA) with Tukey's multiple comparisons tests, two-way ANOVA with Tukey's multiple comparisons tests, two-way ANOVA with Fisher's least significant difference (LSD) tests or unpaired two-tailed Student's *t*-tests were performed for most statistical analysis using Prism. Pearson's correlation coefficients and linear regression were also calculated for some statistical analysis using Prism. *P* values less than 0.05 were considered statistically significant.

References and Notes

1. J. Banchereau, R. M. Steinman, Dendritic cells and the control of immunity. *Nature* **392**, 245-252 (1998).
2. D. Alvarez, E. H. Vollmann, U. H. von Andrian, Mechanisms and consequences of dendritic cell migration. *Immunity* **29**, 325-342 (2008).
3. A. Lanzavecchia, F. Sallusto, The instructive role of dendritic cells on T cell responses: lineages, plasticity and kinetics. *Curr Opin Immunol* **13**, 291-298 (2001).
4. J. Zhu, H. Yamane, W. E. Paul, Differentiation of effector CD4 T cell populations (*). *Annu Rev Immunol* **28**, 445-489 (2010).
5. N. J. Tubo, M. K. Jenkins, CD4+ T Cells: guardians of the phagosome. *Clin Microbiol Rev* **27**, 200-213 (2014).
6. Y. Nakanishi, B. Lu, C. Gerard, A. Iwasaki, CD8(+) T lymphocyte mobilization to virus-infected tissue requires CD4(+) T-cell help. *Nature* **462**, 510-513 (2009).
7. C. H. Liu, Y. T. Fan, A. Dias, L. Esper, R. A. Corn, A. Bafica, F. S. Machado, J. Aliberti, Cutting edge: dendritic cells are essential for in vivo IL-12 production and development of resistance against Toxoplasma gondii infection in mice. *J Immunol* **177**, 31-35 (2006).
8. C. J. Henry, D. A. Ornelles, L. M. Mitchell, K. L. Brzoza-Lewis, E. M. Hiltbold, IL-12 produced by dendritic cells augments CD8+ T cell activation through the production of the chemokines CCL1 and CCL17. *J Immunol* **181**, 8576-8584 (2008).
9. W. Hu, T. D. Troutman, R. Edukulla, C. Pasare, Priming microenvironments dictate cytokine requirements for T helper 17 cell lineage commitment. *Immunity* **35**, 1010-1022 (2011).

10. N. W. Palm, R. K. Rosenstein, R. Medzhitov, Allergic host defences. *Nature* **484**, 465-472 (2012).

11. V. Durai, K. M. Murphy, Functions of Murine Dendritic Cells. *Immunity* **45**, 719-736 (2016).

12. Y. Gao, S. A. Nish, R. Jiang, L. Hou, P. Licona-Limon, J. S. Weinstein, H. Zhao, R. Medzhitov, Control of T helper 2 responses by transcription factor IRF4-dependent dendritic cells. *Immunity* **39**, 722-732 (2013).

13. J. W. Williams, M. Y. Tjota, B. S. Clay, B. Vander Lugt, H. S. Bandukwala, C. L. Hrusch, D. C. Decker, K. M. Blaine, B. R. Fixsen, H. Singh, R. Sciammas, A. I. Sperling, Transcription factor IRF4 drives dendritic cells to promote Th2 differentiation. *Nat Commun* **4**, 2990 (2013).

14. R. Tussiwand, B. Everts, G. E. Grajales-Reyes, N. M. Kretzer, A. Iwata, J. Bagaitkar, X. Wu, R. Wong, D. A. Anderson, T. L. Murphy, E. J. Pearce, K. M. Murphy, Klf4 expression in conventional dendritic cells is required for T helper 2 cell responses. *Immunity* **42**, 916-928 (2015).

15. A. Hoshino, Y. Tanaka, H. Akiba, Y. Asakura, Y. Mita, T. Sakurai, A. Takaoka, S. Nakaike, N. Ishii, K. Sugamura, H. Yagita, K. Okumura, Critical role for OX40 ligand in the development of pathogenic Th2 cells in a murine model of asthma. *Eur J Immunol* **33**, 861-869 (2003).

16. A. S. MacDonald, E. A. Patton, A. C. La Flamme, M. I. Araujo, C. R. Huxtable, B. Bauman, E. J. Pearce, Impaired Th2 development and increased mortality during Schistosoma mansoni infection in the absence of CD40/CD154 interaction. *J Immunol* **168**, 4643-4649 (2002).

17. S. J. Jenkins, G. Perona-Wright, A. G. Worsley, N. Ishii, A. S. MacDonald, Dendritic cell expression of OX40 ligand acts as a costimulatory, not polarizing, signal for optimal Th2 priming and memory induction in vivo. *J Immunol* **179**, 3515-3523 (2007).

18. I. S. Grewal, J. Xu, R. A. Flavell, Impairment of antigen-specific T-cell priming in mice lacking CD40 ligand. *Nature* **378**, 617-620 (1995).

19. S. Constant, C. Pfeiffer, A. Woodard, T. Pasqualini, K. Bottomly, Extent of T cell receptor ligation can determine the functional differentiation of naive CD4+ T cells. *J Exp Med* **182**, 1591-1596 (1995).

20. H. Yamane, J. Zhu, W. E. Paul, Independent roles for IL-2 and GATA-3 in stimulating naive CD4+ T cells to generate a Th2-inducing cytokine environment. *J Exp Med* **202**, 793-804 (2005).

21. N. van Panhuys, F. Klauschen, R. N. Germain, T-cell-receptor-dependent signal intensity dominantly controls CD4(+) T cell polarization In Vivo. *Immunity* **41**, 63-74 (2014).

22. J. S. Shin, M. Ebersold, M. Pypaert, L. Delamarre, A. Hartley, I. Mellman, Surface expression of MHC class II in dendritic cells is controlled by regulated ubiquitination. *Nature* **444**, 115-118 (2006).

23. G. Baravalle, H. Park, M. McSweeney, M. Ohmura-Hoshino, Y. Matsuki, S. Ishido, J. S. Shin, Ubiquitination of CD86 is a key mechanism in regulating antigen presentation by dendritic cells. *J Immunol* **187**, 2966-2973 (2011).

24. T. Samji, S. Hong, R. E. Means, The Membrane Associated RING-CH Proteins: A Family of E3 Ligases with Diverse Roles through the Cell. *Int Sch Res Notices* **2014**, 637295 (2014).

25. G. van Niel, R. Wubbolts, T. Ten Broeke, S. I. Buschow, F. A. Ossendorp, C. J. Melief, G. Raposo, B. W. van Balkom, W. Stoorvogel, Dendritic cells regulate exposure of MHC class II at their plasma membrane by oligoubiquitination. *Immunity* **25**, 885-894 (2006).

26. J. Oh, J. S. Shin, Molecular mechanism and cellular function of MHCII ubiquitination. *Immunol Rev* **266**, 134-144 (2015).

27. O. Bannard, S. J. McGowan, J. Ersching, S. Ishido, G. D. Victora, J. S. Shin, J. G. Cyster, Ubiquitin-mediated fluctuations in MHC class II facilitate efficient germinal center B cell responses. *J Exp Med* **213**, 993-1009 (2016).

28. J. Oh, N. Wu, G. Baravalle, B. Cohn, J. Ma, B. Lo, I. Mellman, S. Ishido, M. Anderson, J. S. Shin, MARCH1-mediated MHCII ubiquitination promotes dendritic cell selection of natural regulatory T cells. *J Exp Med* **210**, 1069-1077 (2013).

29. J. Oh, J. S. A. Perry, H. Pua, N. Irgens-Moller, S. Ishido, C. S. Hsieh, J. S. Shin, MARCH1 protects the lipid raft and tetraspanin web from MHCII proteotoxicity in dendritic cells. *J Cell Biol* **217**, 1395-1410 (2018).

30. B. Pulendran, D. Artis, New paradigms in type 2 immunity. *Science* **337**, 431-435 (2012).

31. C. von Garnier, L. Filgueira, M. Wikstrom, M. Smith, J. A. Thomas, D. H. Strickland, P. G. Holt, P. A. Stumbles, Anatomical location determines the distribution and function of dendritic cells and other APCs in the respiratory tract. *J Immunol* **175**, 1609-1618 (2005).

32. L. S. van Rijt, S. Jung, A. Kleinjan, N. Vos, M. Willart, C. Duez, H. C. Hoogsteden, B. N. Lambrecht, In vivo depletion of lung CD11c+ dendritic cells during allergen challenge abrogates the characteristic features of asthma. *J Exp Med* **201**, 981-991 (2005).

33. J. Loschko, H. A. Schreiber, G. J. Rieke, D. Esterhazy, M. M. Meredith, V. A. Pedicord, K. H. Yao, S. Caballero, E. G. Pamer, D. Mucida, M. C. Nussenzweig, Absence of MHC

class II on cDCs results in microbial-dependent intestinal inflammation. *J Exp Med* **213**, 517-534 (2016).

34. B. N. Lambrecht, H. Hammad, Biology of lung dendritic cells at the origin of asthma. *Immunity* **31**, 412-424 (2009).

35. M. Guilliams, F. Ginhoux, C. Jakubzick, S. H. Naik, N. Onai, B. U. Schraml, E. Segura, R. Tussiwand, S. Yona, Dendritic cells, monocytes and macrophages: a unified nomenclature based on ontogeny. *Nat Rev Immunol* **14**, 571-578 (2014).

36. A. De Gassart, V. Camosseto, J. Thibodeau, M. Ceppi, N. Catalan, P. Pierre, E. Gatti, MHC class II stabilization at the surface of human dendritic cells is the result of maturation-dependent MARCH I down-regulation. *Proc Natl Acad Sci U S A* **105**, 3491-3496 (2008).

37. A. A. Itano, S. J. McSorley, R. L. Reinhardt, B. D. Ehst, E. Ingulli, A. Y. Rudensky, M. K. Jenkins, Distinct dendritic cell populations sequentially present antigen to CD4 T cells and stimulate different aspects of cell-mediated immunity. *Immunity* **19**, 47-57 (2003).

38. C. Jakubzick, J. Helft, T. J. Kaplan, G. J. Randolph, Optimization of methods to study pulmonary dendritic cell migration reveals distinct capacities of DC subsets to acquire soluble versus particulate antigen. *J Immunol Methods* **337**, 121-131 (2008).

39. S. H. Naik, A. I. Proietto, N. S. Wilson, A. Dakic, P. Schnorrer, M. Fuchsberger, M. H. Lahoud, M. O'Keeffe, Q. X. Shao, W. F. Chen, J. A. Villadangos, K. Shortman, L. Wu, Cutting edge: generation of splenic CD8+ and CD8- dendritic cell equivalents in Fms-like tyrosine kinase 3 ligand bone marrow cultures. *J Immunol* **174**, 6592-6597 (2005).

40. Q. Yan, J. Brehm, M. Pino-Yanes, E. Forno, J. Lin, S. S. Oh, E. Acosta-Perez, C. C. Laurie, M. M. Cloutier, B. A. Raby, A. M. Stilp, T. Sofer, D. Hu, S. Huntsman, C. S.

Eng, M. P. Conomos, D. Rastogi, K. Rice, G. Canino, W. Chen, R. G. Barr, E. G. Burchard, J. C. Celedon, A meta-analysis of genome-wide association studies of asthma in Puerto Ricans. *Eur Respir J* **49**, (2017).

41. Pan-UKB team. https://pan.ukbb.broadinstitute.org. 2020.

42. P. I. Lin, J. M. Vance, M. A. Pericak-Vance, E. R. Martin, No gene is an island: the flip-flop phenomenon. *Am J Hum Genet* **80**, 531-538 (2007).

43. R. Ishikawa, M. Kajikawa, S. Ishido, Loss of MHC II ubiquitination inhibits the activation and differentiation of CD4 T cells. *Int Immunol* **26**, 283-289 (2014).

44. K. R. Wilson, H. Liu, G. Healey, V. Vuong, S. Ishido, M. J. Herold, J. A. Villadangos, J. D. Mintern, MARCH1-mediated ubiquitination of MHC II impacts the MHC I antigen presentation pathway. *PLoS One* **13**, e0200540 (2018).

45. H. J. Kim, J. Bandola-Simon, S. Ishido, N. W. Wong, V. N. Koparde, M. Cam, P. A. Roche, Ubiquitination of MHC Class II by March-I Regulates Dendritic Cell Fitness. *J Immunol*, (2020).

46. O. A. Kishta, A. Sabourin, L. Simon, T. McGovern, M. Raymond, T. Galbas, A. Majdoubi, S. Ishido, J. G. Martin, J. Thibodeau, March1 E3 Ubiquitin Ligase Modulates Features of Allergic Asthma in an Ovalbumin-Induced Mouse Model of Lung Inflammation. *J Immunol Res* **2018**, 3823910 (2018).

47. L. J. Young, N. S. Wilson, P. Schnorrer, A. Proietto, T. ten Broeke, Y. Matsuki, A. M. Mount, G. T. Belz, M. O'Keeffe, M. Ohmura-Hoshino, S. Ishido, W. Stoorvogel, W. R. Heath, K. Shortman, J. A. Villadangos, Differential MHC class II synthesis and ubiquitination confers distinct antigen-presenting properties on conventional and plasmacytoid dendritic cells. *Nat Immunol* **9**, 1244-1252 (2008).

48. A. Iwasaki, R. Medzhitov, Regulation of adaptive immunity by the innate immune system. *Science* **327**, 291-295 (2010).

49. M. Dalod, R. Chelbi, B. Malissen, T. Lawrence, Dendritic cell maturation: functional specialization through signaling specificity and transcriptional programming. *EMBO J* **33**, 1104-1116 (2014).

50. C. Perner, C. H. Flayer, X. Zhu, P. A. Aderhold, Z. N. A. Dewan, T. Voisin, R. B. Camire, O. A. Chow, I. M. Chiu, C. L. Sokol, Substance P Release by Sensory Neurons Triggers Dendritic Cell Migration and Initiates the Type-2 Immune Response to Allergens. *Immunity* **53**, 1063-1077 e1067 (2020).

51. C. M. Kane, L. Cervi, J. Sun, A. S. McKee, K. S. Masek, S. Shapira, C. A. Hunter, E. J. Pearce, Helminth antigens modulate TLR-initiated dendritic cell activation. *J Immunol* **173**, 7454-7461 (2004).

52. B. Everts, G. Perona-Wright, H. H. Smits, C. H. Hokke, A. J. van der Ham, C. M. Fitzsimmons, M. J. Doenhoff, J. van der Bosch, K. Mohrs, H. Haas, M. Mohrs, M. Yazdanbakhsh, G. Schramm, Omega-1, a glycoprotein secreted by Schistosoma mansoni eggs, drives Th2 responses. *J Exp Med* **206**, 1673-1680 (2009).

53. M. Y. Gerner, P. Torabi-Parizi, R. N. Germain, Strategically localized dendritic cells promote rapid T cell responses to lymph-borne particulate antigens. *Immunity* **42**, 172-185 (2015).

54. T. Y. Halim, C. A. Steer, L. Matha, M. J. Gold, I. Martinez-Gonzalez, K. M. McNagny, A. N. McKenzie, F. Takei, Group 2 innate lymphoid cells are critical for the initiation of adaptive T helper 2 cell-mediated allergic lung inflammation. *Immunity* **40**, 425-435 (2014).

55. H. L. Miller, P. S. Andhey, M. K. Swiecki, B. A. Rosa, K. Zaitsev, A. C. Villani, M. Mitreva, M. N. Artyomov, S. Gilfillan, M. Cella, M. Colonna, Altered ratio of dendritic cell subsets in skin-draining lymph nodes promotes Th2-driven contact hypersensitivity. *Proc Natl Acad Sci U S A* **118**, (2021).

56. J. A. Walker, A. N. J. McKenzie, TH2 cell development and function. *Nat Rev Immunol* **18**, 121-133 (2018).

57. N. D. Bhattacharyya, C. G. Feng, Regulation of T Helper Cell Fate by TCR Signal Strength. *Front Immunol* **11**, 624 (2020).

58. Y. Matsuki, M. Ohmura-Hoshino, E. Goto, M. Aoki, M. Mito-Yoshida, M. Uematsu, T. Hasegawa, H. Koseki, O. Ohara, M. Nakayama, K. Toyooka, K. Matsuoka, H. Hotta, A. Yamamoto, S. Ishido, Novel regulation of MHC class II function in B cells. *EMBO J* **26**, 846-854 (2007).

59. E. Bettelli, M. Pagany, H. L. Weiner, C. Linington, R. A. Sobel, V. K. Kuchroo, Myelin oligodendrocyte glycoprotein-specific T cell receptor transgenic mice develop spontaneous autoimmune optic neuritis. *J Exp Med* **197**, 1073-1081 (2003).

60. M. L. Caton, M. R. Smith-Raska, B. Reizis, Notch-RBP-J signaling controls the homeostasis of CD8- dendritic cells in the spleen. *J Exp Med* **204**, 1653-1664 (2007).

61. M. J. Barnden, J. Allison, W. R. Heath, F. R. Carbone, Defective TCR expression in transgenic mice constructed using cDNA-based alpha- and beta-chain genes under the control of heterologous regulatory elements. *Immunol Cell Biol* **76**, 34-40 (1998).

62. M. M. Meredith, K. Liu, G. Darrasse-Jeze, A. O. Kamphorst, H. A. Schreiber, P. Guermonprez, J. Idoyaga, C. Cheong, K. H. Yao, R. E. Niec, M. C. Nussenzweig,

Expression of the zinc finger transcription factor zDC (Zbtb46, Btbd4) defines the classical dendritic cell lineage. *J Exp Med* **209**, 1153-1165 (2012).

63. X. Wu, C. G. Briseno, V. Durai, J. C. Albring, M. Haldar, P. Bagadia, K. W. Kim, G. J. Randolph, T. L. Murphy, K. M. Murphy, Mafb lineage tracing to distinguish macrophages from other immune lineages reveals dual identity of Langerhans cells. *J Exp Med* **213**, 2553-2565 (2016).

64. M. Swiecki, S. Gilfillan, W. Vermi, Y. Wang, M. Colonna, Plasmacytoid dendritic cell ablation impacts early interferon responses and antiviral NK and CD8(+) T cell accrual. *Immunity* **33**, 955-966 (2010).

65. D. Kitamura, J. Roes, R. Kuhn, K. Rajewsky, A B cell-deficient mouse by targeted disruption of the membrane exon of the immunoglobulin mu chain gene. *Nature* **350**, 423-426 (1991).

66. A. T. Satpathy, W. Kc, J. C. Albring, B. T. Edelson, N. M. Kretzer, D. Bhattacharya, T. L. Murphy, K. M. Murphy, Zbtb46 expression distinguishes classical dendritic cells and their committed progenitors from other immune lineages. *J Exp Med* **209**, 1135-1152 (2012).

67. U. E. Hopken, J. Droese, J. P. Li, J. Joergensen, D. Breitfeld, H. G. Zerwes, M. Lipp, The chemokine receptor CCR7 controls lymph node-dependent cytotoxic T cell priming in alloimmune responses. *Eur J Immunol* **34**, 461-470 (2004).

68. K. K. Nishimura, J. M. Galanter, L. A. Roth, S. S. Oh, N. Thakur, E. A. Nguyen, S. Thyne, H. J. Farber, D. Serebrisky, R. Kumar, E. Brigino-Buenaventura, A. Davis, M. A. LeNoir, K. Meade, W. Rodriguez-Cintron, P. C. Avila, L. N. Borrell, K. Bibbins-Domingo, J. R. Rodriguez-Santana, S. Sen, F. Lurmann, J. R. Balmes, E. G. Burchard,

Early-life air pollution and asthma risk in minority children. The GALA II and SAGE II studies. *Am J Respir Crit Care Med* **188**, 309-318 (2013).

69. N. Thakur, S. S. Oh, E. A. Nguyen, M. Martin, L. A. Roth, J. Galanter, C. R. Gignoux, C. Eng, A. Davis, K. Meade, M. A. LeNoir, P. C. Avila, H. J. Farber, D. Serebrisky, E. Brigino-Buenaventura, W. Rodriguez-Cintron, R. Kumar, L. K. Williams, K. Bibbins-Domingo, S. Thyne, S. Sen, J. R. Rodriguez-Santana, L. N. Borrell, E. G. Burchard, Socioeconomic status and childhood asthma in urban minority youths. The GALA II and SAGE II studies. *Am J Respir Crit Care Med* **188**, 1202-1209 (2013).

70. S. S. Oh, H. Tcheurekdjian, L. A. Roth, E. A. Nguyen, S. Sen, J. M. Galanter, A. Davis, H. J. Farber, F. D. Gilliland, R. Kumar, P. C. Avila, E. Brigino-Buenaventura, R. Chapela, J. G. Ford, M. A. LeNoir, F. Lurmann, K. Meade, D. Serebrisky, S. Thyne, W. Rodriguez-Cintron, J. R. Rodriguez-Santana, L. K. Williams, L. N. Borrell, E. G. Burchard, Effect of secondhand smoke on asthma control among black and Latino children. *J Allergy Clin Immunol* **129**, 1478-1483 e1477 (2012).

71. D. Taliun, D. N. Harris, M. D. Kessler, J. Carlson, Z. A. Szpiech, R. Torres, S. A. G. Taliun, A. Corvelo, S. M. Gogarten, H. M. Kang, A. N. Pitsillides, J. LeFaive, S. B. Lee, X. Tian, B. L. Browning, S. Das, A. K. Emde, W. E. Clarke, D. P. Loesch, A. C. Shetty, T. W. Blackwell, A. V. Smith, Q. Wong, X. Liu, M. P. Conomos, D. M. Bobo, F. Aguet, C. Albert, A. Alonso, K. G. Ardlie, D. E. Arking, S. Aslibekyan, P. L. Auer, J. Barnard, R. G. Barr, L. Barwick, L. C. Becker, R. L. Beer, E. J. Benjamin, L. F. Bielak, J. Blangero, M. Boehnke, D. W. Bowden, J. A. Brody, E. G. Burchard, B. E. Cade, J. F. Casella, B. Chalazan, D. I. Chasman, Y. I. Chen, M. H. Cho, S. H. Choi, M. K. Chung, C. B. Clish, A. Correa, J. E. Curran, B. Custer, D. Darbar, M. Daya, M. de Andrade, D. L.

DeMeo, S. K. Dutcher, P. T. Ellinor, L. S. Emery, C. Eng, D. Fatkin, T. Fingerlin, L. Forer, M. Fornage, N. Franceschini, C. Fuchsberger, S. M. Fullerton, S. Germer, M. T. Gladwin, D. J. Gottlieb, X. Guo, M. E. Hall, J. He, N. L. Heard-Costa, S. R. Heckbert, M. R. Irvin, J. M. Johnsen, A. D. Johnson, R. Kaplan, S. L. R. Kardia, T. Kelly, S. Kelly, E. E. Kenny, D. P. Kiel, R. Klemmer, B. A. Konkle, C. Kooperberg, A. Kottgen, L. A. Lange, J. Lasky-Su, D. Levy, X. Lin, K. H. Lin, C. Liu, R. J. F. Loos, L. Garman, R. Gerszten, S. A. Lubitz, K. L. Lunetta, A. C. Y. Mak, A. Manichaikul, A. K. Manning, R. A. Mathias, D. D. McManus, S. T. McGarvey, J. B. Meigs, D. A. Meyers, J. L. Mikulla, M. A. Minear, B. D. Mitchell, S. Mohanty, M. E. Montasser, C. Montgomery, A. C. Morrison, J. M. Murabito, A. Natale, P. Natarajan, S. C. Nelson, K. E. North, J. R. O'Connell, N. D. Palmer, N. Pankratz, G. M. Peloso, P. A. Peyser, J. Pleiness, W. S. Post, B. M. Psaty, D. C. Rao, S. Redline, A. P. Reiner, D. Roden, J. I. Rotter, I. Ruczinski, C. Sarnowski, S. Schoenherr, D. A. Schwartz, J. S. Seo, S. Seshadri, V. A. Sheehan, W. H. Sheu, M. B. Shoemaker, N. L. Smith, J. A. Smith, N. Sotoodehnia, A. M. Stilp, W. Tang, K. D. Taylor, M. Telen, T. A. Thornton, R. P. Tracy, D. J. Van Den Berg, R. S. Vasan, K. A. Viaud-Martinez, S. Vrieze, D. E. Weeks, B. S. Weir, S. T. Weiss, L. C. Weng, C. J. Willer, Y. Zhang, X. Zhao, D. K. Arnett, A. E. Ashley-Koch, K. C. Barnes, E. Boerwinkle, S. Gabriel, R. Gibbs, K. M. Rice, S. S. Rich, E. K. Silverman, P. Qasba, W. Gan, N. T.-O. f. P. M. Consortium, G. J. Papanicolaou, D. A. Nickerson, S. R. Browning, M. C. Zody, S. Zollner, J. G. Wilson, L. A. Cupples, C. C. Laurie, C. E. Jaquish, R. D. Hernandez, T. D. O'Connor, G. R. Abecasis, Sequencing of 53,831 diverse genomes from the NHLBI TOPMed Program. *Nature* **590**, 290-299 (2021).

72. A. C. Y. Mak, S. Sajuthi, J. Joo, S. Xiao, P. M. Sleiman, M. J. White, E. Y. Lee, B. Saef, D. Hu, H. Gui, K. L. Keys, F. Lurmann, D. Jain, G. Abecasis, H. M. Kang, D. A. Nickerson, S. Germer, M. C. Zody, L. Winterkorn, C. Reeves, S. Huntsman, C. Eng, S. Salazar, S. S. Oh, F. D. Gilliland, Z. Chen, R. Kumar, F. D. Martinez, A. C. Wu, E. Ziv, H. Hakonarson, B. E. Himes, L. K. Williams, M. A. Seibold, E. G. Burchard, Lung Function in African American Children with Asthma Is Associated with Novel Regulatory Variants of the KIT Ligand KITLG/SCF and Gene-By-Air-Pollution Interaction. *Genetics* **215**, 869-886 (2020).

73. E. Y. Lee, A. C. Y. Mak, D. Hu, S. Sajuthi, M. J. White, K. L. Keys, W. Eckalbar, L. Bonser, S. Huntsman, C. Urbanek, C. Eng, D. Jain, G. Abecasis, H. M. Kang, S. Germer, M. C. Zody, D. A. Nickerson, D. Erle, E. Ziv, J. Rodriguez-Santana, M. A. Seibold, E. G. Burchard, Whole-Genome Sequencing Identifies Novel Functional Loci Associated with Lung Function in Puerto Rican Youth. *Am J Respir Crit Care Med* **202**, 962-972 (2020).

74. C. J. Willer, Y. Li, G. R. Abecasis, METAL: fast and efficient meta-analysis of genomewide association scans. *Bioinformatics* **26**, 2190-2191 (2010).

75. G. T. Consortium, The GTEx Consortium atlas of genetic regulatory effects across human tissues. *Science* **369**, 1318-1330 (2020).

Acknowledgments

We wish to acknowledge the following GALA II and SAGE study collaborators: S. Thyne, UCSF; H. J. Farber, Texas Children's Hospital; D. Serebrisky, Jacobi Medical Center; R. Kumar, Lurie Children's Hospital of Chicago; E. Brigino-Buenaventura, Kaiser Permanente; M. A. LeNoir, Bay Area Pediatrics; K. Meade, UCSF Benioff Children's Hospital, Oakland; W. Rodríguez-Cintrón, VA Hospital, Puerto Rico; P. C. Ávila, Northwestern University; J. R. Rodríguez-Santana, Centro de Neumología Pediátrica; L. N. Borrell, City University of New York; A. Davis, UCSF Benioff Children's Hospital, Oakland; and S. Sen, University of Tennessee. We acknowledge the families and patients for the participation and thank the numerous health care providers and community clinics for the support and participation in GALA II and SAGE. In particular, we thank the recruiters who obtained the data: D. Alva, G. Ayala-Rodríguez, L. Caine, E. Castellanos, J. Colón, D. DeJesus, B. López, B. López, L. Martos, V. Medina, J. Olivo, M. Peralta, E. Pomares, J. Quraishi, J. Rodríguez, S. Saeedi, D. Soto, and A. Taveras. We thank D.A. Nickerson from the University of Washington Northwest Genomics Center, and S. Germer, M.C. Zody, and L.W. and C. Reeves from the New York Genome Center for whole genome sequencing. We thank G. Abecasis and H. M. Kang from the TOPMed Informatics Research Center for whole-genome sequencing data quality control and processing. We thank the Institute of Human Genetics (UCSF, San Francisco, CA) including C. Chu, C. Julian, and E. Wan for single cell RNA sequencing. We thank I. Mellman (Genentech, South San Francisco, CA) for MHCII$^{K>R}$ mice. We thank A.K. Proebstel (UCSF, San Francisco, CA) for technical assistance with EAE experiments. We thank M. Fassett, K.M. Ansel, D. Shepard, and A. Ma (UCSF, San Francisco, CA) for helpful discussion. We dedicate this work to the memory of X. Huang (UCSF, San Francisco, CA), who passed away during the study. We acknowledge

the studies and participants who provided biological samples and data for TOPMed. **Funding:** This work was supported by Sandler Asthma Basic Research Center (J.-S.S), NIH (R01GM105800 and R35GM131702 to J-S.S.; R01HL117004, X01HL134589, and R01MD010443 to E.G.B.), DoD (W81XWH1810110 to J.-S.S.), the American Association of Immunologists (Careers in Immunology Fellowship to J.-S.S. and C.A.C.), the UCSF Biomedical Sciences (BMS) graduate program (to C.A.C) and the IMSD program funded by NIH (to C.A.C). The GALA II Study, SAGE, and E.G.B. were supported by the Sandler Family Foundation; the American Asthma Foundation; the RWJF Amos Medical Faculty Development Program; the Harry Wm. and Diana V. Hind Distinguished Professor in Pharmaceutical Sciences II; the National Heart, Lung, and Blood Institute (NHLBI): R01HL117004, X01HL134589; the National Institute on Minority Health and Health Disparities (NIMHD) (R01MD010443). Whole-genome sequencing for the TOPMed program was supported by the National Heart, Lung, and Blood Institute (NHLBI). Whole-genome sequencing for "NHLBI TOPMed: Gene-Environment, Admixture and Latino Asthmatics Study" (phs000920) and "NHLBI TOPMed: Study of African Americans, Asthma, Genes and Environments" (phs000921) was performed at the New York Genome Center (3R01HL117004-02S3) and the University of Washington Northwest Genomics Center (HHSN268201600032I). Centralized read mapping and genotype calling, along with variant quality metrics and filtering were provided by the TOPMed Informatics Research Center (3R01HL-117626-02S1; contract HHSN268201800002I). Phenotype harmonization, data management, sample-identity QC, and general study coordination were provided by the TOPMed Data Coordinating Center (3R01HL-120393-02S1; contract HHSN268201800001I). Whole-genome sequencing of part of GALA II was performed by the New York Genome Center under The Centers for Common Disease Genomics of the Genome

Sequencing Program (GSP) grant (UM1 HG008901). The GSP Coordinating Center (U24 HG008956) contributed to cross-program scientific initiatives and provided logistical and general study coordination. GSP is funded by the National Human Genome Research Institute, the National Heart, Lung, and Blood Institute, and the National Eye Institute. The content is solely the responsibility of the authors and does not necessarily represent the official views of the NIH. **Author contributions:** C.A.C and J.-S.S. conceived the study, designed the experiments, interpreted the data, and wrote the manuscript. C.A.C. performed and analyzed most experiments. X.R. and X.H. performed AHR and PAS staining experiments. S.L.G. performed EAE experiments. H.K.L. maintained and genotyped mice and provided retroviral vector cloning. A.W.S. provided single cell transcriptomics analysis and advice. H.-E.L. and R.M.L. contributed to worm infection experiments. B.J.L. and J.G.C. contributed to influenza infection experiments. D.H., A.C.Y.M., C.E., J.R.R.-S., M.L., Q.Y., J.C.C., and E.G.B. performed whole-genome sequencing sample preparations, combined GWAS meta-analysis, and eQTL analysis, and provided advice. S.S.Z. contributed to EAE experiments. S.I., J.G.C. and R.M.L. contributed critical reagents. All authors read and critiqued the study. **Competing interests:** R.M.L. is a member of the Scientific Advisory Board at Genentech. The authors declare that they have no competing interests. **Data and materials availability:** The GEO accession number for single-cell RNA sequencing data is GSE183861. All other data needed to evaluate the conclusions in the paper are present in the paper or the Supplementary Materials. MHCII (K>R) mice are available from J.-S.S. under a material transfer agreement with Genentech.

List of Supplementary Files

Data file S2.1. Sensitivity analysis on the top ten associations from the trans-ethnic meta-analysis.

Data file S2.2. This file contains data extracted from publicly available asthma genome-wide association studies (GWAS) summary statistics from Pan-UK Biobank.

Data file S2.3. Three genetic variants with alternative alleles associated with lower asthma risk were also associated with lower MARCH1 expression in multiple tissues in GTEx.

Figures

Fig. 2.1. MARCH1 is required for the development of T_H2 cell immunity and experimental asthma.

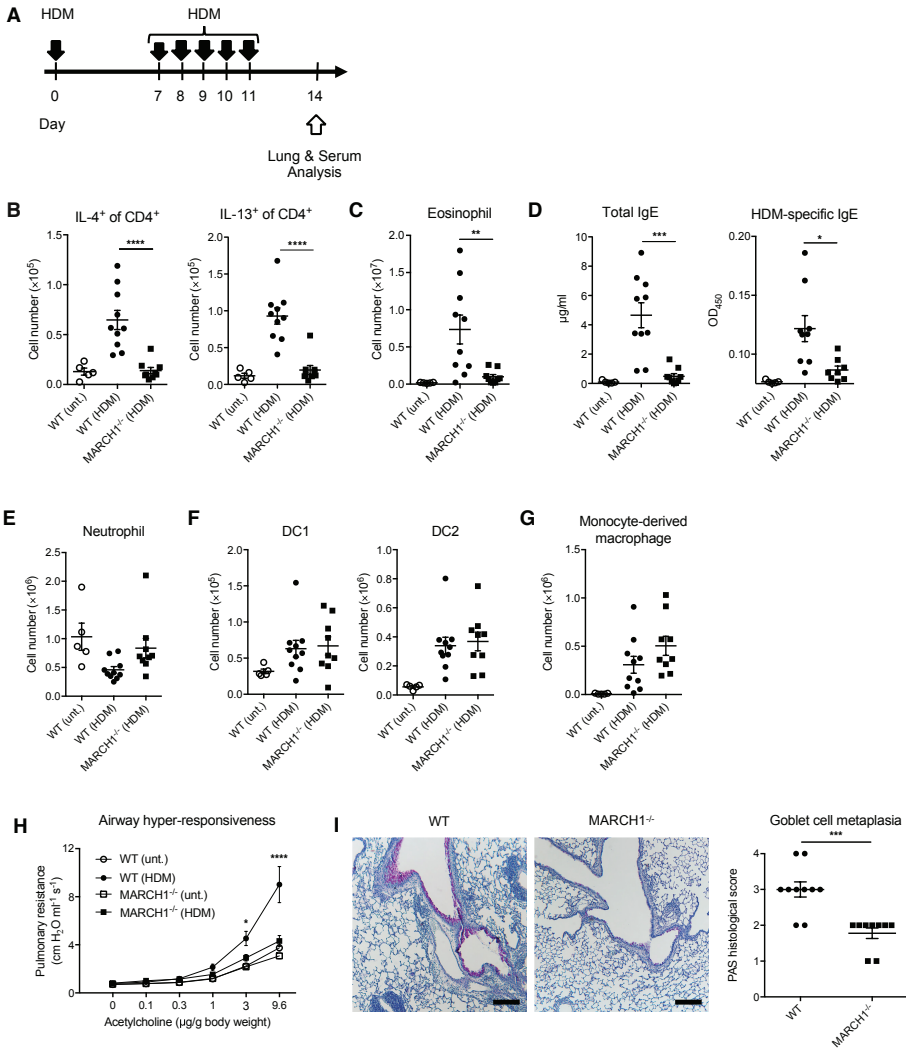

(A) Experimental outline of HDM extract challenge. Solid black arrows indicate oropharyngeal aspiration of 10 µg of HDM. **(B)** Total numbers of IL-4 or IL-13 competent $CD4^+$ T cells in lungs of WT or MARCH1$^{-/-}$ mice untreated or treated with HDM. **(C)** Total numbers of eosinophils in lungs. **(D)** Serological IgE titers and OD values for HDM-specific IgE antibodies as determined by ELISA. **(E** to **G)** Total numbers of neutrophils **(E)**, DC1 or DC2 **(F)**, and monocyte-derived macrophages **(G)** in lungs. Data in **(B** to **G)** are pooled from two independent experiments with each experiment having four to five mice of each genotype administered with HDM and two to three untreated control mice. **(H)** Pulmonary resistance to acetylcholine. **(I)** Representative images of PAS-stained lung sections (magnification, ×5; scale bars, 200µm) and scoring of the stain. Data in **(H** and **I)** are obtained from one experiment with 7 to 10 mice of each genotype for every condition. Data are shown as means ± SEM. Statistical significance was determined by one-way ANOVA with Tukey's multiple comparisons test **(B** to **D)**, two-way ANOVA with Tukey's multiple comparisons test **(H)**, or unpaired Student's *t*-test **(I)**. **P*<0.05; ***P*<0.01; ****P*<0.001; *****P*<0.0001.

Fig. 2.2. The role of MARCH1 in promoting T_H2 cell immunity depends on its expression by DCs.

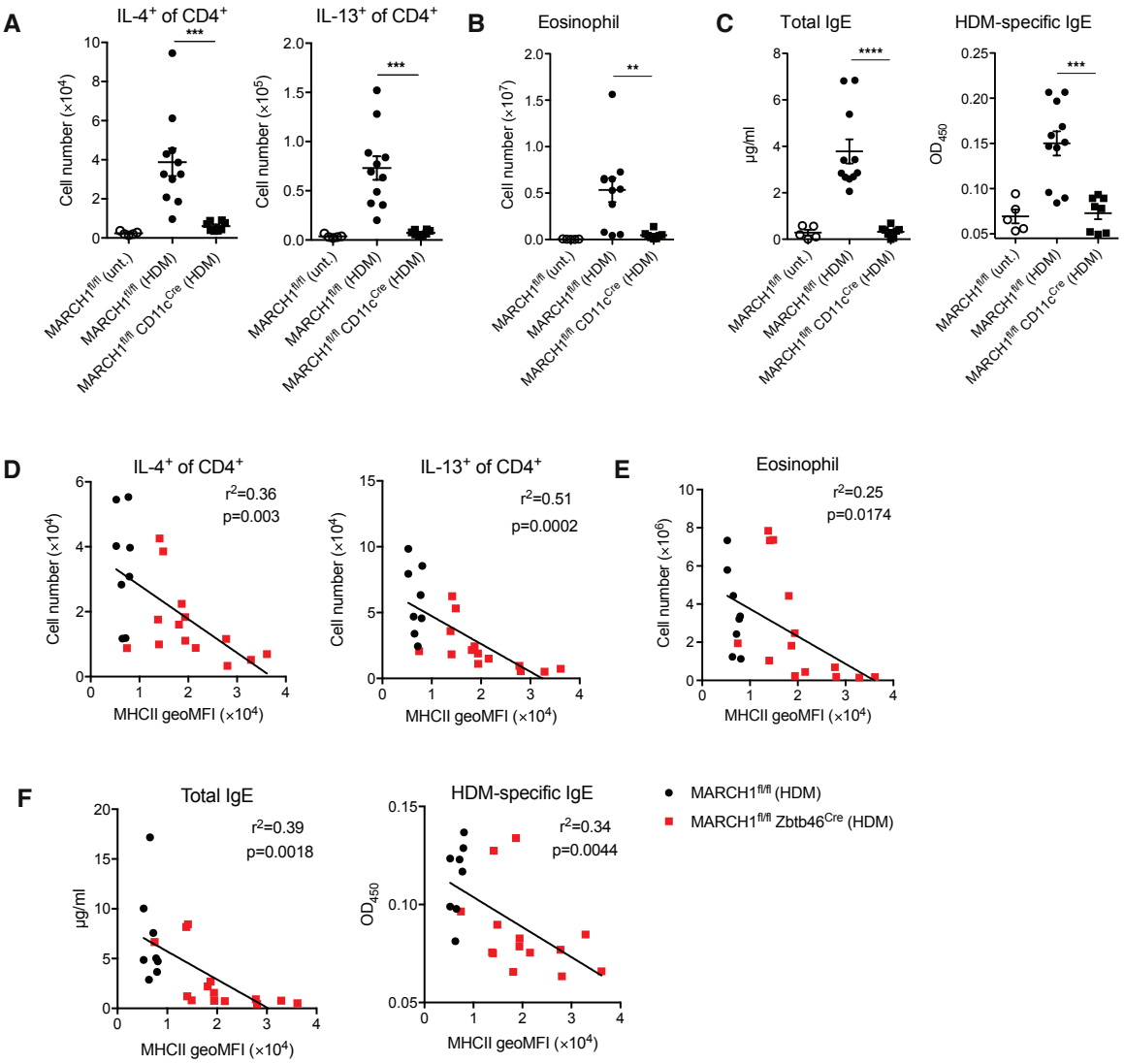

(A) Total numbers of IL-4 or IL-13 competent $CD4^+$ T cells in lungs of $MARCH1^{fl/fl}$ or $MARCH1^{fl/fl}$ CD11cCre mice untreated or treated with HDM. **(B)** Total numbers of eosinophils in lungs. **(C)** Serological IgE titers and OD values for HDM-specific IgE antibodies as determined by ELISA. Data in **(A** to **C)**, are pooled from two independent experiments with three to six mice administered with HDM and two to three untreated control mice. Data are shown as means ± SEM. Statistical significance was determined by one-way ANOVA with Tukey's multiple comparisons test. $^{**}P<0.01$; $^{***}P<0.001$; $^{****}P<0.0001$. **(D** to **F)** Total numbers of IL-4 or IL-13 competent $CD4^+$ T cells **(D)**, eosinophils **(E)**, and serological IgE titers and HDM-specific IgE antibodies **(F)** in $MARCH1^{fl/fl}$ or $MARCH1^{fl/fl}$ $Zbtb46^{Cre}$ mice treated with HDM. Data are shown in relation to the surface expression of MHCII [geometric mean fluorescence intensity (geoMFI)] in lung DC1 (gated as shown in fig. S2.1). Data in **(D** to **F)** are pooled from two independent experiments with each experiment having four to seven mice administered with HDM. Data in **(D** to **F)** are shown with statistical r^2 values, *P*-values, and trend lines determined from linear regression analysis.

Fig. 2.3: MARCH1 promotes T_H2 cell development through LN-resident DCs.

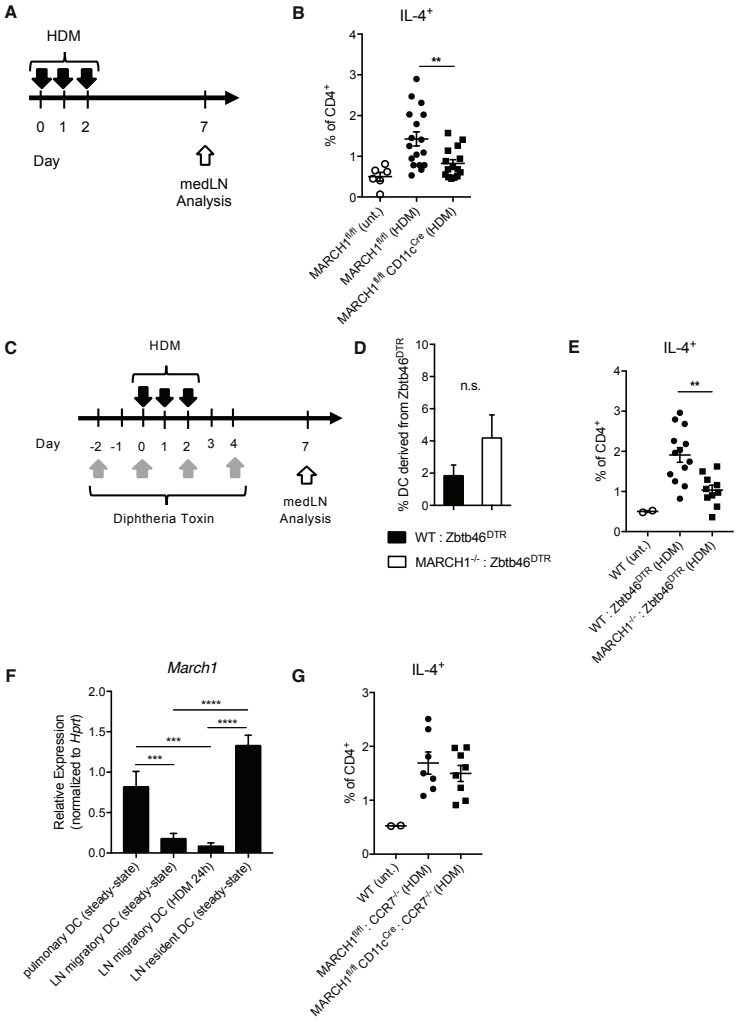

(A) Experimental outline of HDM administration. Solid black arrows indicate oropharyngeal aspiration of 10 μg of HDM. **(B)** Percentage of IL-4 competent $CD4^+$ T cells in medLNs of $MARCH1^{fl/fl}$ and $MARCH1^{fl/fl}$ $CD11c^{Cre}$ mice. Untreated mice were used as negative controls. Data are pooled from three independent experiments with each experiment having five to six mice per treated group. **(C)** Experimental outline of DT and HDM treatment for WT:$Zbtb46^{DTR}$ or $MARCH1^{-/-}$:$Zbtb46^{DTR}$ mixed BM chimeric mice. **(D)** Percentage of DCs in the medLN derived from the $Zbtb46^{DTR}$ BM after DT treatment of WT:$Zbtb46^{DTR}$ or $MARCH1^{-/-}$:$Zbtb46^{DTR}$ mixed BM chimeric mice. Not significant (n.s.), $P>0.1$. **(E)** Percentage of IL-4 competent $CD4^+$ T cells in medLNs of WT:$Zbtb46^{DTR}$ or $MARCH1^{-/-}$:$Zbtb46^{DTR}$ mixed BM chimeric mice after diphtheria toxin (DT) and HDM treatment. Untreated mice were used as negative controls. Data are from one experiment with 10 to 12 mice per treated group. **(F)** *March1* mRNA levels in FACS-purified pulmonary or medLN DCs normalized to the levels of *Hprt* housekeeping gene. Each bar represents at least three measurements. **(G)** Percentage of IL-4 competent $CD4^+$ T cells in medLNs of $MARCH1^{fl/fl}$:$CCR7^{-/-}$ or $MARCH1^{fl/fl}$ CD11cCre:$CCR7^{-/-}$ mixed BM chimeric mice. Untreated mice were used as negative controls. Data are from one experiment with seven to eight mice per treated group. Data are shown as means ± SEM. Statistical significance was determined by one-way ANOVA with Tukey's multiple comparisons test (**B** and **E** to **G**) or unpaired Student's *t*-test. $^{**}P<0.01$; $^{***}P<0.001$; $^{****}P<0.0001$.

Fig. 2.4. MARCH1 expression in LN-resident DCs promotes up-regulation of GATA-3 and down-regulation of T-bet in developing T_H2 cells.

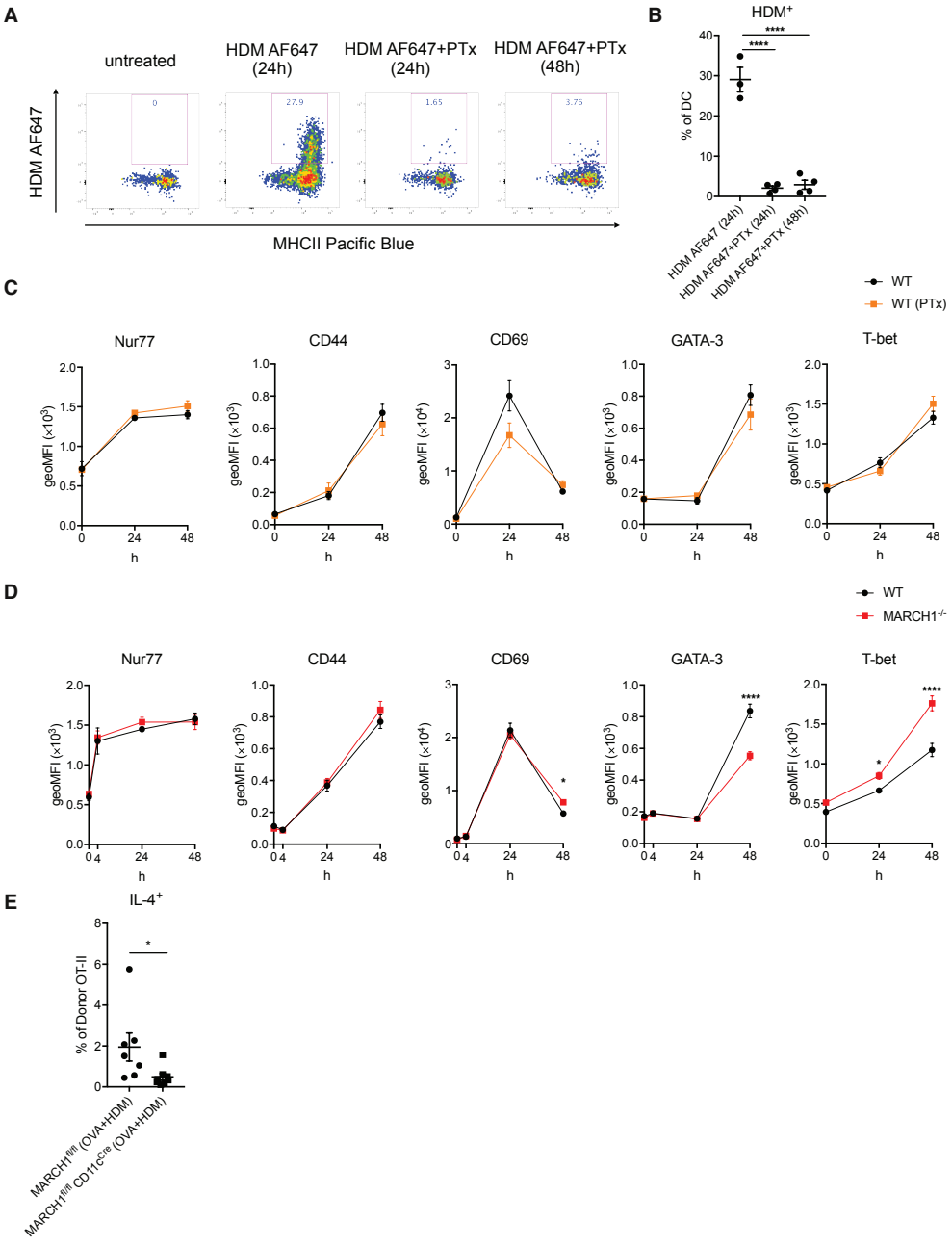

(A and **B)** WT mice were oropharyngeally administered with HDM conjugated to Alexa Fluor 647 (HDM AF647) alone or together with PTx. medLNs were isolated 24 or 48 hours later, and the frequency of HDM^+ DCs was determined by flow cytometry. A WT mouse remained untreated for gating purposes. Representative flow cytometry plots **(A)** and percentages of medLN DCs bearing HDM (**B)** are shown. Data are from one experiment with three to four mice per group. **(C)** Expression kinetics of CD69, CD44, Nur77, GATA-3, or T-bet in adoptively transferred OT-II cells. Mice that had received OT-II $CD4^+$ T cells were oropharyngeally administered with the mixture of HDM and OVA alone or together with PTx. medLNs were isolated, and the expression of designated molecules in OT-II $CD4^+$ T cells was determined by

geometric mean fluorescence intensity (geoMFI). Data are from two independent experiments with each experiment having two to five mice at each time point per group. **(D)** Expression kinetics of CD69, CD44, Nur77, GATA-3, or T-bet in adoptively transferred OT-II cells. WT or MARCH1$^{-/-}$ mice that had received OT-II CD4^{+} T cells were oropharyngeally administered with the mixture of HDM and OVA. medLNs were isolated, and the expression of designated molecules in OT-II CD4^{+} T cells was determined by geoMFI. Data are from three independent experiments with each experiment having three to five mice at each time point per group. **(E)** Percentages of IL-4 competent OT-II T cells in the medLNs. MARCH1$^{fl/fl}$ or MARCH1$^{fl/fl}$ CD11c^{Cre} mice that had received OT-II CD4^{+} T cells were oropharyngeally administered with the mixture of HDM and OVA. medLNs were isolated on day 7, and the frequency of IL-4 competent OT-II T cells was determined. Data are from one experiment with seven to eight recipient mice per group. Data are shown as means ± SEM. Statistical significance was determined by one-way ANOVA with Tukey's multiple comparisons test **(B)**, two-way ANOVA with Fisher's LSD test **(C** and **D)**, or unpaired Student's *t*-test **(E)**. **P*<0.05; *****P*<0.0001.

Fig. 2.5. Ubiquitin-dependent turnover of MHCII and CD86 promotes up-regulation of GATA-3 and down-regulation of T-bet in developing T_H2 cells.

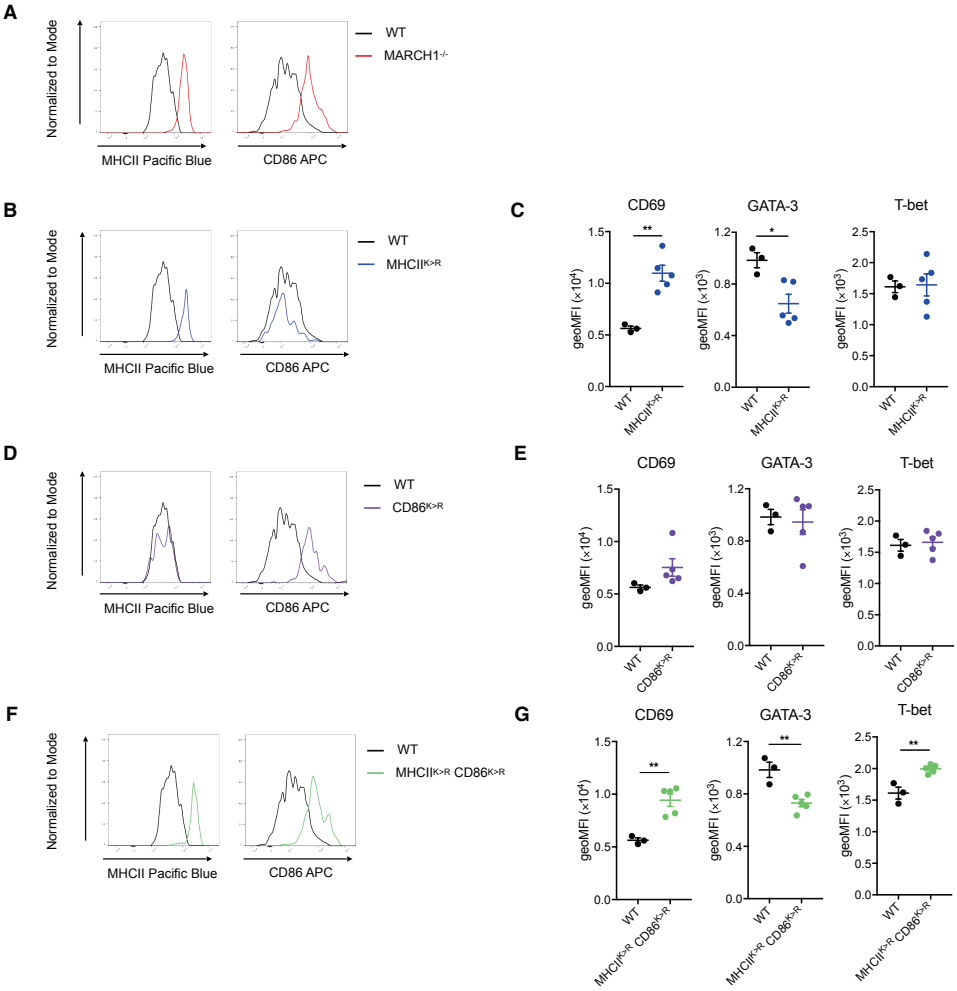

(A) Representative histograms showing MHCII and CD86 abundance on the surface of medLN resident DCs in a MARCH1$^{-/-}$ mouse in comparison to a WT mouse. **(B)** Representative histograms showing MHCII and CD86 abundance on the surface of medLN resident DCs in a MHCII$^{K>R}$ mouse in comparison to a WT mouse. **(C)** Expression level of CD69, GATA-3, or T-bet in adoptively transferred OT-II cells in medLN of WT or MHCII$^{K>R}$ mice at 48 hours after challenge with the mixture of HDM and OVA. **(D)** Representative histograms showing MHCII and CD86 abundance on the surface of medLN resident DCs in a CD86$^{K>R}$ mouse in comparison to a WT mouse. **(E)** Expression level of CD69, GATA-3, or T-bet in adoptively transferred OT-II cells in medLN of WT or CD86$^{K>R}$ mice at 48 hours after challenge with the mixture of HDM and OVA. **(F)** Representative histograms showing MHCII and CD86 abundance on the surface of medLN resident DCs in a MHCII$^{K>R}$CD86$^{K>R}$ mouse in comparison to a WT mouse. **(G)** Expression level of CD69, GATA-3, or T-bet in adoptively transferred OT-II cells in medLN of WT or MHCII$^{K>R}$CD86$^{K>R}$ mice at 48 hours after challenge with the mixture of HDM and OVA. Data in **(A**, **B**, **D**, and **F)** are obtained from one experiment with one mouse per genotype. Data in **(C**, **E**, and **G)** are obtained from one experiment with three to five mice per group. Data are shown as means ± SEM. Statistical significance was determined by unpaired Student's *t*-test. **P*<0.05; ***P*<0.01.

Fig. 2.6. Ubiquitination of MHCII and CD86 promotes T_H2 cell immune development in a cooperative fashion.

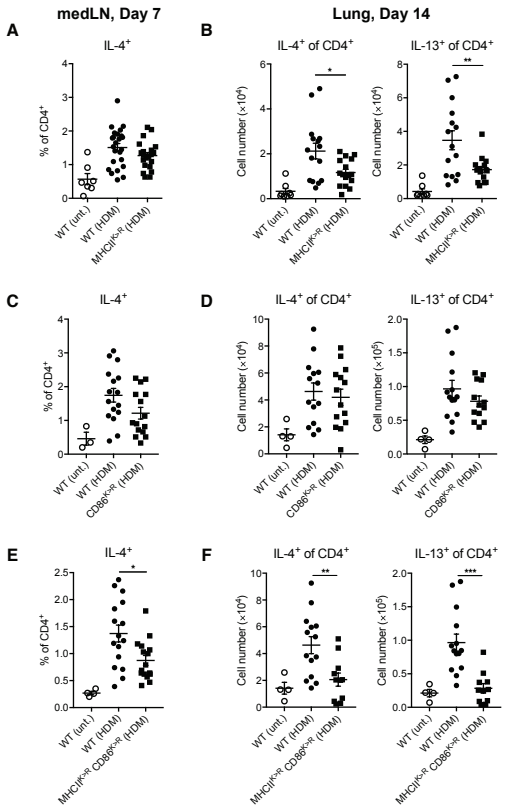

(A) Percentages of IL-4 competent $CD4^+$ T cells in medLNs of WT or $MHCII^{K>R}$ mice at day 7 after HDM challenge (experimental outline shown in Fig. 2.3A). Untreated mice were used as negative controls. Data are pooled from four independent experiments with each experiment having five to six mice per treated group. **(B)** Total numbers of IL-4 or IL-13 competent $CD4^+$ T cells in lungs of WT or $MHCII^{K>R}$ mice at day 14 after repetitive HDM challenge (experimental outline shown in Fig. 2.1A). Untreated mice were used as negative controls. Data are pooled from three independent experiments with each experiment having five to six mice per treated group. **(C)** Percentages of IL-4 competent $CD4^+$ T cells in medLNs of WT or $CD86^{K>R}$ mice after HDM challenge. Untreated mice were used as negative controls. Data are pooled from 2 independent experiments with each experiment having seven to eight mice per treated group. **(D)** Total numbers of IL-4 or IL-13 competent $CD4^+$ T cells in lungs of WT or $CD86^{K>R}$ mice at day 14 after repetitive HDM challenge. Untreated mice were used as negative controls. Data are pooled from two independent experiments with each experiment having six to eight mice per treated group. **(E)** Percentages of IL-4 competent $CD4^+$ T cells in medLNs of WT or $MHCII^{K>R}CD86^{K>R}$ mice at day 7 after HDM challenge. Untreated mice were used as negative controls. Data are pooled from two independent experiments with each experiment having eight mice per treated group. **(F)** Total numbers of IL-4 or IL-13 competent $CD4^+$ T cells in lungs of WT or $MHCII^{K>R}CD86^{K>R}$ mice at day 14 after repetitive HDM challenge. Untreated mice were used as negative controls. Data are pooled from two independent experiments with each experiment having four to seven mice per treated group. Data are shown as means ± SEM. Statistical significance was determined by one-way ANOVA with Tukey's multiple comparisons test. *P<0.05; **P<0.01; ***P<0.001.

Supplementary Figures

Fig. S2.1. Flow cytometry gating strategy.

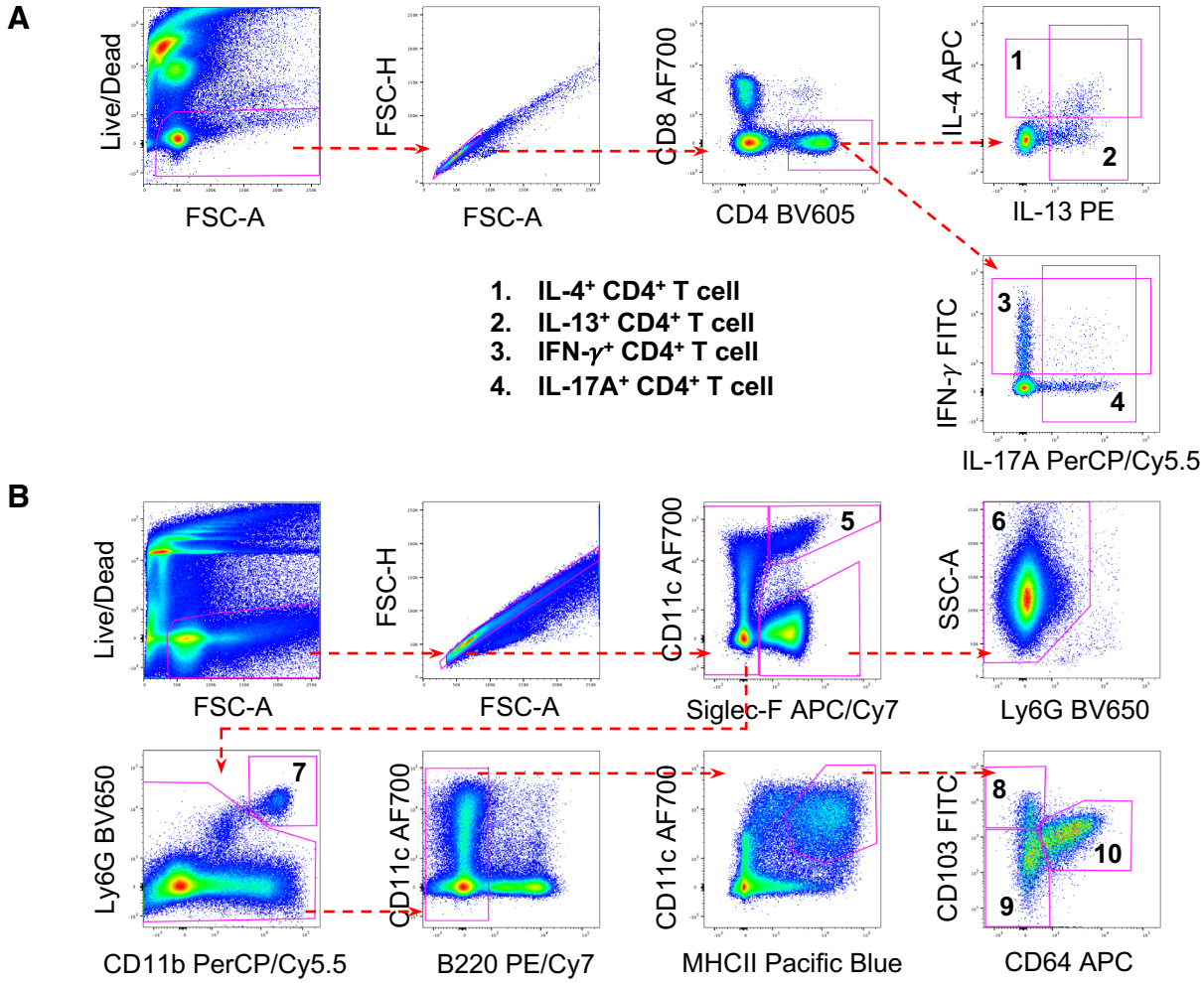

(A and **B)** Gating strategy to determine cytokine competent $CD4^+$ T cells **(A)** and myeloid cells **(B)** in the lungs. Numbers (1-10) refer to the cell populations labelled on the plots.

Fig. S2.2. MARCH1 is required for the development of T_H2 cell immunity to *Aspergillus fumigatus* extract and parasitic worms.

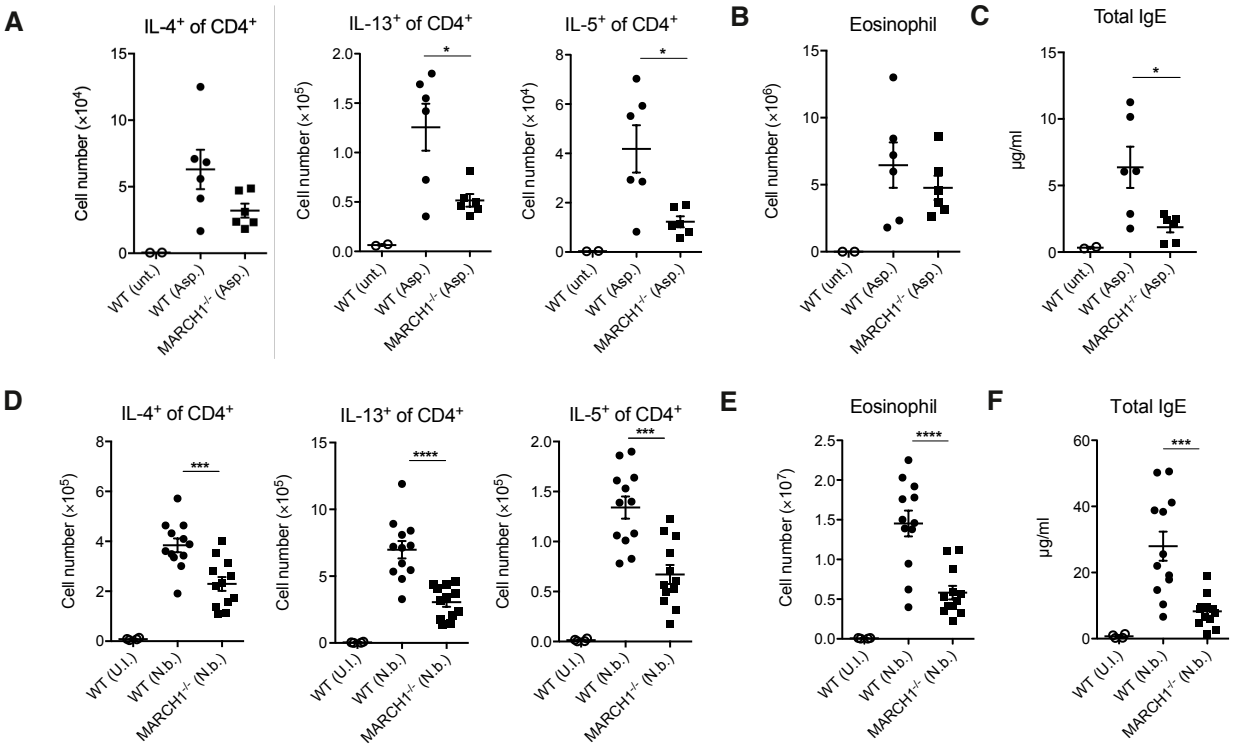

(A to **C)** WT and MARCH1$^{-/-}$ mice were given oropharyngeal cellular extract of *Aspergillus fumigatus* (Asp.) on days 0, 7, 8, 9, and 10 and analyzed at day 13. Total numbers of IL-4, IL-13, or IL-5 competent CD4$^+$ T cells **(A)** and eosinophils **(B)** in lungs were determined by flow cytometry. Serum IgE titers **(C)** were determined by ELISA. Untreated mice were used as negative controls. Data in **(A** to **C)** are from one experiment with six mice per Asp.-treated group. **(D** to **F)** WT and MARCH1$^{-/-}$ mice were infected with 500 L3 *Nippostrongylus brasiliensis* (N.b.) larvae and analyzed at day 13 after infection. Total numbers of IL-4, IL-13, or IL-5 competent CD4$^+$ T cells **(D)** and eosinophils **(E)** in lungs were determined by flow cytometry. Serum IgE titers **(F)** were determined by ELISA. Uninfected mice were used as negative controls. Data in **(D** to **F)** are pooled from two independent experiments with six mice per N.b.-infected group. Data are shown as means ± SEM. Statistical significance was determined by one-way ANOVA with Tukey's multiple comparisons test. **P*<0.05; ****P*<0.001; *****P*<0.0001.

Fig. S2.3. MARCH1 is dispensable for the development of T_H1, T_H17, or cytotoxic $CD8^+$ T cell immunity to influenza virus or autoimmune self-antigen.

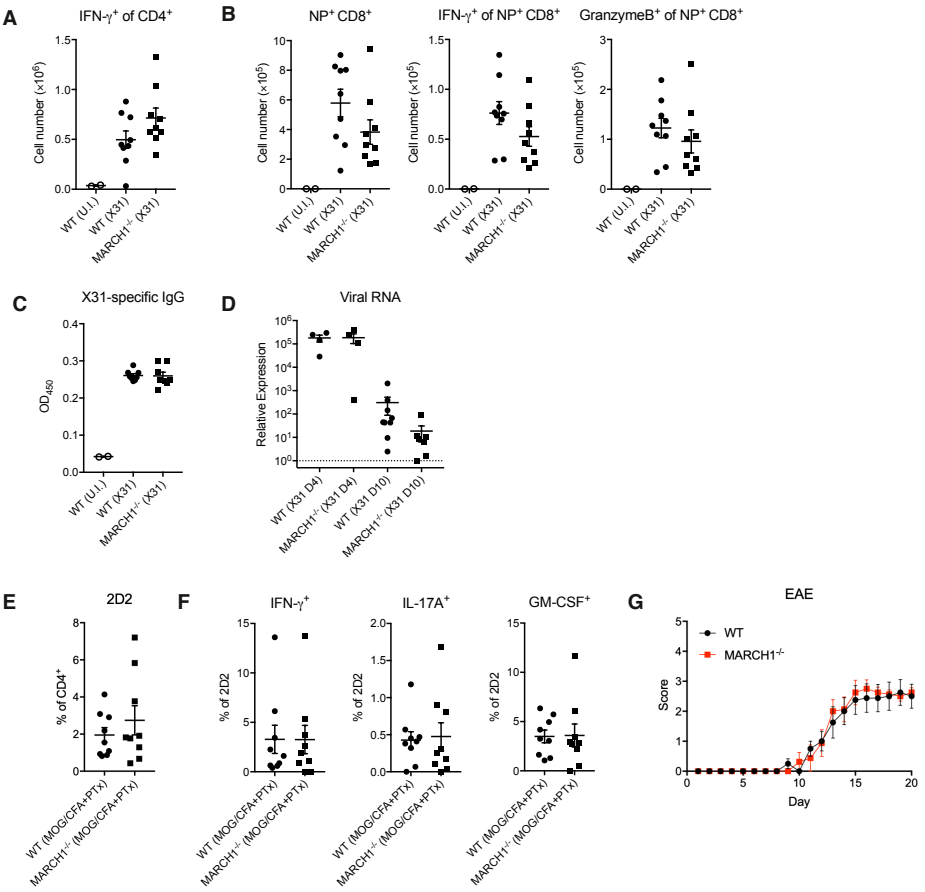

(A) Total numbers of IFN-γ competent $CD4^+$ T cells in lungs of WT or MARCH1$^{-/-}$ mice uninfected or infected with 1×10^5 TCID50 of X31 influenza virus. **(B)** Total numbers of $CD8^+$ T cells specific for X31 nucleoprotein$_{366\text{-}374}$ (NP) and the numbers of IFN-γ or Granzyme B competent NP-specific $CD8^+$ T cells in lungs. **(C)** OD values for X31-specific IgG antibodies as determined by ELISA. Data in **(A** to **C)** are obtained from one experiment with nine mice of each genotype infected with X31 and two uninfected control mice. **(D)** Abundance of viral RNA in the lungs. RNA that encodes viral PA protein was quantitated by qRT-PCR at day 4 or 10 after infection. Values were normalized to the mouse with the least viral burden. Data are obtained from one experiment with four mice of each genotype at day 4 and seven to nine mice of each genotype at day 10. **(E)** Frequency of adoptively-transferred myelin oligodendrocyte glycoprotein (MOG)-specific 2D2 TCR transgenic T cells in the inguinal lymph node at day 6 after subcutaneous injection of 100 μg MOG$_{35\text{-}55}$ peptide emulsified in CFA. Mice were also injected with 200 ng of PTx on day 0 and 2. Data are obtained from one experiment with eight mice of each genotype. **(F)** Frequency of IFN-γ, IL-17A, or GM-CSF competent 2D2 T cells. Data are obtained from one experiment with eight mice of each genotype. **(G)** Clinical scores of experimental autoimmune encephalomyelitis (EAE) development in WT or MARCH1$^{-/-}$ mice. Data are obtained from one experiment with 10 mice of each genotype. Data are shown as means ± SEM. Statistical significance was not determined by one-way ANOVA with Tukey's multiple comparisons test **(A** to **D)**, unpaired Student's *t*-test **(E** and **F)** or two-way ANOVA with Fisher's LSD test **(G)**.

Fig. S2.4. MARCH1 deletion efficiency in MARCH1$^{fl/fl}$ Zbtb46^{Cre} mice.

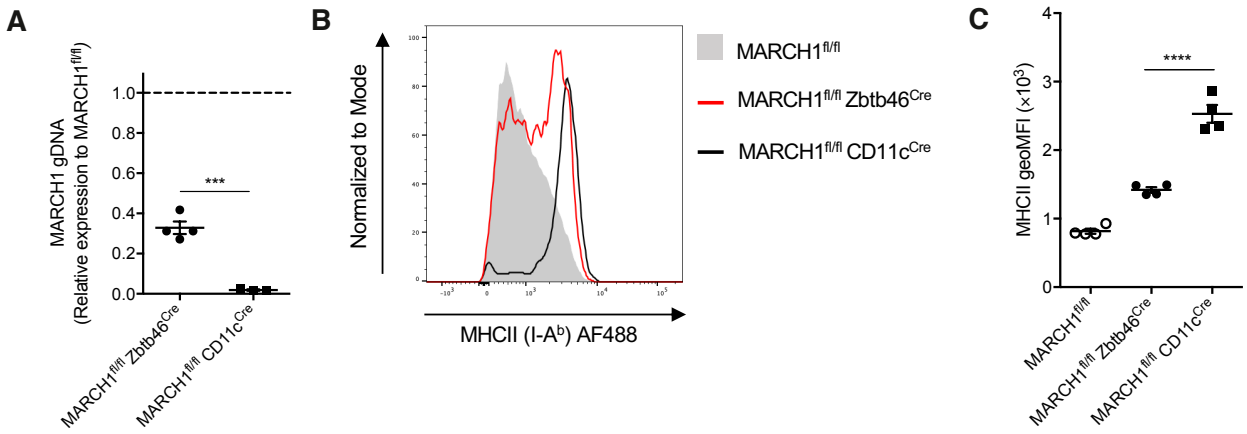

(A) Quantification of the genomic DNA encoding MARCH1 loxp site in DCs isolated from spleens of MARCH1$^{fl/fl}$, MARCH1$^{fl/fl}$ Zbtb46^{Cre}, and MARCH1$^{fl/fl}$ CD11c^{Cre} mice. Data are presented relative to the amount of the genomic DNA detected in MARCH1$^{fl/fl}$ DCs. Data in **(A)** are from one experiment with three to four mice per group. **(B** and **C)** Representative histograms showing the MHCII surface expression in splenic DCs **(B)** and quantification of MHCII surface expression **(C)** by geometric mean fluorescence intensity (geoMFI). Data in **(B** and **C)** are pooled from two experiments with each experiment having two mice of each genotype. Data are shown as means ± SEM. Statistical significance was determined by Student's *t*-test **(A)** or one-way ANOVA with Tukey's multiple comparisons test **(C)**. ***P<0.001; ****P<0.0001.

Fig. S2.5. MARCH1 expressed by macrophages, plasmacytoid DCs, or B cells does not play a significant role in T_H2 cell priming.

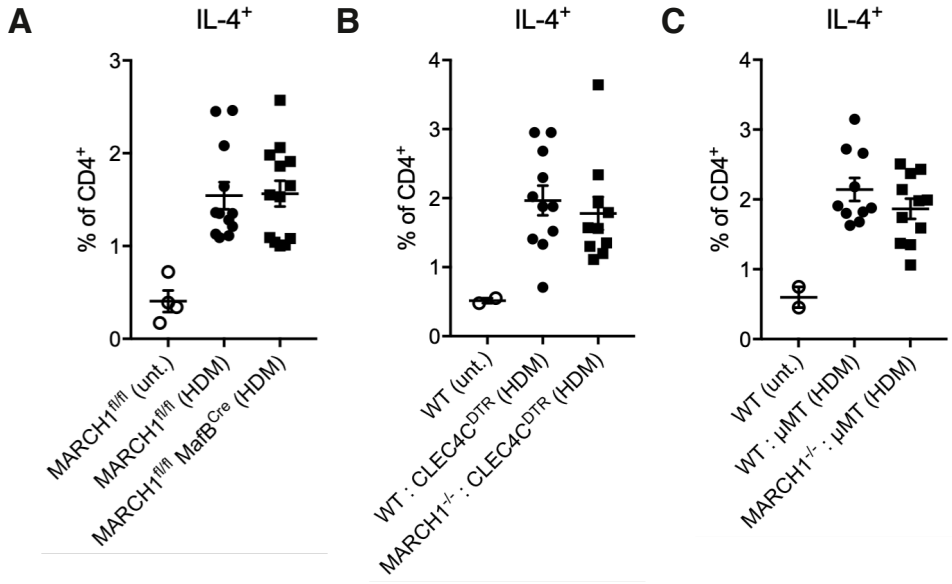

(A) Percentages of IL-4 competent $CD4^+$ T cells in medLNs of $MARCH1^{fl/fl}$ and $MARCH1^{fl/fl}$ MafBCre mice treated with HDM. Untreated mice were used as negative controls. Data are from two independent experiments with six to seven mice per group. **(B)** Percentages of IL-4 competent $CD4^+$ T cells in medLNs of WT:$CLEC4C^{DTR}$ or $MARCH1^{-/-}$:$CLEC4C^{DTR}$ BM chimeric mice treated with DT and HDM. Untreated mice. Data are from one experiment with 10 to 11 mice per treated group. **(C)** Percentage of IL-4 competent $CD4^+$ T cells in medLNs of WT:µMT or $MARCH1^{-/-}$:µMT mixed BM chimeric mice treated with HDM. Untreated mice were used negative controls. Data are from one experiment with 10 to 11 mice per HDM-treated group. Statistical significance was not determined by one-way ANOVA with Tukey's multiple comparisons test. Data are shown as means ± SEM.

Fig. S2.6. MARCH1 is dispensable for pulmonary DC homeostasis, capture of HDM allergen, migration to the draining lymph node, or transcriptional reprograming during migration.

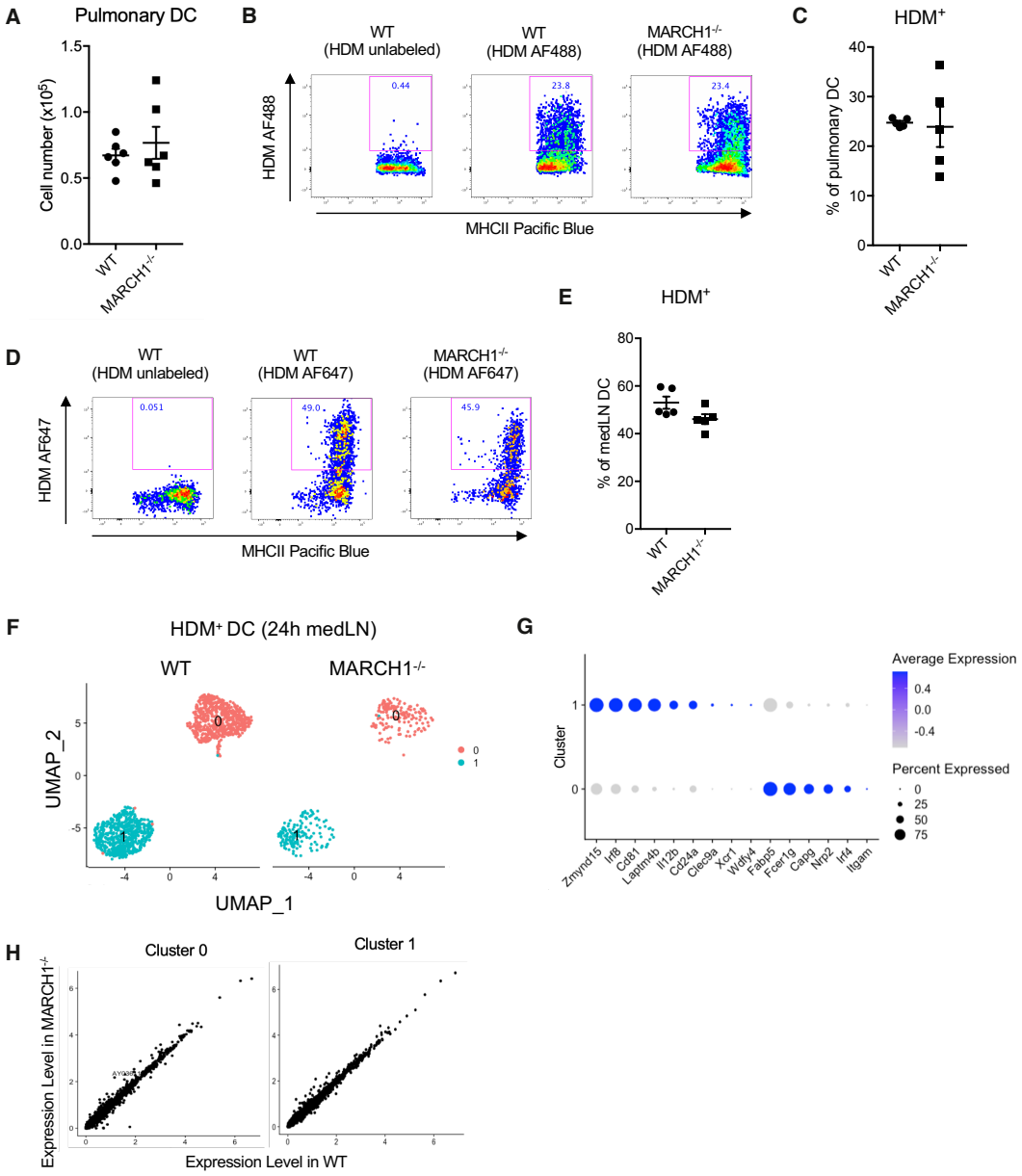

(A) Total numbers of lung DCs (SiglecF^{-}B220^{-}CD11c^{+}MHCII^{+}CD64^{-} cells) in naïve WT and MARCH1$^{-/-}$ mice. Data are pooled from two experiments with two to four mice per group. **(B** and **C)** WT and MARCH1$^{-/-}$ mice were treated with fluorescent HDM (HDM AF488) via oropharyngeal aspiration and 24 hours later, pulmonary DCs were analyzed by flow cytometry. A control mouse was treated with non-fluorescent HDM for gating purposes. Representative flow cytometry plots **(B)** and percentages of pulmonary DCs bearing fluorescent HDM **(C)** are shown. Data are from one experiment with five mice per group. **(D** and **E)** WT and MARCH1$^{-/-}$ mice were treated with fluorescent HDM (HDM AF647) via oropharyngeal aspiration and 24 hours later, medLN DCs were analyzed by flow cytometry. A control mouse was injected with

non-fluorescent HDM for gating purposes. Shown are representative flow cytometry plots **(D)** and percentages of medLN DCs bearing fluorescent HDM **(E)**. Data are from one experiment with five mice per group. Statistical significance was not determined by unpaired Student's *t*-test. Data are shown as means ± SEM. **(F** to **H)** CD45.1/.1 Zbtb46^{GFP} :CD45.2/.2 Zbtb46^{GFP} MARCH1$^{-/-}$ mixed BM chimeric mice were treated with fluorescent HDM (HDM AF647) by oropharyngeal aspiration. HDM^{+} DCs derived from WT or MARCH1$^{-/-}$ BM (CD45.1^{+}CD11c^{+}GFP^{+}AF647^{+} cells and CD45.2^{+}CD11c^{+}GFP^{+}AF647^{+} cells, respectively) were sorted from medLN 24 h later and analyzed by single-cell RNA sequencing. UMAP plots show clustering of 1227 WT and 217 MARCH1$^{-/-}$ DCs **(F)** and dot plots show average expression of various transcripts differentially expressed between the two clusters **(G)**. Scatter plots show average expression of individual genes in WT and MARCH1$^{-/-}$ DCs of each cluster **(H)**. Note that AY036118 is the only gene differently expressed between WT and MARCH1$^{-/-}$ DCs by more than 2-fold ($Log_2FC>1$ or $Log_2FC<-1$) with adjusted $P<0.05$. Data are from one experiment with cells pooled from 5 mice.

Fig. S2.7. FACS gating strategy for purifying pulmonary or medLN DC populations.

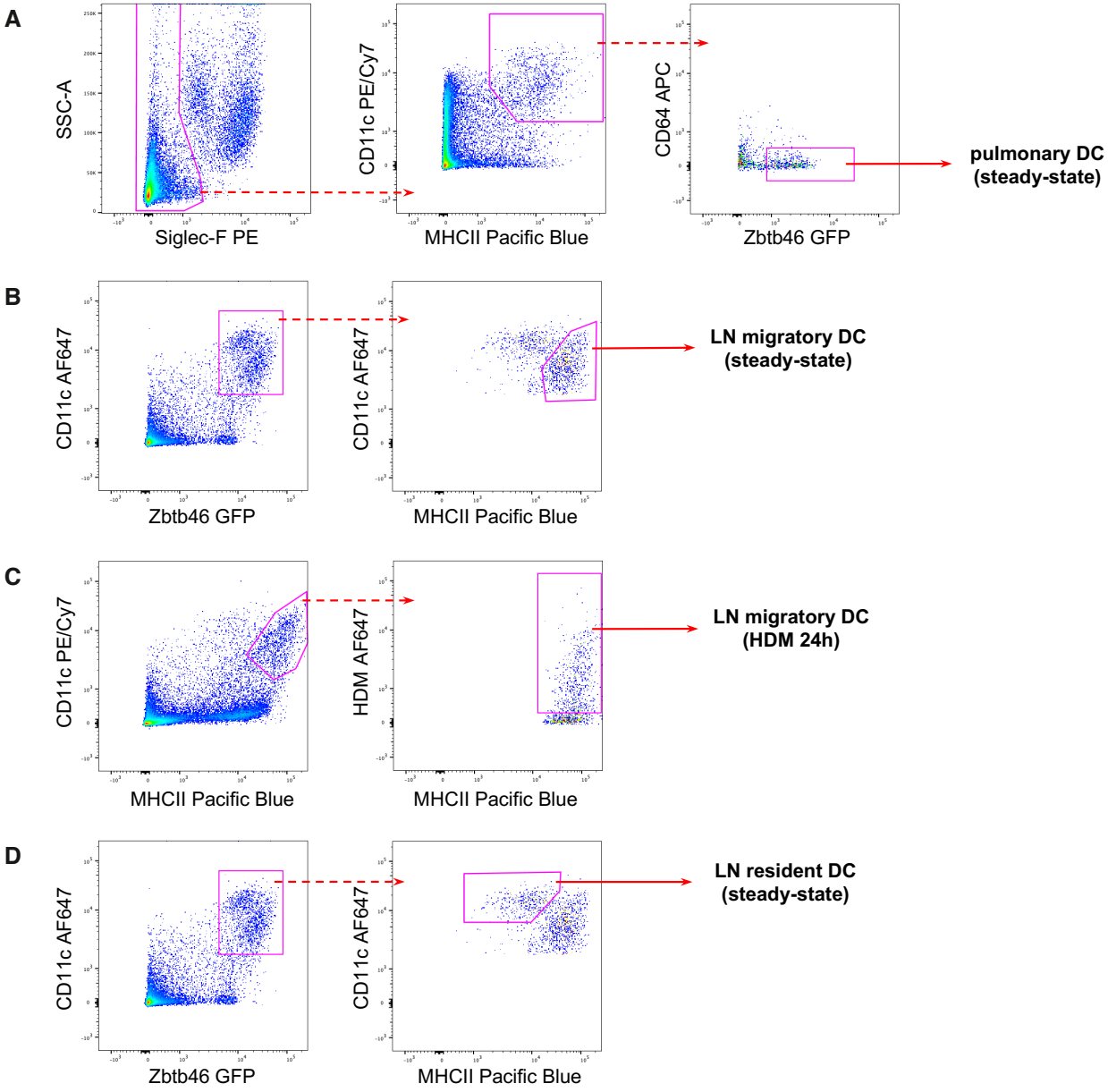

(A to **D)** Cell suspensions from lungs or medLNs were enriched for DCs by depleting B cells, T cells and neutrophils through negative selection using an EasySep magnet and then stained and sorted with a FACS Aria II. Flow cytometry plots show the gating strategies used for purifying pulmonary DCs at steady state **(A)**, LN migratory DCs at steady-state **(B)**, LN migratory DCs bearing fluorescent HDM at 24 hours after challenge **(C)**, or LN-resident DCs at steady state **(D)**. In some of the sorts, Zbtb46^{GFP} reporter mice were used to facilitate the discrimination and isolation of the DCs. The sorts are representative of three to 10 mice and approximately 10,000 DCs were sorted for each population to determine MARCH1 mRNA transcript level by quantitative real-time PCR.

Fig. S2.8. Gating of OT-II T cells and extent of expression of activation markers, GATA-3 and T-bet.

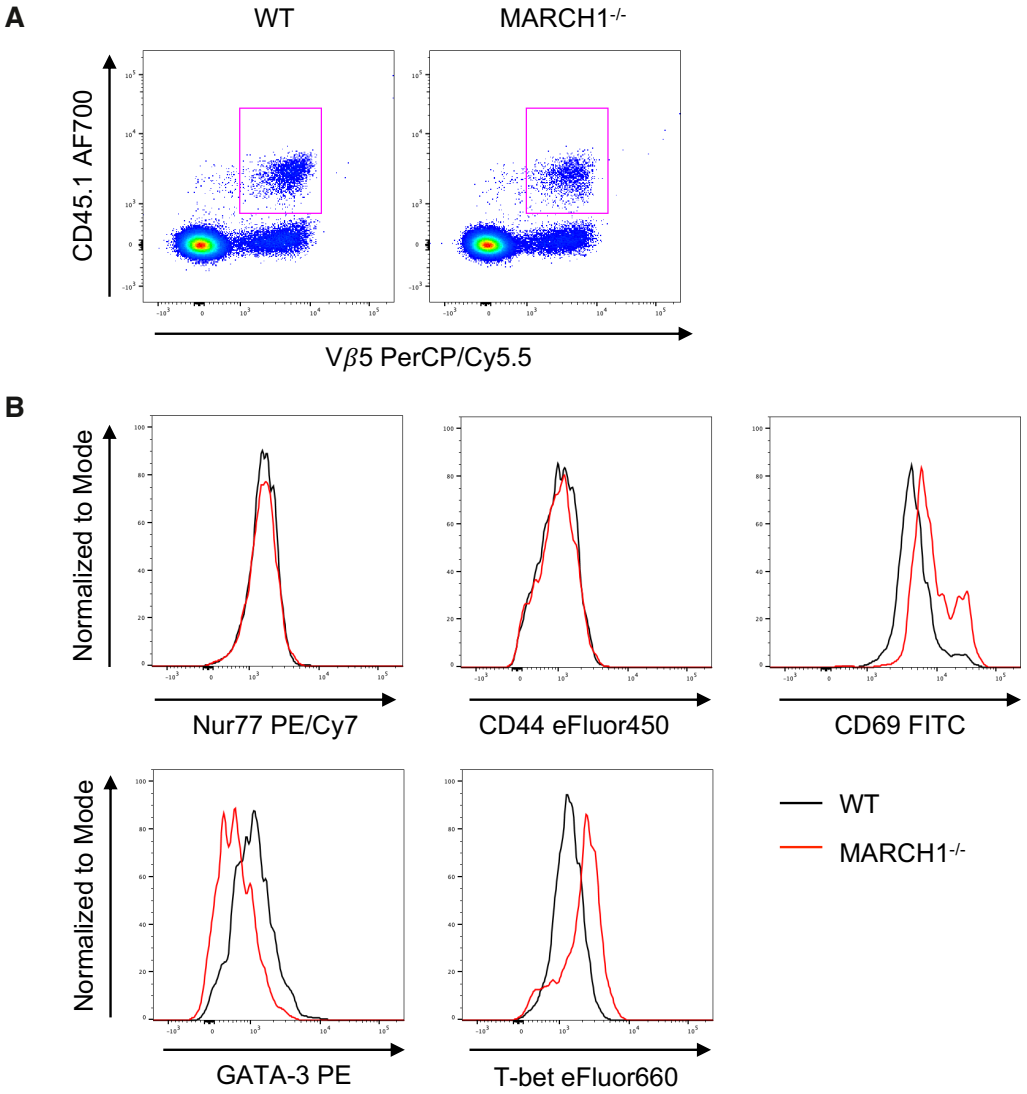

(A and **B)** Flow cytometry plots of $CD4^+$ T cells showing the gating of adoptively transferred OT-II cells **(A)** in the medLN of a WT or a $MARCH1^{-/-}$ mouse at 48 hours after HDM and OVA challenge and histograms showing the extent of expression of Nur77, CD44, CD69, GATA-3 or T-bet **(B)** in the adoptively transferred OT-II cells. Data are representative from 3 independent experiments with each experiment having three to five mice.

Fig. S2.9. Gating of LN-resident DCs.

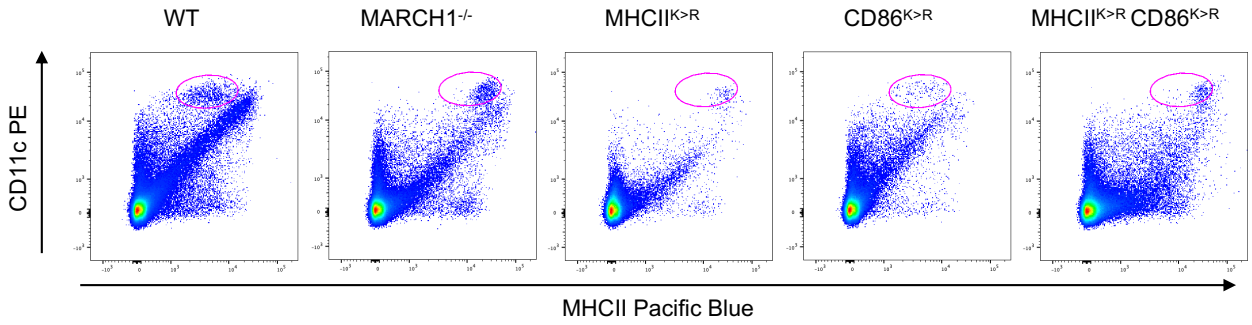

Flow cytometry plots (excluding $B220^+$ B cells) showing the gating of LN-resident DCs in the medLN of WT, $MARCH1^{-/-}$, $MHCII^{K>R}$, $CD86^{K>R}$ or $MHCII^{K>R}$ $CD86^{K>R}$ mice.

Fig. S2.10. MARCH1 facilitates MHCII turnover.

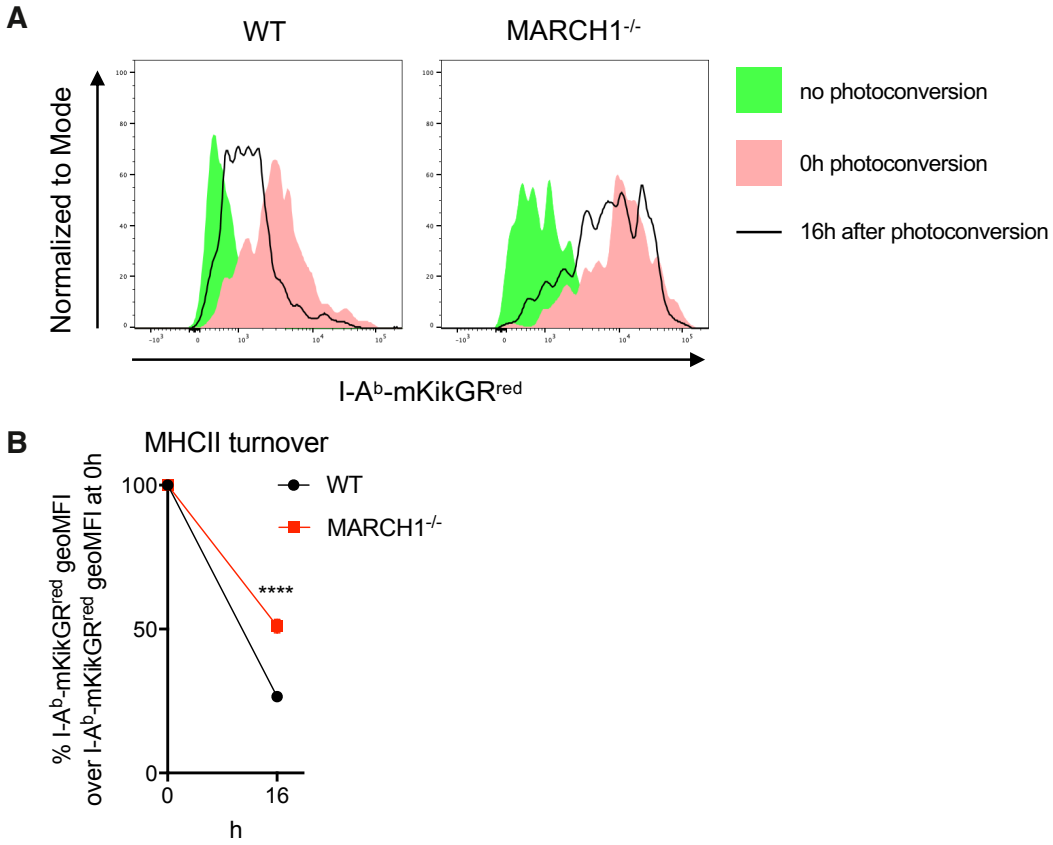

(A) WT or MARCH1$^{-/-}$ BMDCs were retrovirally transduced with MSCV-I-Thy1.1 plasmid encoding an I-A$_b$-mKikGR fusion protein (the mKikGR is fused to the cytoplasmic tail of MHCII β chain). The cells were exposed to violet light at day 9 or 10 of culture and analyzed by flow cytometry at the indicated time points. mKikGR^{red} fluorescence in DCs is shown in the histograms, which included a "no photoconversion" control. **(B)** The rate of MHCII turnover was determined by the percent of mKikGR^{red} fluorescence left at 16 hours after photoconversion. Data are obtained from one experiment with two to three replicates per condition. Data are shown as means ± SEM. Statistical significance was determined by two-way ANOVA with Fisher's LSD test. ****P<0.0001.

Fig. S2.11. eQTL violin plots of associations between genotypes of rs6815724, rs6815345, rs2036903 with MARCH1 expression in lung tissue.

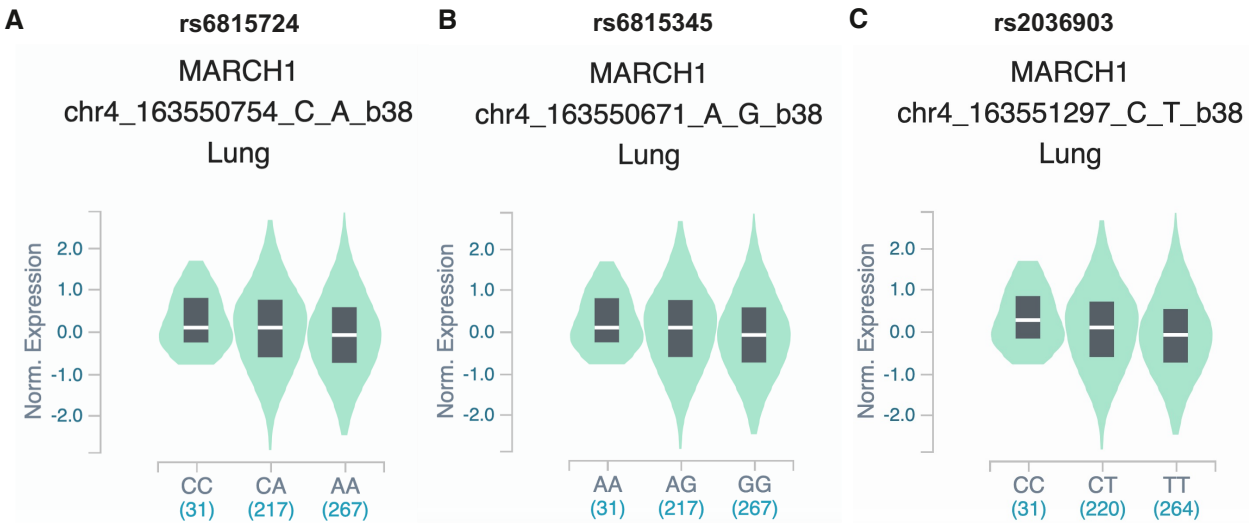

(A) Violin plots of three variants were acquired from the GTEx Project version 8 database and show that protective A allele of rs6815724 **(A)**, G allele of rs6815345 **(B)**, and T allele of rs2036903 **(C)** are associated with lower MARCH1 expression in lung. Note that these three variants were nominally associated with lower asthma risk in trans-ethnic meta-analysis (see table S2.2).

Supplementary Tables

Table S3.1. Demographics of GALA II and SAGE participants included in this study.

Q1/Q3, quantile 1/3. African/Indigenous American/European indicate the corresponding global ancestry proportion.

	African American (N=1379)		Mexican (N=1353)		Puerto Rican (N=2118)		Overall (N=4860)	
	Control (N=503)	Case (N=876)	Control (N=707)	Case (N=646)	Control (N=936)	Case (N=1182)	Control (N=2146)	Case (N=2704)
age (years)								
Median [Q1, Q3]	16.5 [13.1, 18.9]	13.7 [10.9, 17.0]	14.1 [10.9, 17.5]	12.4 [9.98, 15.3]	13.1 [11.1, 15.8]	12.2 [9.97, 15.2]	14.0 [11.3, 17.6]	12.7 [10.3, 15.9]
Sex								
Female	285 (56.7%)	424 (48.4%)	422 (59.7%)	283 (43.8%)	504 (53.8%)	535 (45.3%)	1211 (56.4%)	1242 (45.9%)
Male	218 (43.3%)	452 (51.6%)	285 (40.3%)	363 (56.2%)	432 (46.2%)	647 (54.7%)	935 (43.6%)	1462 (54.1%)
African (%)								
Median [Q1, Q3]	81.8 [75.4, 87.0]	82.6 [76.2, 86.8]	3.39 [1.97, 4.89]	3.48 [2.29, 4.98]	18.1 [13.0, 25.1]	19.0 [13.8, 26.9]	15.6 [4.89, 41.7]	21.5 [8.23, 75.5]
Indigenous American (%)								
Median [Q1, Q3]	< 1	< 1	58.6 [47.7, 74.6]	56.4 [46.5, 68.2]	10.0 [8.31, 11.9]	10.2 [8.56, 12.0]	11.0 [6.02, 47.5]	9.68 [0.967, 17.4]
European (%)								
Median [Q1, Q3]	17.4 [12.5, 23.7]	16.7 [12.4, 22.9]	36.7 [23.0, 47.8]	39.0 [28.3, 48.5]	71.0 [63.5, 76.4]	69.7 [61.9, 75.5]	49.0 [22.8, 69.7]	46.0 [20.4, 68.2]
Sequencing batch								
Batch 1	0 (0%)	449 (51.3%)	0 (0%)	469 (72.6%)	0 (0%)	440 (37.2%)	0 (0%)	1358 (50.2%)
Batch 2	0 (0%)	0 (0%)	0 (0%)	0 (0%)	474 (50.6%)	567 (48.0%)	474 (22.1%)	567 (21.0%)
Batch 3	503 (100%)	427 (48.7%)	707 (100%)	177 (27.4%)	462 (49.4%)	175 (14.8%)	1672 (77.9%)	779 (28.8%)
Current or ever smoker								
No	308 (61.2%)	608 (69.4%)	591 (83.6%)	582 (90.1%)	718 (76.7%)	793 (67.1%)	1617 (75.3%)	1983 (73.3%)
Yes	73 (14.5%)	71 (8.1%)	76 (10.7%)	35 (5.4%)	27 (2.9%)	20 (1.7%)	176 (8.2%)	126 (4.7%)
Missing	122 (24.3%)	197 (22.5%)	40 (5.7%)	29 (4.5%)	191 (20.4%)	369 (31.2%)	353 (16.4%)	595 (22.0%)

Table S2.2. Top ten genetic associations with asthma in trans-ethnic meta-analysis.

Variants were sorted by *P*-value in meta-analysis. Odd ratios (OR) and allele frequency (Freq) were expressed relative to allele 1 (A1), which is also the minor allele; BP, hg38 genomic coordinates on chromosome 4; Reference allele (Ref); AA, African Americans; MX, Mexican Americans; PR: Puerto Ricans; *, suggestively significant asthma association in meta-analysis ($P < 8.20 \times 10^{-3}$). ^, genetic association with asthma at $P < 0.05$ in the replication study, Hartford-PR (table S2.3) or Pan-UK Biobank (data file S2.2). [F], flip-flop genetic association with at $P < 0.05$ in the replication study, Pan-UK Biobank (data file S2.2). [e], eQTLs in GTEx (data file S2.3).

					Meta-analysis			AA			MX			PR			
SNP	BP	Ref	A1	A2	OR	P		Freq	OR	P	Freq	OR	P	Freq	OR	P	
rs6536807	164325654	A	A	G	1.33	2.37E-03	*	0.02	1.06	8.52E-01	0.05	1.20	2.96E-01	0.07	1.45	1.95E-03	*
rs6815724[e, F]	163550754	C	C	A	1.16	2.62E-03	*	0.26	1.20	4.48E-02	0.15	1.13	2.61E-01	0.27	1.15	4.66E-02	
rs6815345[e, F]	163550671	A	A	G	1.16	3.80E-03	*	0.25	1.19	5.84E-02	0.15	1.13	2.63E-01	0.27	1.15	5.38E-02	
rs4691971	164388870	G	G	A	1.29	7.69E-03	*	0.03	1.17	5.26E-01	0.05	1.16	4.09E-01	0.06	1.39	8.66E-03	*
rs72690079	164426854	C	A	C	1.19	8.12E-03	*	0.13	1.25	6.28E-02	0.11	1.12	3.79E-01	0.11	1.19	7.47E-02	
rs7666847[^]	163848106	A	A	G	1.15	8.26E-03		0.24	1.25	1.98E-02	0.24	1.27	9.07E-03	0.13	0.96	6.81E-01	
rs4691973[^, F]	164392771	A	A	C	1.14	9.35E-03		0.28	1.03	7.64E-01	0.16	1.29	2.18E-02	0.25	1.16	4.74E-02	
rs2036903[^, e]	163551297	C	C	T	1.13	1.14E-02		0.28	1.16	1.09E-01	0.15	1.11	3.44E-01	0.27	1.13	8.11E-02	
rs1027755	164386782	C	C	T	1.25	1.30E-02		0.04	1.14	5.38E-01	0.06	1.07	6.85E-01	0.06	1.40	6.33E-03	*
rs1027756	164387898	A	A	C	1.24	1.52E-02		0.05	1.03	8.73E-01	0.05	1.11	5.42E-01	0.06	1.43	4.11E-03	*

Table S2.3. Replication analysis of the top ten associations in the trans-ethnic meta-analysis.

Variants were sorted by *P*-value in meta-analysis. Odd ratios (OR) and allele frequency (Freq) were expressed relative to allele 1 (A1), which is also the minor allele; BP, hg38 genomic coordinates on chromosome 4; Reference allele (Ref); *, suggestively significant asthma association in meta-analysis ($P < 8.20 \times 10^{-3}$). ^, variants with genetic association with asthma at $P < 0.05$ in the replication study, Hartford-Puerto Rico Study (Hartford-PR) or Pan-UK Biobank (data file S2.2). [F], variants with flip-flop genetic association with at $P < 0.05$ in the replication study, Pan-UK Biobank (data file S2.2). [e], eQTLs in GTEx (data file S2.3).

					Meta-analysis			Replication: Hartford-PR		
SNP	BP	Ref	A1	A2	OR	P		Freq	OR	P
rs6536807	164325654	A	A	G	1.33	2.37E-03	*	0.08	1.12	5.57E-01
rs6815724[e, F]	163550754	C	C	A	1.16	2.62E-03	*	0.27	1.05	6.43E-01
rs6815345[e, F]	163550671	A	A	G	1.16	3.80E-03	*	0.26	1.06	5.85E-01
rs4691971	164388870	G	G	A	1.29	7.69E-03	*	0.08	1.08	6.80E-01
rs72690079	164426854	C	A	C	1.19	8.12E-03	*	0.12	0.79	9.68E-02
rs7666847[^]	163848106	A	A	G	1.15	8.26E-03		0.15	0.73	1.79E-02
rs4691973[^, F]	164392771	A	A	C	1.14	9.35E-03		0.27	1.27	2.27E-02
rs2036903[^, e]	163551297	C	C	T	1.13	1.14E-02		0.27	1.07	5.39E-01
rs1027755	164386782	C	C	T	1.25	1.30E-02		0.08	1.08	6.61E-01
rs1027756	164387898	A	A	C	1.24	1.52E-02		0.08	1.13	4.83E-01

Chapter 3: MARCH1-Dependent Restraint of $CD4^+$ T Cell Exhaustion Establishes Airway Allergic Inflammation

One Sentence Summary

MARCH1 in APCs limits T cell exhaustion in allergic asthma.

Abstract

Persistent antigenic signaling leads to T cell exhaustion, a dysfunctional state arising in many chronic infections and cancers. Little is known concerning mechanisms limiting exhaustion in immune stimulatory diseases such as asthma. We report that membrane-associated RING-CH1 (MARCH1), the ubiquitin ligase that mediates surface turnover of MHCII and CD86 in professional APCs, plays an essential role in restraining exhaustion of effector $CD4^+$ T cells in a mouse model of asthma. Mice lacking MARCH1 or the ubiquitin acceptor sites of MHCII and CD86 exhibited increased MHCII and CD86 surface expression on lung APCs, and this increase promoted enhanced expression of immune inhibitory receptors by effector $CD4^+$ T cells and inhibited their proliferation. Remarkably, ablation of MARCH1 in mice with established asthma reduced airway infiltration of eosinophils and Th2 cells. Thus, MARCH1 controls exhaustion of effector $CD4^+$ T cells during allergic airway inflammation and may serve as a therapeutic target for asthma.

Introduction

Professional antigen-presenting cells (APCs) contribute to the induction or effectuation of allergic airway inflammation by sustaining T helper cell activation and proliferation (1). Dendritic cells (DCs) in airways capture inhaled allergens, migrate to the mediastinal lymph node, and present allergens to naïve $CD4^+$ T cells, inducing development of type 2 T helper (Th2) cells (2). However, full-fledged differentiation and maturation of Th2 cells is not completed in the lymph node(3, 4). The tissue of allergen exposure serves an important site for terminal differentiation and effectuation of Th2 cells (5). Tissue conditioning enables T cell production of interleukin (IL)-5 and IL-13 in high levels, which drives recruitment of eosinophils to the airway establishing inflammation (6). Previous studies have shown that tissue DCs and macrophages are important contributors to effector inflammatory responses in allergic asthma. A human cohort study has shown that asthma characterized by high amounts of Th2 cytokines and eosinophils in the airway is accompanied by accumulation of DCs in the airway (7, 8). A mouse asthma model study has shown that depletion of airway DCs during allergen challenge abolished Th2 cell and eosinophilic inflammation, goblet cell hyperplasia, and bronchial hyperreactivity, identifying DCs as key immune cells necessary for Th2 cell stimulation during ongoing airway inflammation (9). Additionally, macrophages in the lung, including those at airway branchpoints termed bronchus-associated macrophages, were found to be critical for effectuation of Th2 cell responses (10). Another mouse study demonstrated that depletion of macrophages impaired local Th2 cell homing and activation in the inflamed lung during IL-13-dependent airway inflammation (11). However, the molecular mechanisms by which DCs and macrophages mediate continuous Th2 cell activation in the airway remain poorly understood.

DCs and other APCs utilize major histocompatibility class II (MHCII) antigen-presenting molecule and the costimulatory molecule CD86 to stimulate antigen-specific $CD4^+$ T cells (12). MHCII and CD86 are both post-translationally modified by a ubiquitin ligase named MARCH1 (13-15). MARCH1 attaches ubiquitin chains to the cytosolic lysine residues of MHCII and CD86 inducing endocytosis and subsequent degradation (14, 16). MARCH1-mediated turnover of MHCII promotes thymic DC selection of regulatory T cells and promotes splenic DC activation of naïve $CD4^+$ T cells (17-19). Yet the role of MARCH1 in APC function in non-lymphoid tissues such as the airways is not known. Because MARCH1 mediates clearance of MHCII and CD86 from the APC surface, MARCH1 may control activation of tissue effector $CD4^+$ T cells and negatively regulate $CD4^+$ T cell-dependent tissue inflammation. Conversely, MARCH1 may sustain effector $CD4^+$ T cell responses by preventing APCs from providing the cells with excessive and/or prolonged antigenic and costimulatory signals as such strong signals could exhaust T cells resulting in poor proliferation and cytokine production (20). In the present study, we investigated how MARCH1 affects lung APC function of driving and maintaining Th2 cell-dependent inflammation in a mouse model of allergic asthma.

Results and Discussion

Wild type (WT) and MARCH1-deficient mice were oropharyngeally administered with house dust mite allergens (HDM) as shown in Fig. 3.1A. On day 14, at the peak of allergic inflammation, lung APCs in MARCH1-deficient mice displayed higher levels of MHCII and CD86 on the surface than those in WT mice indicating that MARCH1 regulates the surface abundance of MHCII and CD86 in lung APCs (Fig. 3.1B). Despite higher levels of MHCII and CD86 on lung APCs, the number of effector $CD4^+$ T cells ($CD44^{hi}CD62L^{lo}CD4^+$ cells) was

significantly lower in MARCH1-deficient mice compared to WT mice (Fig. 3.1C and fig. S3.1A). These findings raised the possibility that the increased MHCII and CD86 on APCs in MARCH1-deficient mice might have induced exhaustion of effector $CD4^+$ T cells impairing proliferation of the T cells. To test this possibility, we examined the expression of PD-1, an immune inhibitory receptor upregulated during T cell exhaustion (20). We found that the percentage of PD-1^+ effector $CD4^+$ T cells was significantly higher in MARCH1-deficient mice than in the WT mice (Fig. 3.1D and fig S3.1B). Several other inhibitory receptors such as CTLA-4, TIGIT, TIM-3, or LAG-3 were also expressed at a higher frequency among effector $CD4^+$ T cells of MARCH1-deficient mice, albeit to a various degree (Fig. 3.1D and fig. S3.1B). Expression of multiple inhibitory receptors is a cardinal feature of T cell exhaustion(20), so we evaluated the percentages of effector $CD4^+$ T cells that express up to four inhibitory receptors. The percentage of effector $CD4^+$ T cells co-expressing more than one inhibitory receptor was higher in MARCH1-deficient mice than in WT mice (Fig. 3.1E), implicating greater T cell exhaustion in MARCH1-deficient mice. To determine whether upregulation of these inhibitory receptors is associated with functional exhaustion, we examined proliferative status of the effector $CD4^+$ T cells by determining the expression of Ki-67, a marker indicative of cell-cycle progression (24). The percentage of Ki-67^+ effector $CD4^+$ T cells was significantly lower in MARCH1-deficient mice than in WT mice (Fig. 3.1F and fig. S3.1C). These results strongly suggest that MARCH1 restrains exhaustion of effector $CD4^+$ T cells during allergic airway inflammation.

To determine if the role of MARCH1 in restraining exhaustion of effector $CD4^+$ T cells is dependent on the expression of this protein in DCs and/or macrophages, but not B cells or other unconventional APCs, we performed similar experiments using $MARCH1^{fl/fl}$ $CD11c^{Cre}$ mice in

which Cre recombinase is expressed under the control of the promoter of CD11c(9, 21, 25), a marker of murine DCs and lung macrophages (fig. S3.2A). As expected, the lung myeloid APCs of MARCH1$^{fl/fl}$ CD11c^{Cre} mice displayed higher levels of MHCII and CD86 on the surface than those of MARCH1$^{fl/fl}$ mice during allergic airway inflammation (fig. S3.2B). The number of effector CD4^{+} T cells was lower in MARCH1$^{fl/fl}$ CD11c^{Cre} mice than in MARCH1$^{fl/fl}$ mice (fig. 3.S2C). The percentage of effector CD4^{+} T cells that express inhibitory receptors such as CTLA-4, TIGIT, and TIM-3 but not PD-1 was significantly higher in MARCH1$^{fl/fl}$ CD11c^{Cre} mice than in MARCH1$^{fl/fl}$ mice (fig. 3.S2D). The percentage of the effector CD4^{+} T cells that concurrently express multiple inhibitory receptors was also higher in MARCH1$^{fl/fl}$ CD11c^{Cre} mice than in MARCH1$^{fl/fl}$ mice (fig. 3.S2E), implicating greater T cell exhaustion in MARCH1$^{fl/fl}$ CD11c^{Cre} mice. Lastly, the frequency of Ki-67-expressing effector CD4^{+} T cells was lower in MARCH1$^{fl/fl}$ CD11c^{Cre} mice than in MARCH1$^{fl/fl}$ mice (fig. 3.S2F). These findings indicate that the role of MARCH1 in restraining exhaustion of effector CD4^{+} T cells during allergic airway inflammation is largely dependent on the expression of this protein in myeloid DCs and/or macrophages, but not B cells or other unconventional APCs.

MARCH1 is not expressed in T cells(15), however MARCH1 deficiency might have caused a defect in the development of effector CD4^{+} T cells in a T cell-extrinsic manner, and this defect could have resulted in functional abnormality of the cells in MARCH1-deficient mice. To bypass this potential problem, we isolated effector CD4^{+} T cells from CD45.1^{+} WT "BoyJ" mice treated with HDM, labeled the cells with cell trace violet (CTV) dye, and transferred the cells to either WT or MARCH1-deficient mice that express CD45.2. These recipient mice were subsequently challenged with HDM, and proliferative responses of transferred T cells were examined by determining dilution of CTV from the cells (Fig. 3.2A). We found the extent of

CTV dilution was significantly lower in MARCH1-deficient mice than in WT mice (Fig. 3.2, B and C). When the same experiment was performed using MARCH1$^{fl/fl}$ CD11c^{Cre} mice and MARCH1$^{fl/fl}$ mice, the transferred T cells proliferated less in MARCH1$^{fl/fl}$ CD11c^{Cre} mice than in MARCH1$^{fl/fl}$ mice (Fig. 3.2D). These findings demonstrate that MARCH1 in myeloid APCs significantly contributes to promoting tissue proliferation of effector CD4^{+} T cells during allergic airway inflammation.

Next, we sought to identify the molecular mechanisms by which MARCH1 suppresses exhaustion of effector CD4^{+} T cells and promotes proliferation of the cells. Our hypothesis was that MARCH1-dependent ubiquitination of MHCII and CD86 allows APCs to express MHCII and CD86 in a regulated fashion, which in turn allows the effector CD4^{+} T cells to express inhibitory receptors in a controlled manner eliciting robust proliferative responses. To test this hypothesis, we generated MHCII$^{K>R}$CD86$^{K>R}$ mice where all the ubiquitin accepting lysines (K) of MHCII and CD86 were mutated to arginines (R) (17, 22). MHCII$^{K>R}$CD86$^{K>R}$ mice and WT mice were treated with HDM as described in Fig. 3.3A. We found that lung APCs in MHCII$^{K>R}$CD86$^{K>R}$ mice displayed increased abundance of MHCII and CD86 on the surface than those in WT mice, which confirms that surface abundance of these two molecules is indeed regulated by ubiquitination (Fig. 3.3B). Remarkably, the number of effector CD4^{+} T cells was significantly low in MHCII$^{K>R}$CD86$^{K>R}$ mice compared to WT mice (Fig. 3.3C). The frequency of effector CD4^{+} T cells that express PD-1, CTLA-4, TIGIT, or TIM-3 was higher in MHCII$^{K>R}$CD86$^{K>R}$ mice than in WT mice (Fig. 3.3D). The percentage of the effector CD4^{+} T cells that concurrently express multiple inhibitory receptors was also higher in MHCII$^{K>R}$CD86$^{K>R}$ mice than in WT mice (Fig. 3.3E). The frequency of Ki-67^{+} effector CD4^{+} T cells was low in MHCII$^{K>R}$ CD86$^{K>R}$ mice compared to WT mice (Fig. 3.3F). Adoptive T cell

transfer experiment showed that MHCII$^{K>R}$CD86$^{K>R}$ mice were inferior in supporting proliferation of HDM-experienced CD4^{+} T cells than in WT mice (Fig. 3.3, G and H), and this poor proliferation was accompanied by increased expression of the inhibitory molecules PD-1 and TIM-3 by the T cells in the MHCII$^{K>R}$CD86$^{K>R}$ mice (Fig. 3.3I). Taken together, ubiquitination of MHCII and CD86 plays a significant role in restraining exhaustion of effector CD4^{+} T cells during allergic airway inflammation.

The findings suggesting that the ubiquitin ligase activity of MARCH1 promotes the proliferation of effector CD4^{+} T cells during allergic airway inflammation led us to hypothesize that inhibiting MARCH1 may exert a therapeutic benefit in allergic asthma by ameliorating inflammation driven by Th2 cells, the pathologic effector CD4^{+} T cells in this disease(6). Since an inhibitor of MARCH1 is not available at present, we conceived an alternative proof of principle experiment that employs a mouse strain where the expression of MARCH1 can be abolished in an inducible manner. MARCH1$^{fl/fl}$ UBC$^{ERT2\text{-}Cre}$ mice express Cre recombinase fused with estrogen receptor (23). Since estrogen receptor is normally localized in the cytosol, Cre is not active in these mice at steady state. However, once the mice intake the ligand of estrogen receptor tamoxifen, the estrogen receptor-Cre fusion protein traffics to the nucleus where Cre is activated and cleaves the MARCH1-encoding DNA disabling the mice to produce MARCH1. MARCH1$^{fl/fl}$ UBC$^{ERT2\text{-}Cre}$ mice and the control UBC$^{ERT2\text{-}Cre}$ mice were administered for 2 weeks with HDM alone, which would induce allergic asthma to both groups of mice. From the third week, the mice were administered with not only HDM but also tamoxifen, which would disable the expression of MARCH1 selectively in MARCH1$^{fl/fl}$ UBC$^{ERT2\text{-}Cre}$ mice. After 7 weeks of HDM treatment in total, lungs were isolated, and APCs, effector CD4^{+} T cells, Th2 cells, and other inflammatory cells were examined (Fig. 3.4A).

First, we examined whether tamoxifen indeed blocked the expression of MARCH1 in MARCH1$^{fl/fl}$ UBC$^{ERT2\text{-}Cre}$ mice. We found that the surface level of MHCII and CD86 was markedly higher in APCs of MARCH1$^{fl/fl}$ UBC$^{ERT2\text{-}Cre}$ mice than that of UBC$^{ERT2\text{-}Cre}$ mice, which confirms the ablation of MARCH1 in MARCH1$^{fl/fl}$ UBC$^{ERT2\text{-}Cre}$ mice. (fig. S3.3A). We also found that the effector CD4^{+} T cells in MARCH1$^{fl/fl}$ UBC$^{ERT2\text{-}Cre}$ mice expressed PD-1, TIM-3, and TIGIT to a higher frequency than those in UBC$^{ERT2\text{-}Cre}$ mice (fig. S3.3B). The frequency of effector CD4^{+} T cells that concurrently express multiple inhibitory receptors was also higher in MARCH1$^{fl/fl}$ UBC$^{ERT2\text{-}Cre}$ mice (fig. S3.3C). This finding is consistent with the role of MARCH1 in restraining the exhaustion of effector CD4^{+} T cells. Next, we examined the frequency of Th2 cells, which produce IL-4, IL-13, and IL-5 driving inflammation in allergic asthma. We also determined the frequency of eosinophils, which are associated with Th2 cells and contribute to inflammation in allergic asthma. We found the number of Th2 cells and eosinophils were both significantly lower in MARCH1$^{fl/fl}$ UBC$^{ERT2\text{-}Cre}$ mice compared to UBC$^{ERT2\text{-}Cre}$ mice (Fig. 3.4, B and C). These findings support our hypothesis that inhibiting MARCH1 could be an effective strategy of ameliorating airway inflammation associated with allergic asthma.

In the present study, we sought to identify the role of MARCH1 in tissue APC function in the context of Th2 cell-driven inflammatory responses in the airway. We found that MARCH1 supports effectuation of Th2 cells during allergic airway inflammation by mediating turnover of MHCII and CD86 in lung APCs. This might seem counter-intuitive since MHCII and CD86 are considered immune-stimulatory ligands that promote activation and expansion of antigen-specific CD4^{+} T cells (12). Nevertheless, mice deficient in either MARCH1 or the ubiquitin acceptor sites of MHCII and CD86 elicited poor effector CD4^{+} T cell responses compared to WT mice. The effector CD4^{+} T cells in these mice were found to upregulate the expression of a broad

range of inhibitory receptors and proliferate poorly, which are characteristic of exhausted T cells(20). Indeed, this is in accordance with the existing model that persistent antigenic signaling drives T cell exhaustion. Thus, we conclude that MARCH1-dependent control of MHCII and CD86 grants tissue APCs an ability to sustain robust effector $CD4^+$ T cell responses by limiting T cell exhaustion and that this function plays a significant role in sustaining airway inflammation associated with asthma.

It is notable that a study from others has shown that MARCH1-deficient mice exhibited defective Th2 cell responses but competent eosinophilia in the lung when immunized with ovalbumin and alum and later challenged with ovalbumin intranasally (26). This discrepancy may represent inherent differences in the mouse models of asthma. It is also notable that we did not address the distinct contribution of MARCH1 among myeloid APCs (i.e. DC or macrophage subsets) to effectuation of Th2 cell responses in this study. A recent work from our group showed that MARCH1 played a specific role in DC function of inducing Th2 cell responses to HDM allergens by enabling Th2 cell development in the lymph node (27). MARCH1 may also function in airway DCs by allowing these cells to restrain exhaustion of the Th2 cells that have trafficked from the lymph node into the airway. Alternatively, but not exclusively, MARCH1 may carry this function through macrophages as mice lacking MARCH1 specifically in macrophages ($MARCH1^{fl/fl}$ $MafB^{Cre}$ mice) (28) exhibited diminished Th2 cell inflammation although eosinophilia developed normally (unpublished data). In any case, our study reveals that MARCH1-dependent control of antigen presentation and costimulatory signals by lung APCs plays a relevant role for optimal effector $CD4^+$ T cell responses during allergic airway inflammation.

T cell exhaustion has been considered a maladaptive phenomenon that arises in chronic viral infections and cancers (29). However, our study suggests that this phenomenon could be forcefully induced by inhibiting MARCH1 and that MARCH1 inhibition could bring a therapeutic benefit for the control of immune-stimulatory diseases such as allergic asthma. Therefore, we propose that developing MARCH1 inhibitors could be one of the exciting avenues for future research with clinical relevance.

Materials and Methods

Mice

Wild-type C57BL/6J and B6.SJL-PtprcaPepcb/BoyJ (CD45.1^{+} "BoyJ") mice were purchased from The Jackson Laboratory and maintained in our colony. MARCH1$^{-/-}$, MARCH1$^{fl/fl}$, CD11c^{Cre}, MHCII$^{K>R}$, CD86$^{K>R}$, and UBC$^{ERT2\text{-}Cre}$ mice were previously described (15, 17, 18, 21-23). MARCH1$^{fl/fl}$ CD11c^{Cre} mice were generated by breeding MARCH1$^{fl/fl}$ mice with CD11c^{Cre} mice. MHCII$^{K>R}$CD86$^{K>R}$ mice were generated by breeding MHCII$^{K>R}$ mice and CD86$^{K>R}$ mice MARCH1$^{fl/fl}$ UBC$^{ERT2\text{-}Cre}$ were generated by breeding MARCH1$^{fl/fl}$ mice with UBC$^{ERT2\text{-}Cre}$ mice. Mice were housed in a specific-pathogen free facility in the Laboratory Animal Research Center at UCSF. Mice of both sexes were used at 5-20 weeks of age when initiating an experiment and whenever possible, littermates or mice of distinct genotypes were co-housed in the same cage. Sample sizes were guided by previous studies. Mouse genotypes were not blinded from the investigator. All experiments conformed to ethical principles and guidelines approved by the Institutional Animal Care and Use Committee at UCSF.

HDM-induced allergic asthma protocol

On days 0 and 7-11, naïve mice were anesthetized with isoflurane and given 10 μg HDM extract (*Dermatophagoides pteronyssinus*, Stallergenes Greer, catalog no. NC0419530) by oropharyngeal aspiration. On day 14, mice were euthanized, and lungs were collected for flow cytometry. For experiments involving tamoxifen, mice were also challenged on the days of tamoxifen administration with 10 μg HDM extract (days 14, 17, 20, 24, 28, 31, 35, 38, 42, and 45) and euthanized on day 49.

Cell preparation for flow cytometry

Lungs were digested with Collagenase D (Roche) and DNase I (Roche) for 30 min at 37°C and dissociated in C tubes with a gentleMACS Dissociator (Miltenyi Biotec). The digest was stopped with cold FACS buffer (0.5% BSA in PBS) and centrifuged at 500g for 5 min at 4°C. Cell pellets were resuspended in red blood cell lysis buffer for 5 min at room temperature (RT) and washed with FACS buffer. Cell suspensions were filtered with 70-micron nylon mesh strainers. Cells were centrifuged and resuspended in 1ml FACS buffer and counted with a Z2 Particle Counter (Beckman Coulter). Lung cells then were stained for surface and/or intracellular markers, or in some experiments also stimulated for intracellular cytokine accumulation and staining.

Surface staining of cells

Fc receptors of lung cells were blocked with anti-mouse CD16/32 (Trustain fcX clone 93, BioLegend) antibody for 10 min on ice. Cells were stained with mixtures of fluorochrome-labeled antibodies in FACS buffer containing 0.5% BSA and 2mM EDTA in PBS for 30 min on ice. Antibodies used for surface staining included anti-mouse eFluor450 CD44 (IM7; eBioscience), anti-mouse CD62L (MEL-14; BioLegend), anti-mouse Pacific Blue I-A/I-E

MHCII (M5/114.15.2, BioLegend), anti-mouse BV605 CD4 (GK1.5 or RM4-5; BioLegend), anti-mouse BV605 TIM-3 (RMT3-23; BioLegend), anti-mouse BV650 Ly6G (1A8; BioLegend), anti-mouse PE CD4 (GK1.5; BioLegend), anti-mouse PE PD-1 (RMP1-30; BioLegend), anti-mouse PE CD86 (GL-1; BD Pharmingen), anti-mouse PE/Cy7 CD44 (IM7; BioLegend), anti-mouse PE/Cy7 B220 (RA3-6B2; BioLegend), anti-mouse APC TIGIT (1G9; BioLegend), anti-mouse APC CD45.1 (A20; BioLegend), anti-mouse Alexa Fluor 700 CD4 (GK1.5), anti-mouse Alexa Fluor 700 CD11c (N418; BioLegend), anti-mouse APC/Cy7 (MEL-14; BioLegend), or anti-mouse APC/Cy7 Siglec-F (E50-2440; BD Pharmingen). Cells were also stained with propidium iodide (Invitrogen) or in case of intracellular staining with either Live/Dead Fixable Red Dead Cell Stain (Invitrogen) or eFluor780 Fixable Viability Dye (eBioscience) as a live/dead stain. Cells were washed and resuspended in FACS buffer for flow cytometry analysis on a BD LSRII machine.

Intracellular staining of cells

For staining of CTLA-4, LAG-3 or Ki-67, surface-stained cells were prepared with the Foxp3 Transcription Factor Staining Buffer Kit (eBioscience) and stained with mixtures of fluorochrome-labeled antibodies in Permeabilization Buffer (eBioscience) for 30 min on ice. Antibodies used for intracellular staining included anti-mouse PerCP/Cy5.5 CTLA-4 (UC10-4B9, BioLegend), anti-mouse PE/Cy7 Ki-67 (B56, BD Pharmingen), anti-mouse APC CTLA-4 (UC10-4B9, BioLegend), or anti-mouse LAG-3 (C9B7W, BioLegend). Cells were washed and resuspended in FACS buffer for flow cytometry analysis on a BD LSRII machine.

Intracellular cytokine staining

Cells were stimulated *ex vivo* with stimulation cocktail of PMA (10 ng/ml, Sigma-Aldrich) plus ionomycin (1 μg/ml, Sigma-Aldrich) in the presence of protein transport blocker

Brefeldin A (10 μg/ml, Sigma-Aldrich) for 3h in a 37°C CO_2 incubator. After stimulation, cells were blocked with anti-mouse CD16/32 antibody for 10 min on ice then stained with anti-mouse BV605 CD4 (GK1.5) and with eFluor780 Fixable Viability Dye as a live/dead stain for 30 min on ice. Cells were fixed with IC Fixation Buffer (Invitrogen) and permeabilized with Permeabilization Buffer. Cells were stained intracellularly with anti-mouse FITC IL-5 (TRFK5, Leinco Technologies), anti-mouse PE IL-13 (eBio13A, eBioscience) and anti-mouse APC IL-4 (11B11, BioLegend) in Permeabilization Buffer for 30 min on ice. Cells were washed and resuspended in FACS buffer for flow cytometry analysis on a BD LSRII machine.

Adoptive transfer of HDM-experienced T cells

T cells were isolated using the EasySep CD4+ T cell Isolation Kit (StemCell Technologies) from single-cell suspensions of lungs derived from $CD45.1^+$ donor mice at day 14 of HDM-induced allergic asthma protocol. For each experiment, lung $CD4^+$ T cells were pooled from multiple donor mice. Purified lung T cells were labeled with Cell Trace Violet (CTV) (Life Technologies) for 20 min at 37°C and quenched with RPMI supplemented with 10% FBS. Cells ($\sim 0.5\text{-}1\times10^6$) were transferred via retro-orbital injection into recipient mice. Recipient mice were administered 10 μg HDM on days 0-3 after transfer. On day 4, recipient mice were euthanized, and lungs were collected for determining proliferation of donor T cells by staining lung cells with anti-mouse BV605 CD4 (GK1.5 or RM4-5) or anti-mouse Alexa Fluor 700 CD4 (GK1.5) and anti-mouse APC CD45.1 (A20) antibodies and CTV dilution of the transferred cells was detected by flow cytometry.

Tamoxifen-induced ablation of MARCH1

Tamoxifen was infused in corn oil and injected intraperitoneally at a dose of 50 μg/g.

Software and Statistical analysis

Flow cytometry data were analyzed by FlowJo (TreeStar). Graphs were drawn by Prism (GraphPad). Unpaired two-tailed Student's *t*-test was performed to assess the significance.

References

1. Schuijs, M. J., H. Hammad, and B. N. Lambrecht. 2019. Professional and 'Amateur' Antigen-Presenting Cells In Type 2 Immunity. *Trends Immunol* 40: 22-34.
2. Lambrecht, B. N., and H. Hammad. 2009. Biology of lung dendritic cells at the origin of asthma. *Immunity* 31: 412-424.
3. Van Dyken, S. J., J. C. Nussbaum, J. Lee, A. B. Molofsky, H. E. Liang, J. L. Pollack, R. E. Gate, G. E. Haliburton, C. J. Ye, A. Marson, D. J. Erle, and R. M. Locksley. 2016. A tissue checkpoint regulates type 2 immunity. *Nat Immunol* 17: 1381-1387.
4. Tibbitt, C. A., J. M. Stark, L. Martens, J. Ma, J. E. Mold, K. Deswarte, G. Oliynyk, X. Feng, B. N. Lambrecht, P. De Bleser, S. Nylen, H. Hammad, M. Arsenian Henriksson, Y. Saeys, and J. M. Coquet. 2019. Single-Cell RNA Sequencing of the T Helper Cell Response to House Dust Mites Defines a Distinct Gene Expression Signature in Airway Th2 Cells. *Immunity* 51: 169-184 e165.
5. Hondowicz, B. D., D. An, J. M. Schenkel, K. S. Kim, H. R. Steach, A. T. Krishnamurty, G. J. Keitany, E. N. Garza, K. A. Fraser, J. J. Moon, W. A. Altemeier, D. Masopust, and M. Pepper. 2016. Interleukin-2-Dependent Allergen-Specific Tissue-Resident Memory Cells Drive Asthma. *Immunity* 44: 155-166.
6. Locksley, R. M. 2010. Asthma and allergic inflammation. *Cell* 140: 777-783.
7. Greer, A. M., M. A. Matthay, J. Kukreja, N. R. Bhakta, C. P. Nguyen, P. J. Wolters, P. G. Woodruff, J. V. Fahy, and J. S. Shin. 2014. Accumulation of BDCA1(+) dendritic cells in interstitial fibrotic lung diseases and Th2-high asthma. *PLoS One* 9: e99084.

8. Woodruff, P. G., B. Modrek, D. F. Choy, G. Jia, A. R. Abbas, A. Ellwanger, L. L. Koth, J. R. Arron, and J. V. Fahy. 2009. T-helper type 2-driven inflammation defines major subphenotypes of asthma. *Am J Respir Crit Care Med* 180: 388-395.

9. van Rijt, L. S., S. Jung, A. Kleinjan, N. Vos, M. Willart, C. Duez, H. C. Hoogsteden, and B. N. Lambrecht. 2005. In vivo depletion of lung CD11c+ dendritic cells during allergen challenge abrogates the characteristic features of asthma. *J Exp Med* 201: 981-991.

10. Tang, X.-Z., L. S. M. Kreuk, C. Cho, R. J. Metzger, and C. D. C. Allen. 2020. Bronchus-associated macrophages are positioned for soluble antigen capture from the airway lumen and for local Th2 cell activation. *bioRxiv*: 2020.2009.2018.247742.

11. Borthwick, L. A., L. Barron, K. M. Hart, K. M. Vannella, R. W. Thompson, S. Oland, A. Cheever, J. Sciurba, T. R. Ramalingam, A. J. Fisher, and T. A. Wynn. 2016. Macrophages are critical to the maintenance of IL-13-dependent lung inflammation and fibrosis. *Mucosal Immunol* 9: 38-55.

12. Banchereau, J., and R. M. Steinman. 1998. Dendritic cells and the control of immunity. *Nature* 392: 245-252.

13. De Gassart, A., V. Camosseto, J. Thibodeau, M. Ceppi, N. Catalan, P. Pierre, and E. Gatti. 2008. MHC class II stabilization at the surface of human dendritic cells is the result of maturation-dependent MARCH I down-regulation. *Proc Natl Acad Sci U S A* 105: 3491-3496.

14. Baravalle, G., H. Park, M. McSweeney, M. Ohmura-Hoshino, Y. Matsuki, S. Ishido, and J. S. Shin. 2011. Ubiquitination of CD86 is a key mechanism in regulating antigen presentation by dendritic cells. *J Immunol* 187: 2966-2973.

15. Matsuki, Y., M. Ohmura-Hoshino, E. Goto, M. Aoki, M. Mito-Yoshida, M. Uematsu, T. Hasegawa, H. Koseki, O. Ohara, M. Nakayama, K. Toyooka, K. Matsuoka, H. Hotta, A. Yamamoto, and S. Ishido. 2007. Novel regulation of MHC class II function in B cells. *EMBO J* 26: 846-854.

16. Shin, J. S., M. Ebersold, M. Pypaert, L. Delamarre, A. Hartley, and I. Mellman. 2006. Surface expression of MHC class II in dendritic cells is controlled by regulated ubiquitination. *Nature* 444: 115-118.

17. Oh, J., N. Wu, G. Baravalle, B. Cohn, J. Ma, B. Lo, I. Mellman, S. Ishido, M. Anderson, and J. S. Shin. 2013. MARCH1-mediated MHCII ubiquitination promotes dendritic cell selection of natural regulatory T cells. *J Exp Med* 210: 1069-1077.

18. Oh, J., J. S. A. Perry, H. Pua, N. Irgens-Moller, S. Ishido, C. S. Hsieh, and J. S. Shin. 2018. MARCH1 protects the lipid raft and tetraspanin web from MHCII proteotoxicity in dendritic cells. *J Cell Biol* 217: 1395-1410.

19. Kim, H. J., J. Bandola-Simon, S. Ishido, N. W. Wong, V. N. Koparde, M. Cam, and P. A. Roche. 2020. Ubiquitination of MHC Class II by March-I Regulates Dendritic Cell Fitness. *J Immunol*.

20. Wherry, E. J., and M. Kurachi. 2015. Molecular and cellular insights into T cell exhaustion. *Nat Rev Immunol* 15: 486-499.

21. Caton, M. L., M. R. Smith-Raska, and B. Reizis. 2007. Notch-RBP-J signaling controls the homeostasis of CD8- dendritic cells in the spleen. *J Exp Med* 204: 1653-1664.

22. Ishikawa, R., M. Kajikawa, and S. Ishido. 2014. Loss of MHC II ubiquitination inhibits the activation and differentiation of CD4 T cells. *Int Immunol* 26: 283-289.

23. Ruzankina, Y., C. Pinzon-Guzman, A. Asare, T. Ong, L. Pontano, G. Cotsarelis, V. P. Zediak, M. Velez, A. Bhandoola, and E. J. Brown. 2007. Deletion of the developmentally essential gene ATR in adult mice leads to age-related phenotypes and stem cell loss. *Cell Stem Cell* 1: 113-126.

24. Gerdes, J., H. Lemke, H. Baisch, H. H. Wacker, U. Schwab, and H. Stein. 1984. Cell cycle analysis of a cell proliferation-associated human nuclear antigen defined by the monoclonal antibody Ki-67. *J Immunol* 133: 1710-1715.

25. von Garnier, C., L. Filgueira, M. Wikstrom, M. Smith, J. A. Thomas, D. H. Strickland, P. G. Holt, and P. A. Stumbles. 2005. Anatomical location determines the distribution and function of dendritic cells and other APCs in the respiratory tract. *J Immunol* 175: 1609-1618.

26. Kishta, O. A., A. Sabourin, L. Simon, T. McGovern, M. Raymond, T. Galbas, A. Majdoubi, S. Ishido, J. G. Martin, and J. Thibodeau. 2018. March1 E3 Ubiquitin Ligase Modulates Features of Allergic Asthma in an Ovalbumin-Induced Mouse Model of Lung Inflammation. *J Immunol Res* 2018: 3823910.

27. Castellanos, C. A., X. Ren, S. L. Gonzalez, H. K. Li, A. W. Schroeder, H. E. Liang, B. J. Laidlaw, D. Hu, A. C. Y. Mak, C. Eng, J. R. Rodriguez-Santana, M. LeNoir, Q. Yan, J. C. Celedon, E. G. Burchard, S. S. Zamvil, S. Ishido, R. M. Locksley, J. G. Cyster, X. Huang, and J. S. Shin. 2021. Lymph node-resident dendritic cells drive TH2 cell development involving MARCH1. *Sci Immunol* 6: eabh0707.

28. Wu, X., C. G. Briseno, V. Durai, J. C. Albring, M. Haldar, P. Bagadia, K. W. Kim, G. J. Randolph, T. L. Murphy, and K. M. Murphy. 2016. Mafb lineage tracing to distinguish

macrophages from other immune lineages reveals dual identity of Langerhans cells. *J Exp Med* 213: 2553-2565.

29. Saeidi, A., K. Zandi, Y. Y. Cheok, H. Saeidi, W. F. Wong, C. Y. Q. Lee, H. C. Cheong, Y. K. Yong, M. Larsson, and E. M. Shankar. 2018. T-Cell Exhaustion in Chronic Infections: Reversing the State of Exhaustion and Reinvigorating Optimal Protective Immune Responses. *Front Immunol* 9: 2569.

Figures

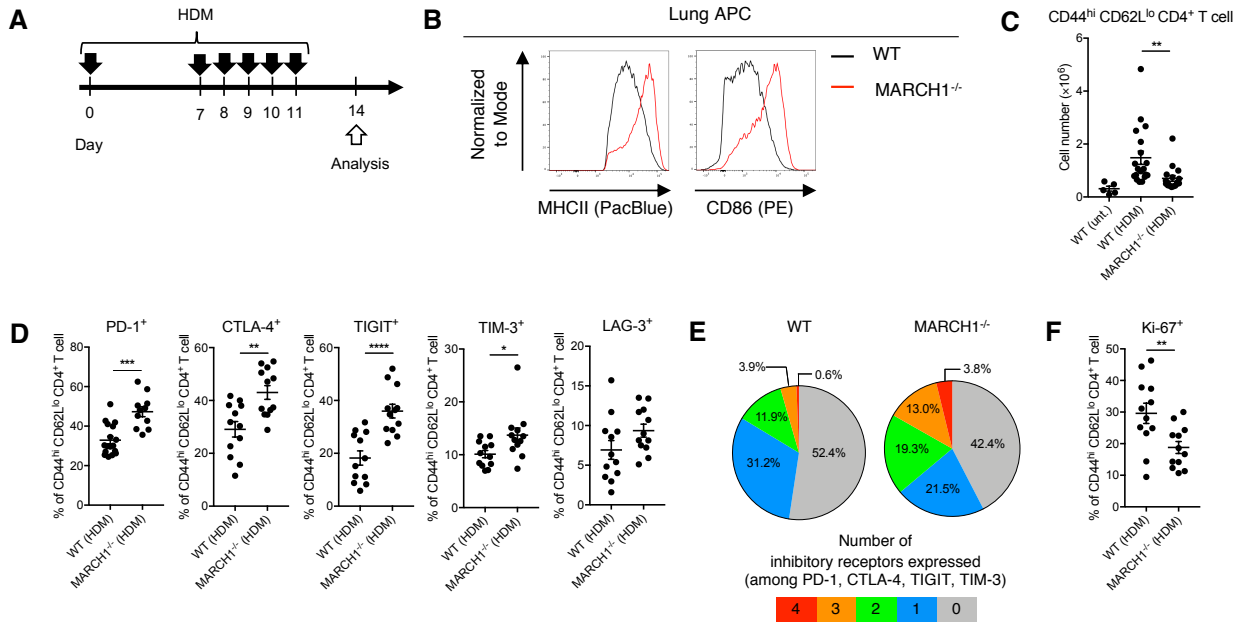

(A) Experimental outline of HDM challenge. Solid black arrows indicate oropharyngeal aspiration of 10 µg of HDM. **(B)** Representative histograms showing MHCII and CD86 surface expression in lung tissue APCs (gated as Siglec-F^{-} B220^{-} CD11c^{+} MHCII^{+}) of WT and MARCH1$^{-/-}$ mice. Data are representative from two experiments with four to five mice per group. **(C)** Total number of CD44^{hi} CD62L^{lo} effector CD4^{+} T cells in the lungs of WT or MARCH1$^{-/-}$ mice untreated or treated with HDM. Data are pooled from three experiments with two to seven mice per group. **(D)** Frequency of effector CD4^{+} T cells in the lungs expressing PD-1, CTLA-4, TIGIT, TIM-3 or LAG-3. Data are obtained from two to three experiments with five to seven mice per group. **(E)** Composition of effector CD4^{+} T cells that express single or multiple inhibitory receptors in WT or MARCH1$^{-/-}$ mice. Average frequency of cells expressing 0, 1, 2, 3 or 4 distinct inhibitory receptors are indicated as percentage in the pie charts. **(F)** Frequency of effector CD4^{+} T cells in the lungs expressing Ki-67. Data are from two experiment with six mice per group. *P<0.05; **P<0.01; ***P<0.001; ****P<0.0001 (Student's t-test). Data are shown as mean ± standard error from the mean (SEM).

Fig. 3.2. MARCH1 promotes expansion of effector CD4$^+$ T cells during allergic airway inflammation.

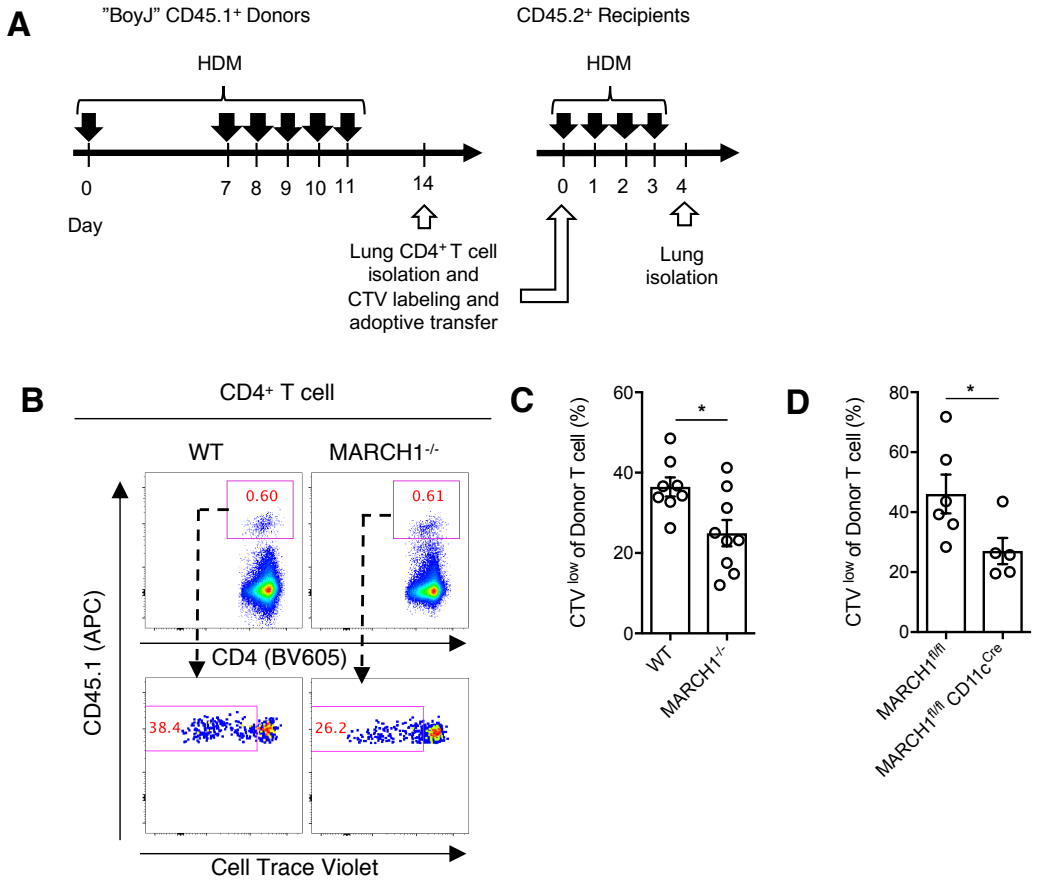

(A) Experimental protocol for adoptive transfer of HDM-experienced CD4$^+$ T cells. **(B)** Representative flow cytometry plots indicating proliferation of transferred CD4$^+$ T cells (CD4$^+$CD45.1$^+$) in WT or MARCH1$^{-/-}$ recipient mice. Numbers indicate percentages of cells in the indicated gate. **(C)** Summary of data from **(B)** showing the percentage of transferred T cells proliferating in WT or MARCH1$^{-/-}$ recipient mice. Data are pooled from two experiments with 4-5 mice per group. **(D)** The percentage of transferred T cells proliferating in MARCH1$^{fl/fl}$ or MARCH1$^{fl/fl}$ CD11c^{Cre} recipient mice. Data are obtained from one experiment with 5-7 mice per group. *P<0.05 (Student's t-test). Data are shown as mean ± SEM.

Fig. 3.3. Ubiquitination of MHCII and CD86 negatively regulates the expression of inhibitory receptors by effector CD4$^+$ T cells and suppresses exhaustion of these cells during allergic airway inflammation.

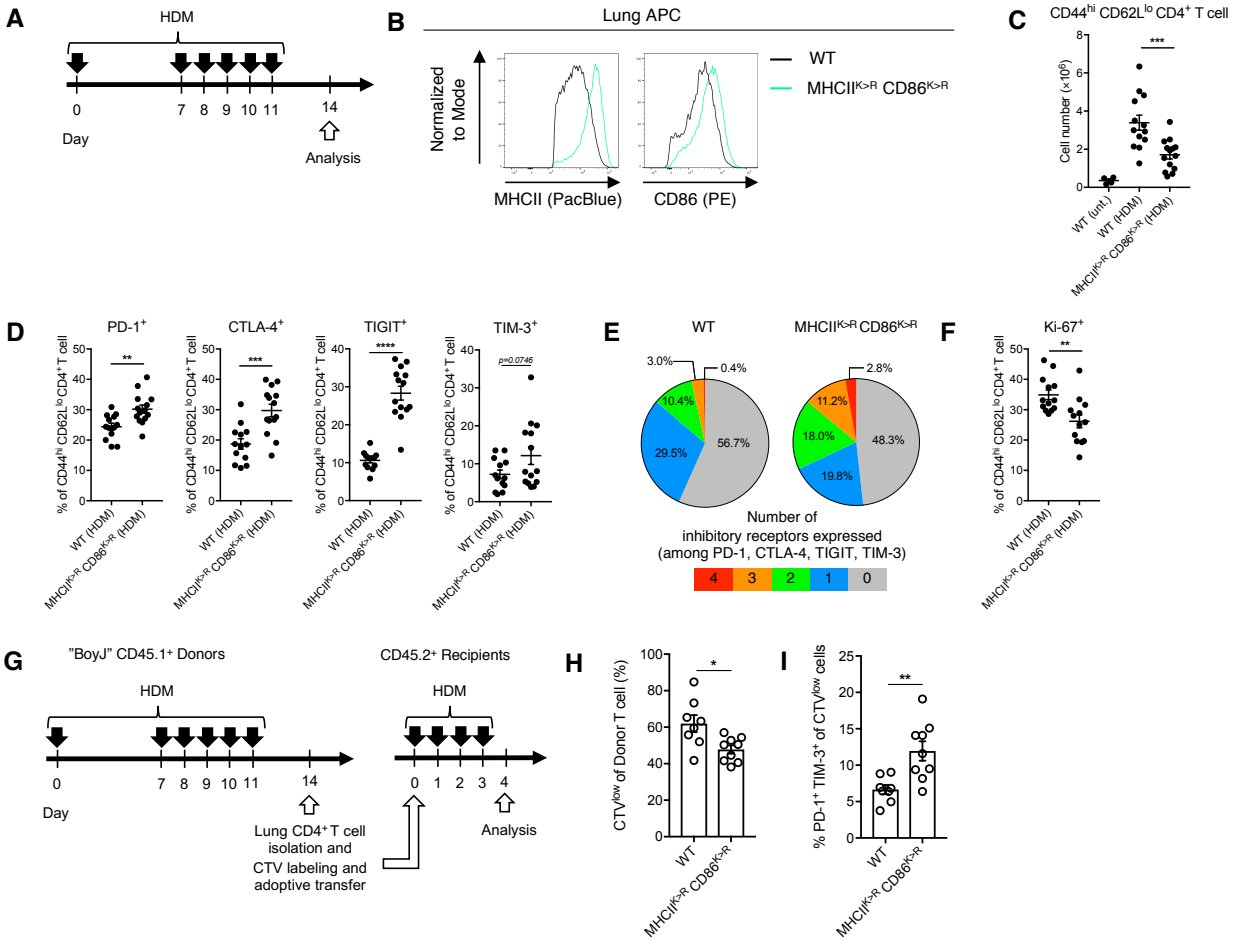

(A) Experimental outline of HDM challenge. **(B)** Representative histograms showing the surface levels of MHCII or CD86 in lung tissue APCs of WT or MHCII$^{K>R}$CD86$^{K>R}$ mice. Data are representative from one experiment with eight mice per group. **(C)** Total number of CD44^{hi} CD62L^{lo} effector CD4$^+$ T cells in the lungs of WT or MHCII$^{K>R}$CD86$^{K>R}$ mice untreated or treated with HDM. **(D)** Frequency of effector CD4$^+$ T cells expressing PD-1, CTLA-4, TIGIT, or TIM-3. **(E)** Composition of effector CD4$^+$ T cells that express single or multiple inhibitory receptors in WT or MHCII$^{K>R}$CD86$^{K>R}$ mice. Average frequency of cells expressing 0, 1, 2, 3 or 4 distinct inhibitory receptors are indicated as percentage in the pie charts. **(F)** Frequency of effector CD4$^+$ T cells expressing Ki-67. Data in **(C-F)** are from two experiments with two untreated mice and six to eight WT or MHCII$^{K>R}$CD86$^{K>R}$ mice challenged with HDM. **(G)** Experimental protocol for adoptive transfer of HDM-experienced CD4$^+$ T cells. **(H)** The percentage of transferred T cells proliferating in WT or MHCII$^{K>R}$CD86$^{K>R}$ mice. **(I)** The percentage of transferred T cells expressing PD-1 and TIM-3 simultaneously in WT or MHCII$^{K>R}$CD86$^{K>R}$ mice. Data in **(H and I)** are from one experiment with eight to nine mice per group. *P<0.05; **P<0.01; ***P<0.001; ****P<0.0001 (Student's t-test). Data are shown as mean ± SEM.

Fig. 3.4. MARCH1 ablation after establishment of allergic airway inflammation reduces Th2 cell effector function and eosinophilia to chronic HDM exposure.

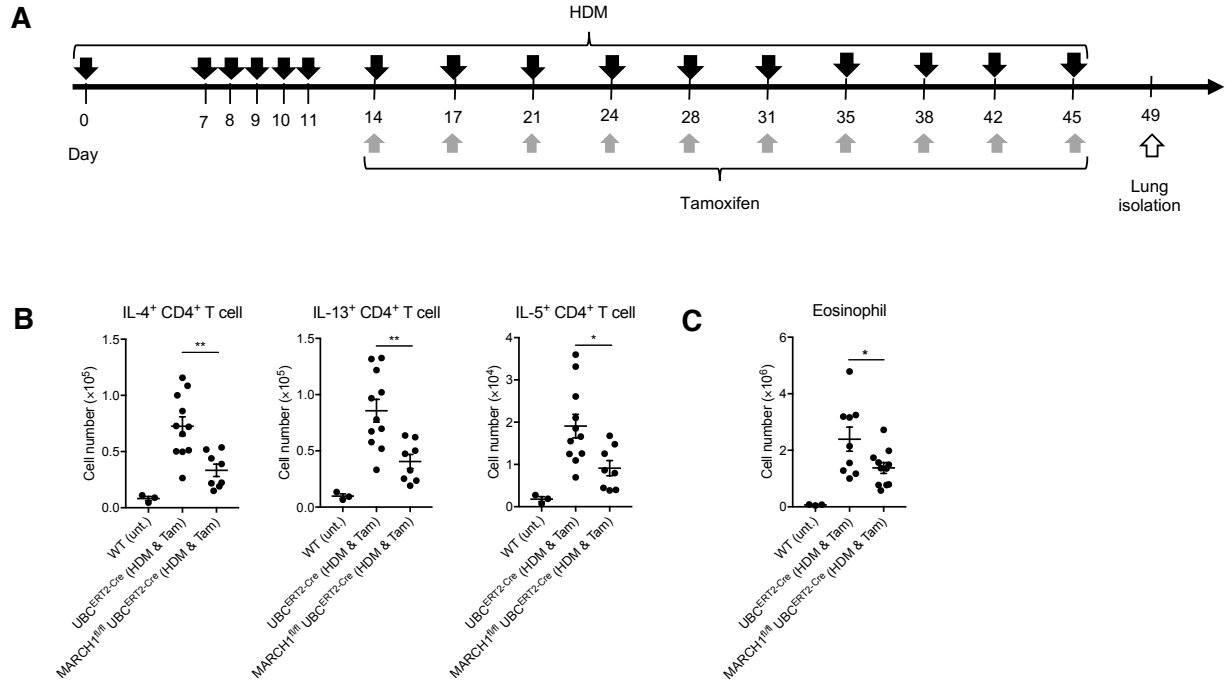

(A) Experimental outline of HDM challenge (black arrows) and tamoxifen injection (gray arrows). **(B)** Total numbers of IL-4, IL-13, or IL-5 competent $CD4^+$ T cells in lungs of untreated mice or $UBC^{ERT2\text{-}Cre}$ or $MARCH1^{fl/fl}$ $UBC^{ERT2\text{-}Cre}$ mice treated with HDM and tamoxifen (Tam). **(C)** Total numbers of eosinophils in lungs of untreated mice or $UBC^{ERT2\text{-}Cre}$ or $MARCH1^{fl/fl}$ $UBC^{ERT2\text{-}Cre}$ mice treated with HDM and tamoxifen. Data in **(B and C)** are representative from two experiments with three untreated mice and eight to 11 $UBC^{ERT2\text{-}Cre}$ or $MARCH1^{fl/fl}$ $UBC^{ERT2\text{-}Cre}$ treated with HDM and tamoxifen. $*P<0.05$; $**P<0.01$ (Student's *t*-test). Data are shown as mean ± SEM.

Supplementary Figures

Fig. S3.1. Flow cytometry plots of effector CD4$^+$ T cells in the lungs of WT and MARCH1$^{-/-}$ mice.

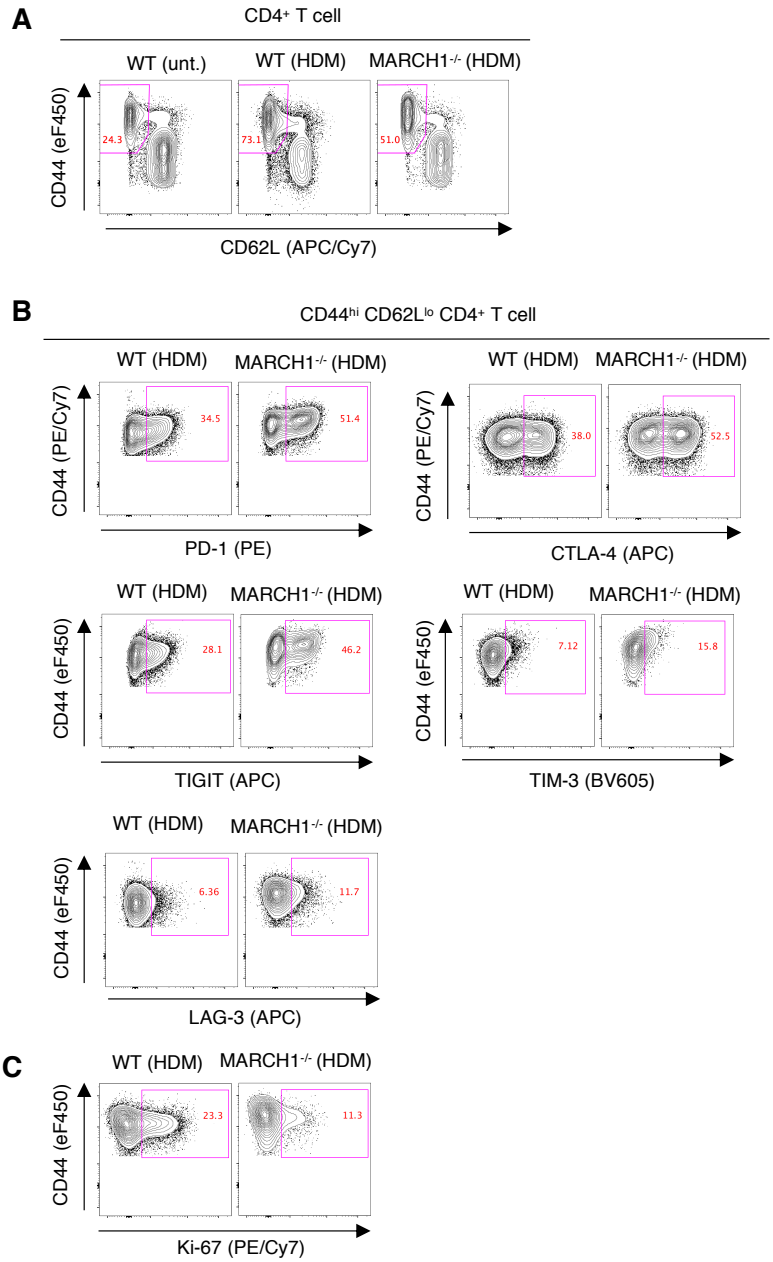

(A) Representative flow cytometry plots indicating the frequency of CD44^{hi} CD62L^{lo} effector CD4$^+$ T cells in the lungs of WT or MARCH1$^{-/-}$ mice untreated or treated with HDM. Data are representative of three experiments with two to seven mice per group. **(B)** Representative flow cytometry plots indicating the frequency of effector CD4$^+$ T cells expressing PD-1, CTLA-4, TIGIT, TIM-3 or LAG-3. Data are representative of one to three experiments with four to seven mice per group. **(C)** Representative flow cytometry plots indicating the frequency of effector CD4$^+$ T cells expressing Ki-67. Data are representative of one experiment with six mice per group.

Fig. S3.2. MARCH1 in myeloid APCs promotes effector CD4$^+$ T cell accumulation and controls inhibitory receptor expression during HDM-induced allergic airway inflammation.

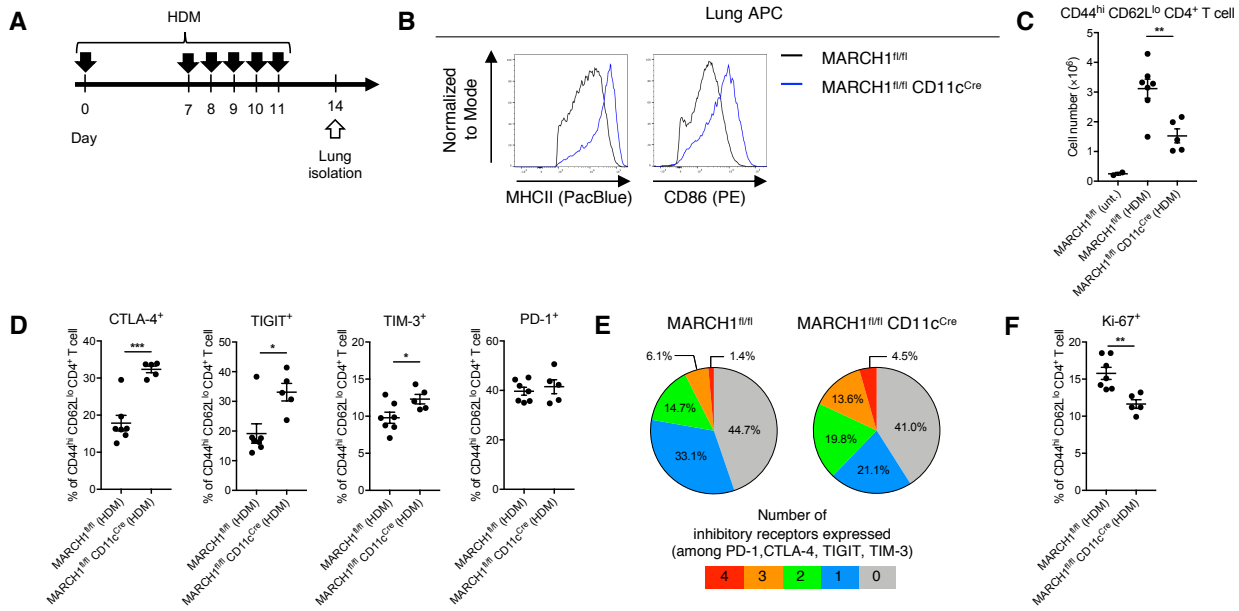

(A) Experimental outline of HDM challenge. **(B)** Representative histograms showing the surface levels of MHCII or CD86 in lung tissue APCs of MARCH1$^{fl/fl}$ or of MARCH1$^{fl/fl}$ CD11c^{Cre} mice. Data are representative from two experiments with four to five mice per group. **(C)** Total number of CD44^{hi} CD62L^{lo} effector CD4$^+$ T cells in MARCH1$^{fl/fl}$ or MARCH1$^{fl/fl}$ CD11c^{Cre} mice untreated or treated with HDM. **(D)** Frequency of effector CD4$^+$ T cells expressing PD-1, CTLA-4, TIGIT, TIM-3, or PD-1. **(E)** Composition of effector CD4$^+$ T cells that express single or multiple inhibitory receptors in MARCH1$^{fl/fl}$ or MARCH1$^{fl/fl}$CD11c^{Cre} mice. Average frequency of cells expressing 0, 1, 2, 3 or 4 distinct inhibitory receptors are indicated as percentage in the pie charts. **(F)** Frequency of effector CD4$^+$ T cells expressing Ki-67. Data in **(C-F)** are from one experiment with five to seven mice per group. *P<0.05; **P<0.01; ***P<0.001 (Student's t-test). Data are shown as mean ± SEM.

Fig. S3.3. Tamoxifen treatment increases the surface expression of MHCII and CD86 by lung APCs and increases the expression of inhibitory receptors by effector CD4^{+} T cells in MARCH1$^{fl/fl}$ UBC$^{ERT2\text{-}Cre}$ mice.

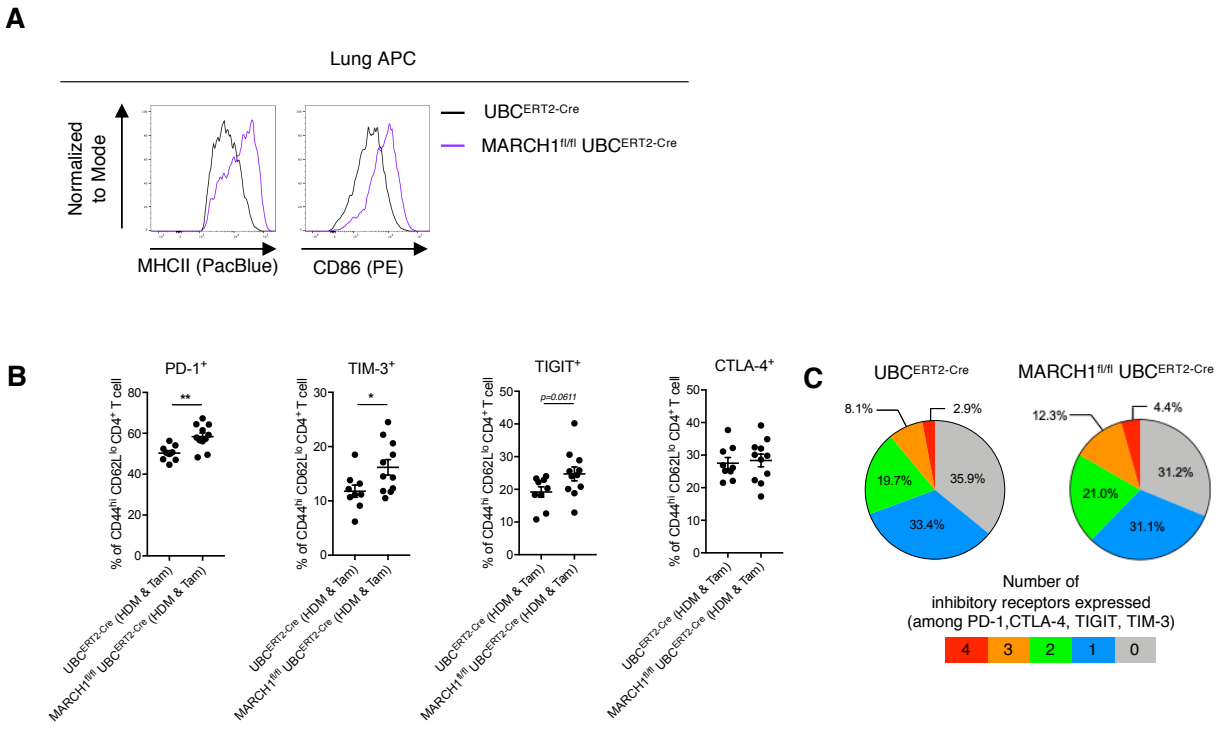

(A) Representative histograms showing MHCII and CD86 surface expression in lung tissue APCs of MARCH1$^{fl/fl}$ UBC$^{ERT2\text{-}Cre}$ mice in comparison to UBC$^{ERT2\text{-}Cre}$ control mice after HDM challenge and tamoxifen treatment. Data are representative from one experiment with nine to 11 mice per group. **(B)** Frequency of effector CD4^{+} T cells expressing PD-1, TIM-3, TIGIT, or CTLA-4 in UBC$^{ERT2\text{-}Cre}$ or MARCH1$^{fl/fl}$ UBC$^{ERT2\text{-}Cre}$ mice. **(C)** Composition of effector CD4^{+} T cells that express single or multiple inhibitory receptors in UBC$^{ERT2\text{-}Cre}$ or MARCH1$^{fl/fl}$ UBC$^{ERT2\text{-}Cre}$ mice. Average frequency of cells expressing 0, 1, 2, 3 or 4 distinct inhibitory receptors are indicated as percentage in the pie charts. Data in **(B and C)** are from one experiment with nine to 11 mice per group. *P<0.05; **P<0.01(Student's t-test). Data are shown as mean ± SEM.

Publishing Agreement

It is the policy of the University to encourage open access and broad distribution of all theses, dissertations, and manuscripts. The Graduate Division will facilitate the distribution of UCSF theses, dissertations, and manuscripts to the UCSF Library for open access and distribution. UCSF will make such theses, dissertations, and manuscripts accessible to the public and will take reasonable steps to preserve these works in perpetuity.

I hereby grant the non-exclusive, perpetual right to The Regents of the University of California to reproduce, publicly display, distribute, preserve, and publish copies of my thesis, dissertation, or manuscript in any form or media, now existing or later derived, including access online for teaching, research, and public service purposes.

DocuSigned by:
Carlos Castellanos
3453E8F76CBC437...
Author Signature

12/15/2021
Date